東京大学理学部紀要

第二類　地質学 鉱物学 地理学 地球物理学

第十冊　第一篇

JOURNAL

OF THE

FACULTY OF SCIENCE

UNIVERSITY OF TOKYO

SECTION II

GEOLOGY, MINERALOGY, GEOGRAPHY, GEOPHYSICS

Vol. X　Part I

TOKYO
Published by the University
September 30, 1956

The "Journal of the Faculty of Science" is the continuation of the "Journal of the College of Science" published by this University in forty-five volumes (1887-1925), and is issued in five sections:

Section I.—Mathematics, Astronomy, Physics, Chemistry
Section II.—Geology, Mineralogy, Geography, Geophysics
Section III.—Botany
Section IV.—Zoology
Section V.—Anthropology

All communications relating to this Journal should be addressed to the Dean of the Faculty of Science, University of Tokyo.

Nepheline Syenites and Associated Alkalic Rocks of the Fukushin-zan District, Korea

By

Akiho MIYASHIRO and Tami MIYASHIRO

Geological Institute, Faculty of Science, Tokyo University

CONTENTS

I. Introduction

A group of alkalic plutonic rocks, including nepheline-syenite, syenite, and granite, is exposed in the Fukushin-zan district* (Pock-chinsan district), Heikô-gun, Kôgen-do in central Korea (Fig. 1). The district measures 32 km from NW to SE, having Fukukei Station* (Pock-kae Station) of the Keigen Line in the center. Fukushin-zan is the name of a mountain, highest in this district (816 m high), and located at 127°10′E and 38°31′N. In this paper the writers intend to give detailed petrographical and mineralogical descriptions of the alkalic rocks, together with discussions on their origin.

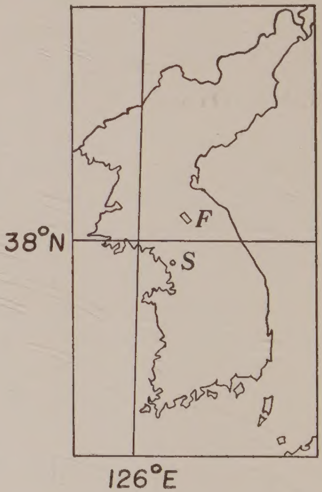

Fig. 1. Location of the Fukushin-zan district in Central Korea. F, Fukushin-zan district; S, Seoul.

This plutonic complex was studied from long ago by many Japanese geologists, among whom Hazime YOSHIZAWA (1932) and Yoshio KINOSAKI made most important contributions, though the results of the latter have not been published yet. (Prof. KINOSAKI kindly provided the writers with a part of his unpublished data.) Nobufusa

* These are names expressed in Japanese, the corresponding Korean ones being shown in the succeeding parentheses.

SAITO began a chemical study of this complex in 1942. He analysed nearly 80 rocks, which have been collected mainly by KINOSAKI. A. MIYASHIRO began the present study in 1943 in close relation with SAITO. In 1945 it became impossible owing to political affairs for him to revisit the district, but his laboratory work was continued for a few years more in collaboration with T. MIYASHIRO. Though many field problems remain unsolved, the writers are hoping that this paper will make some contribution to our knowledge of the alkalic rocks.

The writers wish to express their thanks to Emeritus Prof. Seitaro TSUBOI and Prof. Hisashi KUNO of the Tokyo University for their kind advice. Their hearty thanks are due to Prof. Nobufusa SAITO for his informations on the chemistry of the complex and also for his kind advice and arrangements for the field work of A. Miyashiro. Prof. Yoshio KINOSAKI kindly showed his unpublished data, including his geological map of the eastern part of the district. A. MIYASHIRO wishes to express his gratitude to Dr. Iwao TATEIWA, Prof. Toshiya MIYAZAWA, Mr. Takao YAMAGUCHI for their advice and help for his field work, and also to Mr. Shûzo BAN and Mr. Yoshimitsu OYAMA for various facilities during his trip to the district. Dr. Kenzo YAGI and Mr. Masao YAMASAKI kindly read the manuscript with friendly criticism.

II. General Statements

1. Geological History of the Fukushin-zan District

The oldest rocks in this district are more or less regionally metamorphosed sediments that are generally regarded as a member of the Shôgen System (Upper pre-Cambrian). In grade of metamorphism they are different in different part of the district. Thus, they are composed of staurolite-kyanite-bearing mica-schist, garnet-bearing mica schist, mica-schist, phyllite, slates, quartzite and limestone, with a small quantity of amphibolite*.

After the regional metamorphism, the alkalic masses now under consideration were emplaced partly along and partly across the

* The mode of occurrence of kyanite in druses in kyanite-quartz-veins cutting through schists of the Shôgen system at Saiho-ri was described in detail in another paper (MIYASHIRO, 1951b).

schistosity or bedding planes of the pre-existing rocks.

After an interval of time, calc-alkalic granitic masses intruded at various parts of the district, penetrating the alkalic masses at places (e. g. at Shôra-san). The geologic ages of these intrusions are not known yet.

After a long period of erosion, these plutonic masses were exposed to the surface, and further later, in Quaternary period parts of the district were covered by olivine-basalt lava owing to a volcanic activity in the adjacent area.

2. General Features and Divisions of the Alkalic Rocks

The alkalic rocks of the district were emplaced into the older sedimentary and meta-sedimentary rocks, generally with sharp contacts. At certain places materials from the alkalic masses caused fairly intense metasomatic replacement of the country rocks.

The most striking feature of this complex, easily recognized in the field, is the strong structural and textural contrast between the rocks of the eastern half of the district and those of the western half. The contrast is also accompanied by mineralogical and chemical differences between the two groups of rocks. This fact is shown synoptically in Table 1. Thus, the rocks of the complex may be divided into two rock groups: *group W* of the western half of the district and *group E* of the eastern half.

Table 1. Comparison of groups W and E

	Rocks of group W	Rocks of group E
Texture	(1) Unfoliated* or weakly gneissose. (2) Coarse-grained, or porphyritic with a small quantity of groundmass.	(1) Gneissose. (2) Porphyritic with a large quantity of groundmass.
Mineralogy	(1) Small microcline grains are absent or scanty. (2) Amphiboles of the hasingsite group are present.	(1) Small microcline grains are abundant. (2) Amphiboles of the riebeckite group are present.
Chemistry	(1) Richer in Al_2O_2, CaO, and K_2O. (2) Poorer in SiO_2, Fe_2O_3, and Na_2O.	(1) Poorer in Al_2O_3, CaO, and K_2O. (2) Richer in SiO_2, Fe_2O_3 and Na_2O.

* In this paper the term "unfoliated" indicates want of any preferred orientation.

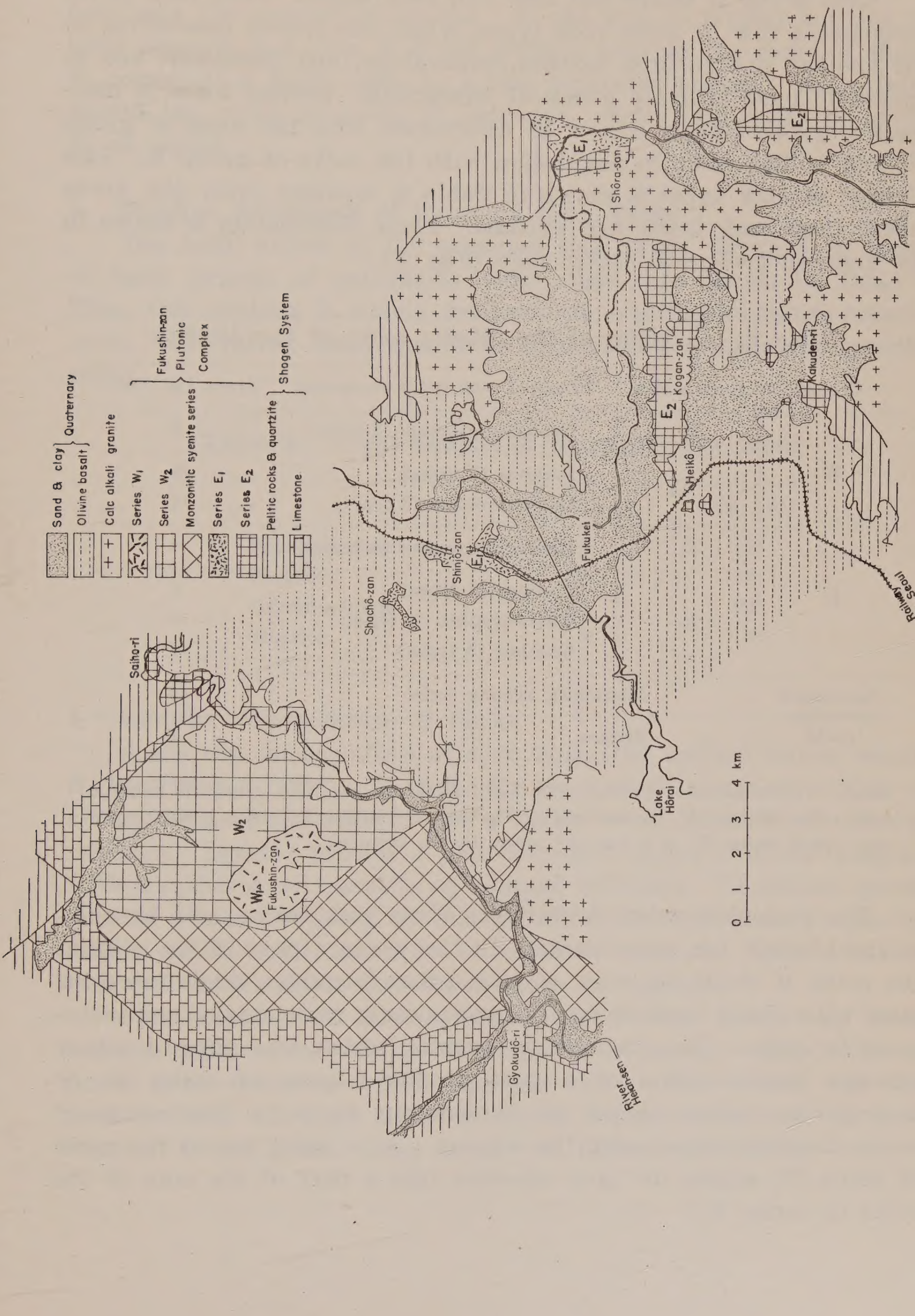

Fig. 2. Geologic sketch map of the Fukushin-zan district, Korea. Compiled by A. MIYASHIRO on the basis of the survey by H. YOSHIZAWA, Y. KINOSAKI and A. MIYASHIRO.

Each group is subdivided into two rock series. Each rock series comprises a few or more rock types, which are closely resembling to one another in structure, texture, mineralogy, and chemistry, and so appear to have intimate genetical connection. Besides these, a monzonitic syenite series occurs in association with the rocks of group W, and fenites occur in association with the rocks of group E. This division of rock types is shown in Table 2, together with the areas where these rock types are exposed. Their distribution is shown in the annexed geological sketch map (Fig. 2.)

Table 2. Divisions of the alkalic rocks of the district

Groups	Rock series	Principal rock types comprised	Areas (sq. km.)
W	W_1	Nepheline-syenites (3 types)	5
	W_2	Syenites (3 types)	22
		Quartz-syenites (3 types)	11
E	E_1	Nepheline-syenites (4 types)	4
	E_2	Syenites (5 types)	4
		Quarz-syenites (4 types)	4
		Granites (5 types)	4
Associated crystalline rocks	Monzonitic syenite series		44
	Fenites		1

Note: The monzonitic syenite series and fenites are in close genetical relation with series W_2 and E_2 respectively. (The monzonitic syenite series in this paper was called series W_3 in a few old papers by the writers.)

The geological relations between these rock series will be summarized below for convenience. In the western part of the district the rocks of series W_2 were emplaced first forming a single intrusive mass with sharp contacts to the pre-existing sedimentary and metamorphic rocks. The monzonitic syenite series was formed either through contamination of a part of the magma of series W_2 or through the metasomatism of pre-existing rocks by the action of emanations associated with the magma. At a later period the rocks of series W_1 appear to have intruded into a part of the area of the rocks of series W_2.

In the eastern part the rocks of series E_2 appear to have intruded first into the crystalline schists. As the area is largely covered by later deposits and lava, it is not certain whether the rocks of series E_2 constitute a single mass or a few separated masses. At a later period the rocks of series E_1 intruded, partly into rocks of series E_2 at places.

3. Relative Abundance of Principal Rock Types

The areal extent of the principal rock types, grouped in terms of their degree of saturation with silica, are shown in Table 3. Thus, this complex is mainly composed of syenitic and quartz syenitic rocks, with rather small quantities of nepheline-syenitic and granitic rocks.

Table 3. Areal extents of principal rock types

	Area (sq. km.)	Area (%)
Nepheline-syenites	9	17
Syenites	26	48
Quartz-syenites	15	28
Granites	4	7

4. Adopted Nomenclature of Rocks

As to the nomenclature of rock types, the writers follow mainly H. ROSENBUSCH (1910). Granite denotes a rock composed mainly of alkali feldspars and quartz, with a rather small quantity of coloured minerals. Syenite denotes a rock composed mainly of alkali feldspars with a rather small quantity of coloured minerals. Nepheline syenite denotes a rock composed mainly of alkali feldspars and nepheline with a rather small quantity of coloured minerals. Quartz syenite is a rock intermediate between granite and syenite.

Fenite denotes an igneous-looking alkalic rock formed by metasomatic replacement of pre-existing rocks through material transfusion from associated alkalic igneous rocks. This name was first used by W. C. BROGGER (1921) in a very narrow sense and was later widened to the prsent usage by H. von ECKERMANN (1948).

III. Petrography

1. Common Textural Features of Groups W and E

Practically all the rocks of groups W and E have certain textural features in common, which will be conveniently described in this section.

All the rocks under consideration consist of minerals of two contrasted sizes. In other words, larger crystals (usually 1–8 mm in size) are embedded in a fine-grained groundmass, each grain of which is 0.03–0.3 m in size. The larger crystals are of microcline-perthite and/or nepheline. Microcline-perthite is invariably present in all the rocks, while nepheline is confined to nepheline-syenites. The groundmass is composed of, besides some coloured minerals, feldspars, which are represented mainly by albite in the rocks of group W, but by microcline and albite in the rocks of group E. (In some nepheline syenites, nepheline occurs not only as larger crystels but also as a constituent of the groundmass.)

Though all these minerals form xenomorphic crystals, marginal parts of the larger cryatals frequently fill the interstices of the smaller grains of the groundmass, or include them poikilitically. Accordingly the larger cryatals must have crystallized after the groundmass minerals, at least in part. The writers call the larger crystals "*porphyritic minerals*." Special attention should be paid to the fact that the term in this case does not mean crystals which were formed earlier than those of the groundmass, as does in ordinary cases.

Coloured minerals tend to gather loosely to form open clusters together with a small quantity of colourless minerals. Such a textural feature is called "*glomeroplasmatic*". (See, for example, Figs. 1–2 in plate I.)

On the other hand, there are some differences in texture between rocks of group W and of group E as follows:

(1) Rocks of group W contain generally a larger quantity of porphyritic minerals than those of group E. In some rocks of group W the groundmass is so scanty that the rocks are composed almost exclusively of coarse-grained porphyritic minerals, while in some rocks of group E the porphyritic minerals occupy so small parts of

the rocks that the rocks look to the unaided eye as if they were composed only of very fine-grained groundmass.

(2) The average size of porphyritic minerals is larger in rocks of group W than in rocks of group E. For example, the porphyritic minerals are 3 to 8 mm in diameter in nepheline syenites of series W_1, whereas they are 1 to 3 mm in nepheline syenites of series E_1.

(3) Rocks of group W are generally unfoliated (lacking in preferred orientation), or at most weakly gneissose, while those of group E are generally strongly gneissose with parallel arrangement of stretched lenticles of glomeroplasmatic clusters of coloured minerals in the light-coloured matrix (Plate II, Fig. 6; Plate III, Figs. 1–2).

In some cases crystals of aegirine and/or amphibole are prismatic and those of biotite are platy. The direction of the dimensional elongation of those crystals in gneissose rocks are parallel to the direction of gneissosity. In other cases, however, those minerals are equidimensional in form, and show random orientation independent of the gneissosity, which the latter is produced by parallel arrangement of elongated clusters of those equidimensional grains. Though the grains of quartz generally show slightly undulose extinction, few other cataclastic structutres were observed.

In short, the rocks of group W have the appearance of ordinary plutonic rocks to the unaided eye, while those of group E have the appearance of gneissose metamorphic rocks.

2. Series W_1 (Nepheline-Syenites)

Distribution and Structural Relations

The rocks of this series are exposed on and around the summit of Fukushin-zan. They are supposed to have intrnded into rocks of series W_2, though the actual contact between them was not found.

General Features

The rocks are generally unfoliated, porphyritic, and allotriomorphic. The porphyritic minerals are microcline-perthite and nepheline, while groundmass minerals are mainly albite and biotite, usually together with some of the following: cancrinite, sodalite, hastingsite, aegirine, garnet, and minor ingredients (Figs. 1–4 in Plate I). The amount of nepheline is 5–15% in most cases. In some rocks garnet amounts to a fairly large quantity. Aegirine is nearly always rimmed by the garnet.

Principal Rock Types

According to the combinations of coloured silicate minerals present, the rocks of this series may be classified as follows:

(a) Biotite-nepheline-syenite

Main const.: microcline-perthite, albite, nepheline, biotite; usually cancinite; rarely sodalite.

Minor const.: apatite, allanite, carbonate, titanite, zircon, opaque mineral.

(b) Hastingsite-biotite-nepheline-syenite

Main const.: Microcline-perthite, albite, nepheline, biotite, hastingsite; usually canarinite, garnet.

Minor const.: sodalite, apatite, allanite, titanite, zircon, opaque mineral.

(c) Aegirine-hastingsite-biotite-nepheline-syenite

Main const.: microcline-perthite, albite, nepheline, biotite, hastingsite, aegirine; usually garnet.

Minor const.: sodalite, cancrinite, apatite, carbonate, titanite, zircon, opaque mineral.

Relations between the Principal Rock Types

Biotite-nepheline-syenite, is exposed in the south-eastern part of the summit, hastingsite-biotite-nepheline-syenite in the central part, and aegirine-hastingsite-biotite-nepheline-syenite in the north-western part. Perhaps they grade into each other.

Chemical Characters

SAITO analysed 13 rock samples from this series. The average chemical composition of each principal rock type, calculated therefrom, are shown in Table 4. The average mineral composition was calculated from the average of all the types, using chemical analyses of the constituent minerals as far as possible. The result is shown in Table 5. The procedure of the calculation is outlined below:

The amounts of apatite, zircon, sodalite, and cancrinite were first determined from the contents of P_2O_5, ZrO_2, Cl, and CO_2 of the rocks respectively. Then, the amounts of coloured minerals: biotite, hastingsite, aegirine, and magnetite were determined by alloting the total amount of $Fe_2O_3+FeO+MgO$ to them in ratios which were estimated from observations under the microscope. The remaining part of TiO_2 was used up to make titanite. The amount of garnet was also estimated from observations under the microscope. The remaining parts of K_2O, Na_2O, CaO, and SiO_2 were used up to make the molecules of orthoclase, albite, and anorthite, and also nepheline, by allotting appropriate amounts of Al_2O_3.

The main sources of error in this procedure probably lie in the estimation of ratios of coloured minerals and of garnet. Some error in the estimation of coloured minerals would cause an error in the amount of K_2O and Na_2O to be allotted to them, and then to the

Table 4. Average compositions of nepheline-syenites of series W_1

	A	B	C	D
SiO_2	55.94	56.03	57.36	56.44
Al_2O_3	23.11	21.43	20.85	21.80
Fe_2O_3	1.81	2.83	2.02	2.22
FeO	1.96	2.16	2.92	2.35
MgO	0.36	0.25	0.42	0.34
CaO	1.23	1.88	1.70	1.60
Na_2O	7.92	7.19	7.81	7.64
K_2O	5.17	5.55	4.87	5.20
H_2O-	0.14	0.21	0.13	0.16
H_2O+	0.83	0.84	0.82	0.83
TiO_2	0.34	0.65	0.42	0.47
ZrO_2	0.30	0.23	0.24	0.26
CO_2	0.43	0.15	0.07	0.22
P_2O_5	0.30	0.33	0.20	0.28
S	0.04	0.04	0.04	0.04
F	0.02	0.06	0.03	0.04
Cl*	(0.28)	(0.09)	(0.08)	(0.15)
MnO	0.21	0.15	0.28	0.21
BaO	0.07	0.09	0.17	0.11
Rare earths	0.10	0.09	0.14	0.11

* Not accurate.

A: Biotite-nepheline-syenite (average of 4 analyses).

B: Hastingsite-biotite-nepheline-syenite (average of 3 analyses).

C: Aegirine-hasingsite-biotite-nepheline-syenite (averege of 5 analyses).

D: Average of A, B, and C.

orthoclase and albite molecules and nepheline. As the total amounts of K_2O and Na_2O, allotted to the coloured minerals are, however, very small, this error would be slight. Error in the estimation of garnet would cause error in the calculated amount of the anorthite molecule, but the effect of this error would be also negligible, because the total amounts of garnet and anorthite are very small.

Subordinate Rodk Types

(i) Dark-coloured rocks

Some rocks of series W_1 are darker to the unaided eye than the ordinary rock types, though they are similar to each other in mineral composition. The difference in colour

Table 5. Mineral composition of average nepheline-syenite of series W_1

Oxides	wt. %	Apatite	Zircon	Biotite	Hastings.	Aegirine	Magnetite	Titanite	Sodalite	Cancrinite	Garnet	An	Or	Ab	Nepheline	Residue
SiO_2	56.44		0.1	1.7	0.7	0.6		0.2	0.5	1.2	0.4	0.5	16.1	30.7	3.6	
Al_2O_3	21.80			0.9	0.2				0.4	1.0	0.2	0.4	4.6	8.7	3.1	+2.3
Fe_2O_3	2.22			0.7	0.1	0.2	1.2									
FeO	2.35			1.2	0.4	0.1	0.6									
MgO	0.34			0.3												
CaO	1.60	0.3			0.2	0.1		0.2		0.3	0.3	0.2				
Na_2O	7.64					0.1			0.3	0.6				5.3	1.5	
K_2O	5.20			0.5									4.2		0.5	
H_2O-	0.16															+0.16
H_2O+	0.83			0.2						0.1						+0.5
TiO_2	0.47			0.1				0.3								+0.1
ZrO_2	0.26		0.3													
CO_2	0.22									0.2						
P_2O_5	0.28	0.3														
S	0.04															+0.04
F	0.04															+0.04
Cl	(0.15)								0.1							
MnO	0.21			0.1												+0.1
BaO	0.11															+0.11
Rare earths	0.11															+0.11
		0.6	0.4	5.7	1.6	1.1	1.8	0.7	1.3	3.4	0.9	1.1	24.9	44.7	8.7	

Bulk molecular composition of modal feldspars: $Or_{34\cdot 0}$ $Ab_{64\cdot 6}$ $An_{1\cdot 4}$

appears to be due mainly to defference in texture. The dark-coloured rocks are finer in grain size and more uniform in the distribution of coloured minerals.

(ii) Vesuvianite-garnet-aegirine-hastingsite-biotite-nepheline-syenite

This rock type was found from a few localities on the northern slope of Fukushin-zan.

Main const.: microcline-perthite, albite, nepheline, biotite, hastingsite, aegirine, garnet, vesuvianite.

Minor const.: cancrinite, allanite, titanite.

3. Series W_2 (Syenites and Quartz-syenites)

Distribution and Structural Relations

The rocks of this series are exposed on the lower flank of Fukushin-zan and also its northern and eastern foot. Various rock types are distributed irregularly within the area. They appear to form a single intrusive mass. The central part of the area of series W_2 is occupied by the rocks of series W_1, which probably intruded later.

General Features

The rocks of this series are generally unfoliated (rarely weakly gneissose), porphyritic, allotriomorphic, and are composed mainly of porphyritic microcline-perthite, embedded in the groundmass consisting mainly of albite and coloured minerals, such as biotite and hastingsite. Microcline occurs not infrequently in the groundmass, and quartz occurs only in the groundmass of quartz-syenite. Muscovite amounts sometimes to a large quantity and may have been formed by deuteric reactions. In some rocks hastingsite occurs in large crystals, comparable with porphyritic crystals of microcline-perthite in size. Aegirine is extremely rare.

Principal Rock Types

(a) Biotite-syenite

Main const.: Microcline-perthite, albite, biotite; frequently microcline, muscovite.

Minor const.: allanite, apatite, titanite, zircon, opaque mineral; sometimes carbonate.

(b) Hastingsite-syenite

Main const.: microcline-perthite, microcline, albite, hastingsite.

Minor const.: apatite, titanite, zircon, opaque mineral.

(c) Hastingsite-biotite-syenite

Main const.: microcline-perthite, albite, hastingsite, biotite; sometimes muscovite.

Minor const.: apatite, garnet, titanite, zircon, opaque mineral; sometimes epidote, carbonate.

(d) Biotite-quartz-syenite

Main const.: microcline-perthite, albite, quartz, biotite; sometimes muscovite.

Minor const.: allanite, apatite, zircon, opaque mineral; sometimes garnet, carbonate.

(e) Hastingsite-biotite-quartz-syenite

Main const.: microcline-perthite, albite, quartz, biotite, hastingsite; sometimes microcline.

Minor const.: apatite, carbonate, titanite, zircon, opaque mineral.

(f) Aegirine-hastingsite-biotite-quartz-syenite

Main const.: microcline-perthite, albite, quartz, aegirine, hastingsite, biotite.

Minor const.: apatite, carbonate, titanite, opaque mineral.

Note:—Biotite-syenite and hastingsite-biotite-syenite probably predominate among these principal rock types.

Chemical Characters

SAITO analyzed 11 rock samples from this series. The average chemical compostions of the principal rock types, calculated therefrom, are shown in Table 6. The results of calculation of average

Table 6. Average compositions of rocks of series W_2

	A	B	C	D	E	F
SiO_2	58.56	59.65	59.11	58.71	60.28	59.50
Al_2O_3	22.23	21.03	21.63	21.88	17.54	19.71
Fe_2O_3	2.47	1.46	1.97	2.58	3.04	2.81
FeO	1.84	2.28	2.06	2.79	3.18	2.99
MgO	0.43	0.22	0.33	0.26	0.80	0.53
CaO	0.58	1.64	1.11	1.33	2.60	1.97
Na_2O	6.19	6.07	6.13	4.66	5.60	5.13
K_2O	5.11	5.51	5.31	5.12	4.96	5.04
H_2O-	0.22	0.38	0.30	0.08	0.12	0.10
H_2O+	1.32	0.49	0.91	1.16	0.21	0.69
TiO_2	0.41	0.36	0.39	0.51	0.94	0.73
ZrO_2	0.20	0.16	0.18		0.26	
CO_2	0.05	0.05	0.05		0.46	
P_2O_5	0.18	0.28	0.23	0.23	0.63	0.43
S	0.04	0.02	0.03		0.12	
F	0.16	0.02	0.09		0.09	
MnO	0.25	0.51	0.38	0.27	0.14	0.21
BaO	0.05	0.24	0.14		0.06	
Rare earths	0.10	0.07	0.09		0.03	

A: Biotite-syenite (average of 5 analyses).
B: Hastingsite-biotite-syenite (1 analysis).
C: Average of A and B.
D: Biotite-quartz-syenite (1 analysis).
E: Aegirine-hastingsite-biotite-quartz-syenite (1 analysis).
F: Average of D and E.

Table 7. Mineral composition of average syenite of series W_2

Oxides	wt. %	Apatite	Zircon	Biotite	Hastings.	Magnetite	Titanite	An	Or	Muscovite	Ab	Quartz	Residue
SiO_2	59.11		0.1	1.7	0.7		0.2	1.1	15.3	3.1	35.5	1.4	
Al_2O_3	21.63			0.9	0.2			0.9	4.3	2.6	10.0		+2.7
Fe_2O_3	1.97			0.7	0.2	1.1							
FeO	2.06			1.2	0.4	0.5							
MgO	0.33			0.3									
CaO	1.11	0.2			0.2		0.2	0.5					
Na_2O	6.13										6.1		
K_2O	5.31			0.5					4.0	0.8			
H_2O-	0.30												+0.3
H_2O+	0.91			0.2						0.3			+0.4
TiO_2	0.39			0.1			0.3						
ZrO_2	0.18		0.2										
CO_2	0.05												+0.05
P_2O_5	0.23	0.2											
S	0.03												+0.03
F	0.09												+0.09
MnO	0.38			0.1									+0.3
BaO	0.14												+0.14
Rare earths	0.09												+0.09
		0.4	0.3	5.7	1.7	1.6	0.7	2.5	23.6	6.8	51.6	1.4	

Bulk molecular compysition of modal feldspars: $Or_{29\cdot2}$ $Ab_{67\cdot7}$ $An_{3\cdot1}$

Table 8. Mineral composition of average quartz-syenite of series W_2

Oxides	wt. %	Apatite	Zircon	Biotite	Hastings.	Aegirine	Magnetite	Titanite	Calcite	An	Or	Muscovite	Ab	Quartz	Residue
SiO_2	59.50		0.1	2.6	0.5	1.2		0.4		0.9	14.2	2.1	28.4	9.1	
Al_2O_3	19.71			1.3	0.2					0.7	4.0	1.8	8.1		+3.6
Fe_2O_3	2.81			0.9	0.1	0.3	1.5								
FeO	2.99			1.8	0.3	0.2	0.7								
MgO	0.53			0.4		0.1									
CaO	1.97	0.5			0.1	0.3		0.4	0.3	0.4					
Na_2O	5.13				0.1	0.1							4.9		
K_2O	5.04			0.8							3.7	0.5			
H_2O-	0.10														+0.10
H_2O+	0.69			0.3								0.2			+0.2
TiO_2	0.73			0.1				0.6							
ZrO_2	(0.26)		0.3												
CO_2	(0.46)								0.2						
P_2O_5	0.43	0.4													
S	(0.12)														(+0.12)
F	(0.09)														(+0.09)
MnO	0.21			0.2											
BaO	(0.06)														(+0.06)
Rare earths	(0.03)														(+0.03)
		0.9	0.4	8.4	1.3	2.2	2.2	1.4	0.5	2.0	21.9	4.6	41.4	9.1	

Bulk molecular composition of modal feldspars: $Or_{32\cdot3}$ $Ab_{64\cdot8}$ $An_{2\cdot9}$

mineral compositions from the averages of syenites and quartz-syenites are shown in Tables 7 and 8 respectively.

Subordinate Rock Types

(i) Epidote-biotite-syenite

Main const.: microcline-perthite, biotite, epidote; sometimes albite, muscovite.

Minor const.: apatite, carbonate, titanite, opaque mineral.

This rock type was found at several separated localities, and probably represents remnants of digested basic inclusions. (Basic inclusions are rather common in rocks of series W_2.) Crystals of epidote are more or less idiomorphic. Analyses of two rocks are shown in Table 9. Refer also to Fig. 6 in Plate I.

This rock type suggests that the temperature of crystallization of the rock was too low for intermediate and basic plagioclase to form, even though the chemical composition of the rock was favourable for the formation of such plagioclases, as will be discussed later.

Table 9. Compositions of epidote-biotite-syenites

	A	B
SiO_2	59.36	55.91
Al_2O_3	20.43	21.71
Fe_2O_3	0.93	1.97
FeO	3.13	3.90
MgO	0.64	1.00
CaO	0.82	3.29
Na_2O	5.89	4.67
K_2O	5.21	5.00
H_2O-	0.24	0.11
H_2O+	1.20	1.14
TiO_2	0.328	0.732
ZrO_2	0.136	
CO_2	0.000	
P_2O_5	0.138	0.483
S	0.017	
F	0.03	
MnO	0.226	0.263
BaO	0.111	
Rare earths	0.186	
	99.076	100.178

A: Epidote-muscovite-biotite-syenite from the southern slope of Fukushin-zan (Specimen No. 11427)

B: Epidote-biotite-syenite from the southern slope of Fukushin-zan. (Specimen No. 11426)

Rocks with such chemical composition do not occur in the other series.

(ii) Biotite-magnetite-syenite

Main const.: microcline-perthite, microcline, albite, biotite, magnetite.

This rock type was found only at one locality.

4. Monzonitic Syenite Series (Monzonitic Syenite, Quartz-Monzonitic Syenite, and Granite) and its Origin

Distribution and Structural Relation

The rocks of this series occur widely at the southern foot of Fukushin-zan, and extends to the south. The actual contact or the relation between the rocks of this series and those of W_2 was not found. This series may represents either a contaminated facies of series W_2, or a certain group of pre-existing rocks which were metasomatized by alkali transfusion perhaps from the magma of series W_2. This mass is concordant with the thick limestone bed on the west. The distribution of the different rock types within the mass is irregular.

General Features

The most distinctive feature of the rocks of this series is the presence of rather idiomorphic crystals of turbid plagioclase (Figs. 1–2 in Plate II). The rocks of the other series contain neither idiomorphic crystals of any kind of mineral nor any crystals of plagioclase except clear albite.

The rocks are unfoliated, granular (non-porphyritic), and hypidiomorphic, and are composed mainly of plagioclase, microcline-perthite, quartz, and coloured minerals such as amphiboles and biotite in various proportions. Plagioclase represents an earlier generation than microcline-perthite and quartz. Crystals of the amphiboles show remarkable sieve-structure (Figs. 3–4 in Plate II).

Principal Rock Types

(a) Hornblende-biotite-monzonitic syenite

Main const.: plagioclase, microcline-perthite, hornblende, biotite.

Minor const.: apatite, epidote, titanite, zircon, opaque mineral.

(b) Hornblende-biotite-puartz-monzonitic syenite

Main const.: plagioclase, microcline-perthite, quartz, hornblende, biotite; sometimes albite, microcline.

Minor const.: apatite, epdote, titanite, zircon, opaque mineral; frequently garnet; sometimes carbonate, fluorite, tourmaline.

(c) Hastingsite-biotite-granite

Main const.: plagioclase, microcline-perthite, quartz, hastingsite, biotite.

Minor const.: titanite, zircon, opaque mineral; sometimes tourmaline.

(d) Leucocratic granite

Main const.: microcline-perthite, quartz.

Minor const.: carbonate, chlorite (secondary?), fluorite, titanite, opaque mineral, zircon.

Chemical Characters

SAITO analyzed 13 rock samples from this series. The average chemical compositions of the principal rock types, calculated therefrom, are shown in Table 10. The mineral compositions, calculated therefrom, are shown in Tables 11–13.

Subordinate Rock Types

(i) Hypersthene-augite-bearing or augite-bearing hornblende-biotite-quartz-monzonite

Main const.: plagioclase, hornblende, biotite, and either hypersthene and augite, or augite alone.

Table 10. Average compositions of rocks of the monzonitic syenite series

	A	B	C
SiO_2	58.12	61.12	70.62
Al_2O_3	18.64	17.51	14.35
Fe_2O_3	3.49	2.28	2.34
FeO	3.58	3.65	1.80
MgO	1.34	0.60	0.69
CaO	2.89	2.52	0.48
Na_2O	5.08	4.99	3.28
K_2O	4.60	4.66	4.46
H_2O-	0.54	0.17	0.20
H_2O+	0.68	1.20	0.86
TiO_2	0.68	0.73	0.22
ZrO_2	0.13	0.19	0.14
CO_2	0.05	0.13	0.04
P_2O_5	0.29	0.25	0.09
S	0.03	0.07	0.02
F	0.04	0.10	0.04
MnO	0.23	0.16	0.31
BaO	0.05	0.13	0.11
Rare earths	0.10	0.05	0.11

A: Hornblende-biotite-monzonitic syenite (1 analysis).

B: Hornblende-biotite-quartz-monzonitic syenite (average of 10 analyses).

C: Hastingsite-biotite-granite (average of 2 analyses).

Table 11. Mineral composition of hornblende-biotite-monzonitic syenite

Oxides	wt. %	Apatite	Zircon	Biotite	Hornblende	Magnetite	Titanite	Epidote	An	Or	Sericite	Ab	Quartz	Residue
SiO_2	58.12		0.1	2.9	2.0		0.4	0.6	2.6	16.9	0.4	28.5	3.7	
Al_2O_3	18.64			1.3	0.6			0.5	2.1	4.7	0.4	8.1		+0.9
Fe_2O_3	3.49			1.2	0.4	1.8		0.1						
FeO	3.58			1.5	1.3	0.8								
MgO	1.34			1.0	0.3									
CaO	2.89	0.3			0.6		0.4	0.4	1.2					
Na_2O	5.08			0.2								4.9		
K_2O	4.60			0.7	0.1					4.4	0.1			
H_2O-	0.54													+0.54
H_2O+	0.68			0.5	0.1									+0.1
TiO_2	0.68			0.1			0.5							+0.1
ZrO_2	0.13		0.1											
CO_2	0.05													+0.05
P_2O_5	0.29	0.3												
S	0.03													+0.03
F	0.04													+0.04
MnO	0.23			0.2										
BaO	0.05													+0.05
Rere earths	0.10													+0.10
		0.6	0.2	9.6	5.4	2.6	1.3	1.6	5.9	26.0	0.9	41.5	3.7	

Bulk molecular composition of modal feldspars: $Or_{34.3}$ $Ab_{58.0}$ $An_{7.7}$

Table 12. Mineral composition of average hornblende-biotite-quartz-monzonitic syenite

Oxides	wt. %	Apatite	Zircon	Biotite	Hornblende	Magnetite	Garnet	Calcite	Titanite	Epidote	An	Or	Ab	Quartz	Residue
SiO_2	61.12		0.1	2.2	3.1		0.2		0.4	0.4	1.3	15.6	29.1	8.7	
Al_2O_3	17.51			1.1	0.9		0.1			0.3	1.1	4.4	8.2		+1.4
Fe_2O_3	2.28			0.9	0.5	0.9									
FeO	3.65			1.3	1.8	0.4	0.2								
MgO	0.60			0.4	0.2										
CaO	2.52	0.3			0.9			0.1	0.4	0.2	0.6				
Na_2O	4.99												5.0		
K_2O	4.66			0.5	0.1							4.1			
H_2O-	0.17														+0.17
H_2O+	1.20			0.4	0.1										+0.7
TiO_2	0.73			0.1					0.6						
ZrO_2	0.19		0.2												
CO_2	0.13							0.1							
P_2O_5	0.25	0.3													
S	0.07														+0.07
F	0.10														+0.10
MnO	0.16			0.2											
BaO	0.13														+0.13
Rare earths	0.05														+0.05
		0.6	0.3	7.1	7.6	1.3	0.5	0.2	1.4	0.9	3.0	24.1	42.3	8.7	

Bulk molecular composition of modal feldspars: $Or_{33.5}$ $Ab_{62.3}$ $An_{4.2}$

Table 13. Mineral composition of average hastingsite-biotite-granite

Oxides	wt. %	Apatite	Zircon	Biotite	Hastings.	Magnetite	Titanite	Or	Ab	Quartz	Residue
SiO_2	70.62		0.1	1.5	1.8		0.1	15.3	19.2	32.6	
Al_2O_3	14.35			0.7	0.5			4.3	5.4		+3.5
Fe_2O_3	2.34			0.9	0.3	1.1					
FeO	1.80			0.5	0.8	0.5					
MgO	0.69			0.4	0.2						+0.1
CaO	0.48	0.1			0.3		0.1				
Na_2O	3.28								3.3		
K_2O	4.46			0.4	0.1			4.0			
H_2O-	0.20										+0.20
H_2O+	0.86			0.3	0.1						+0.5
TiO_2	0.22						0.2				
ZrO_2	0.14		0.1								
CO_2	0.04										+0.04
P_2O_5	0.09	0.1									
S	0.02										+0.02
F	0.04										+0.04
MnO	0.31			0.2							+0.1
BaO	0.11										+0.11
Rare earths	0.11										+0.11
		0.2	0.2	4.9	4.1	1.6	0.4	23.6	27.9	32.6	

Bulk molecular composition of modal feldspars: $Or_{44.3}$ $Ab_{55.7}$

Minor const.: microcline-perthite, quartz, magnetite apatite.
These rock types were found at Fukuman-ri, at the western foot of Fukushin-zan. The pyroxenes are unstable, being rimmed by hornblende.

Origin of this Rock Series.

The principal rock types of the series (monzonitic syenite, quartz-monzonitic syenite, and granite) are considered to represent various stages in progressive mineralogical variations, though it is not certain whether the variation is the results of the progressive digestion of foreign more basic rocks by some alkali magma such as of series W_2,

or the results of progressive metasomatism of some pre-existing more basic rocks by alkalic emanations. The pyroxenes in the subordinate rock types probably represent relics from the more basic rocks.

Monzonitic syenite is composed mainly of plagioclase, microcline-perthite, hornblende, and biotite with subordinate amounts of quartz, etc. Plagioclase is in more or less idiomorphic crystals and appears to be an unstable relic from the basic rocks, for it is partly albitized from its border, producing clinozoisite or epidote as the by-product. The un-albitized core of the plagioclase is cloudy, owing to numerous minute inclusions of alteration product which has not been identified. The core is usually oligoclase in composition, but was probably more basic originally. Quartz and microcline-perthite are replacing plagioclase either from its margin or as irregular patches within the plagioclase.

As the albitization and replacement proceed, the quantity of quartz increases, until the rock becomes quartz-monzonitic syenite, and finally granite. (In monzonitic syenite, un-albitized cores of plagioclase comprise about 20–30% of the rock and quartz only a few %, while in granite the un-albitized cores comprise generally only a few %, and quartz about 35%.) The ratio of microcline-perthite to plagioclase also increases through this process.

As the process goes on, the coloured minerals also show a progressive variation in their compositions. Amphiboles in monzonitic syenite and quartz-monzonitic syenite is brownish green-blue variety of common hornblende with large optical angles. It often shows marginal change to a clear green blue variety with slightly smaller optical angles. As the host rock becomes more quartzose, the amphibole becomes hastingsitic in composition with smaller optical angles (Fig. 8).

5. Series E_1 (Nepheline-syenites)

Distribution and Structural Relations

The rocks of this series are exposed at Shinjô-zan (Shinsong-san) and Shachô-zan (Sachong-san) near Fukukei Station and also at Shôra-san to the east. In the western part of Kogan-zan (Hoam-san), rocks of this series form a few parallel dykes, cutting through E_2 rocks along the plane of gneissosity.

General Features

The rocks of this series are generally gneissose, porphyritic, and allotriomorphic. Porphyritic minerals are microcline-perthite and nepheline, while the groundmass is composed mainly of microcline and albite, usually with some of the following: sodalite, cancrinite, biotite, riebeckite, and aegirine (Figs. 5–6 in Plate II). Nepheline occurs not infrequently in the groundmass, too. The total amount of nepheline ranges from 5 to 15% of the rock in most cases. Biotite occurs most commonly among the coloured minerals.

Principal Rock Types

(a) Biotite-nepheline-syenite

Main const.: microcline-perthite, microcline, albite, npheline, biotite, cancrinite.

Minor const.: sodalite, allanite, apatite, zircon, opaque mineral; sometimes garnet, titanite.

(b) Riebeckite-biotite-nepheline syenite

Main const.: microcline-perthite, microcline, albite, nepheline, riebeckite, biotite.

Minor const.: sodalite, apatite, fluorite, garnet, titanite, opaque mineral,

(c) Aegirine-biotite-nepheline-syenite

Main const.: microcline-perthite, microcline, albite, nepheline; usually cancrinite, aegirine, biotite; rarely sodalite.

Minor const.: apatite, titanite, opaque mineral; frequently allanite, fluorite, garnet, zircon.

(d) Aegirine-riebeckite-biotite-nepheline-syenite

Main const.: microcline-perthite, microcline, albite, nepheline, aegirine, biotite; sometimes cancrinite, riebeckite.

Minor const.: allanite, apatite, garnet, titanite; frequently sodalite, zircon, opaque mineral.

(e) Dark-coloured rocks

Some rocks at Shinjô-zan and Shachô-zan look much darker to the unaided eye than the ordinary nepheline-spenites. The former is dark grey, while the latter is usually light grey with black glomeroplasmatic clusters. It is interesting that the dark-coloured rocks are not so different in mineral and chemical compositions from the associated ordinary nepheline-syenites; namely, they are either aegirine-biotite nepheline-syenite or aegirine-riebeckite-biotite nepheline-syenite in most cases. The main difference between the dark-coloured and ordinary rocks lies in their textures. Thus, in dark-coloured rocks the coloured minerals are in finer grains, and are dispersed fairly evenly nhroughout the rocks, while in the ordinary rocks they form glomeroplasmatic clusters.

Chemical Characters

SAITO analyzed 21 rock samples from this series. The average chemical composition of each principal rock type, calculated therefrom, are shown in Table 14. The result of calculation of the average mineral composition from the average of all types is shown in Table 15.

Table 14. Average compositions of nepheline-syenites of series E_1

	A	B	C	D	E
SiO_2	58.55	58.44	58.28	58.90	58.54
Al_2O_3	20.70	21.70	20.40	20.47	20.82
Fe_2O_3	2.44	2.61	2.66	2.29	2.50
FeO	2.03	1.62	2.06	1.84	1.89
MgO	0.52	0.79	0.54	0.65	0.63
CaO	0.62	1.35	0.66	0.73	0.84
Na_2O	8.21	9.35	8.31	8.09	8.49
K_2O	4.80	3.78	4.53	4.62	4.43
H_2O-	0.26	0.29	0.32	0.31	0.30
H_2O+	1.17	0.26	1.16	0.65	0.81
TiO_2	0.22	0.30	0.43	0.38	0.33
ZrO_2	0.18		0.12	0.25	
CO_2	0.08		0.11	0.08	
P_2O_5	0.19	0.15	0.22	0.29	0.21
S	0.03		0.03	0.02	
F	0.04		0.09	0.09	
Cl*	(0.12)		(0.17)	(0.13)	
MnO	0.21	0.25	0.24	0.23	0.23
BaO	0.07		0.06	0.09	
Rare earths	0.08		0.11	0.02	

* Not accurate.

A: Biotite-nepheline-syenite (average of 6 anaıyses).
B: Riebeckite-biotite-nepheline-syenite (1 analyses).
C: Aegirine-biotite-nepheline-syenite (average of 8 analyses).
D: Begirine-riebeckite-biotite-nepheline-syenite (average of 5 analyses).
E: Average of A, B, C, and D.

Subordinate Rock Types

(i) Vesuvianite-bearing garnet-biotite-nepheline-syenite

A band of vesuvianite-bearing garnet-biotite-nepheline-syenite, about 1 m thick, occurs at Shachô-zan. It looks reddish brown to the unaided eye, owing to its large content of garnet. The garnet is a member of the grossularite-andradite series.

Main const.: microcline, albite,nepheline, cancrinite, biotite, garnet.

Minor const.: vesuvianite, sodalite, apatite opaque mineral.

Biotite and garnet show somewhat antipathetic relation to each other. The rock is chemically characterized by a very high content of CaO and rather high content of K_2O in comparison with the ordinary nepheline-syenites, as is shown in Table 16.

(ii) Garnet-nepheline-syenite

The rock is similar to the above, except the absence of vesuvianite. It was found at several localities at Shinjô-zan and Shachô-zan. It occurs usually as pockets and veins in the oreinary nepheline-syenite.

Table 15. Mineral composition of average nepheline-syenite of series E_1

Oxides	wt. %	Apatite	Zircon	Biotite	Riebeckite	Aegirine	Magnetite	Titanite	Sodalite	Cancrinite	Garnet	An	Or	Ab	Nepheline	Residue
SiO_2	58.54		0.1	1.6	0.8	1.5		1.1	0.6	0.6	0.1	0.4	13.7	34.5	3.5	
Al_2O_3	20.82			0.6					0.5	0.5	0.1	0.4	3.7	9.5	3.0	+2.5
Fe_2O_3	2.50			0.5	0.2	0.6	1.2									
FeO	1.89			1.1	0.2		0.6									
MgO	0.63			0.4	0.1	0.1										
CaO	0.84	0.2				0.2		0.1		0.1	0.1	0.2				−0.1
Na_2O	8.49				0.1	0.3			0.3	0.3				5.8	1.7	
K_2O	4.43			0.5									3.4		0.5	
H_2O-	0.30															+0.30
H_2O+	0.81			0.2												+0.6
TiO_2	0.33			0.1				0.2								
ZrO_2	(0.18)		0.2													
CO_2	(0.09)									0.1						
P_2O_5	0.21	0.2														
S	(0.03)															(+0.03)
F	(0.07)															(+0.07)
Cl	(0.14)								0.1							
MnO	0.23			0.1												+0.1
BaO	(0.07)															(+0.07)
Rare earths	(0.07)															(+0.07)
		0.4	0.3	5.1	1.4	2.7	1.8	1.4	1.5	1.6	0.3	1.0	20.8	49.8	8.7	

Bulk molecular composition of modal feldspars: $Or_{27.9}\ Ab_{70.8}An_{1.3}$

Table 16. Composition of vesuvianite-bearing garnet-biotite-nepheline-syenite from Shachô-zan

SiO_2	54.71
Al_2O_3	22.44
Fe_2O_3	2.23
FeO	1.37
MgO	0.41
CaO	7.45
Na_2O	3.34
K_2O	6.44
H_2O-	0.02
H_2O+	0.51
TiO_2	0.05
P_2O_5	0.31
MnO	0.13
Total	99.41

Note. Specimen No. AM 440628-8. Anal. by T. MIYASHIRO.

Relation between Various Rock Types

All the rock types of series E_1 occur in parallel bands, which are also parallel to the gneissosity of the racks (Fig. 3). At places the banded structure is disturbed by the occurrence of dark-coloured rocks which form contorted irregular masses. At a quarry of Shinjô-zan was found a large concentric structure of dark-and light-coloured rocks.

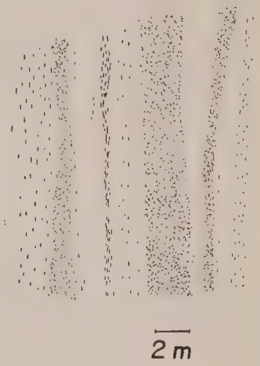

Fig. 3. Banded structure of nepheline-syenite at Shinjô-zan. The light and dark colours are mainly due to a difference in texture. The different bands are similar in mineral and chemical compositions.

6. Series E_2 (Syenites, Quartz-Syenites and Granites)

Distribution and Structural Relations

The rocks of this series are exposed sporadically at the follow ing places: Kogan-zan (Hoam-san), a hill around Kutsugan, a hill

at Kakuden-ri, and the river side of Heian-sen at Saiho-ri (Sepori). The igneous masses at these places may be continuous under the cover of olivine-basalt lava and alluvial deposits. The mass at Saiho-ri is in discordant contact with the mica-schists. The mass at Kakuden-ri metasomatically replaces mica-schists at its contact to form fenites.

General Features

The rocks are porphyritic with strong lineation (Figs. 1–2 in Plate III). They look, however, as if they were fine-grained granular to the unaided eye, because the porphyritic crystals are inconspicuous. The porphyritic crystals are of microcline-perthite, while the groundmass is composed mainly of microcline, albite, and some of the following: quartz, aegirine, riebeckite and biotite.

The different rock types of series E_2 form alternate bands of diverse mineral compositions.

Principal Rock Types

(a) Biotite-syenite
Main nonst: microcline-perthite, albite, biotite.

(b) Riebeckite-syenite
Main const.: microcline, albite, riebeckite; sometimes microcline-perthite.
Minor const.: apatite, fluorite, zircon, opaque mineral.

(c) Riebeckite-biotite-syenite
Main const.: microcline-perthite, microcline, albite, biotite, riebeckite.
Minor const.: apatite, titanite, opaque mineral.

(d) Aegirine-biotite-syenite
Main const.: microcline-perthite, micrgcline, albite, aegirine, biotite.
Minor const.: apatite, fluorite, zircon, opaque mineral.

(e) Aegirine-riebeckite-syenite
Main const.: microcline-perthite, microcline, albite, aegirine, riebeckite.
Minor const.: apatite, fluorite, zircon, opaque mineral.

(f) Biotite-quartz-syenite
Main const.: microcline-perthite, albite, biotite.
Minor const.: quartz, riebeckite, apatite, titanite, opaque mineral.

(g) Riebeckite-quartz-syenite
Main const.: microcline-perthite, microcline, albite, riebeckite.
Minor const.: apatite, titanite, zircon, opaque mineral.

(h) Riebeckite-biotite-quartz-syenite
Main const.: microcline-perthite, albite, quartz, biotite, riebeckite.
Minor const.: zircon, opapue mineral.

(i) Aegirite-riebeckite-quartz-syenite
Main const.: microcline-perthite, microcline, albite, quartz, riebeckite, aegirine.
Minor const.: apatite, titanite, zircon, opapue mineral: rarely fluorite.

(j) Biotite-granite

Main const.: microcline, albite, quartz, biotite.

Minor const.: apatite, titanite, opaque mineral; sometimes fluorite.

(k) Riebeckite-granite

Main const.: microcline, albite, quartz, riebeckite; sometimes microcline-perthite.

Minor const.: zircon; rarely garnet.

(l) Aegirine-granite

Main const.: microcline-perthite, microcline, albite, quartz, aegirine.

Minor const.: zircon.

(m) Riebeckite-biotite-granite

Main const.: microcline, albite, quartz, riebeckite, biotite.

Minor const.: apatite, fluorite, titanite, zircon, opapue mineral.

(n) Leucocratic granite

Main const.: microcline-perthite, microcline, albite, puartz.

Chemical Characters

SAITO analyzed 15 rock samples from this series. The average chemical composition of the principal rock types, calculated therefrom, are shown in Table 17. The results of calculations of the mineral compositions from the average chemical compositions of syenites, quartz-syenites, and granites, are given in Tables 18–20.

Subordinate Rock Types

(i) Aegirine-enigmatite-riebeckite-quartz-syenite

Main const.: microcline, albite, quartz,riebeckite, enigmatite.

Minor const.: aegirine, apatite, zircon.

This rock was found only at a small hill 500 m to the southwest of Heikô (Pyongkang) Station.

(ii) Magnetite-riebeckite-biotite-syenite

Main const.: microcline-perthite, microcline, albite, biotite, riebeckite, magnetite.

Minor const.: apatite, fluorite, titanite, zircon.

Found at Shôra-san only.

7. Fenites and the Fenitization

Preliminary Statement

The actual contacts of alkalic rocks of series E_2 with schists are best observed at Saiho-ri at the northeastern end of the district. There was noticed a slight feldspathization of the schists within the limit of about 1 m from the contact.

At Kakuden-ri near the southern end of the district, a rather intense alkali metasomatism (fenitization) appears to have taken place, judging from scanty evidences obtained in the poorly exposed area. The width of the fenite zone is probably from 10 to 30 m.

Table 17. Average compositions of rocks of series E_2

	A	B	C	D	E	F	G	H	I
SiO_2	61.29	63.29	62.29	63.05	63.61	63.33	73.04	74.19	73.62
Al_2O_3	15.36	16.56	15.96	14.94	15.78	15.36	8.78	12.41	10.60
Fe_2O_3	4.42	4.18	4.30	4.36	3.40	3.88	4.26	2.91	3.59
FeO	2.72	1.28	2.00	3.38	2.82	3.10	1.86	0.48	1.17
MgO	0.64	0.70	0.67	0.47	0.57	0.52	0.40	0.31	0.36
CaO	0.91	0.38	0.65	1.10	0.96	1.03	0.31	0.29	0.30
Na_2O	7.29	7.13	7.21	6.20	5.93	6.07	4.35	3.77	4.06
K_2O	4.98	4.74	4.86	4.19	4.73	4.46	4.66	4.40	4.53
H_2O-	0.26	0.28	0.27	0.10	0.24	0.17	0.18	0.13	0.16
H_2O+	1.04	0.38	0.71	0.58	0.56	0.57	0.39	0.28	0.34
TiO_2	0.81	0.31	0.56	0.62	0.50	0.56	0.46	0.29	0.38
ZrO_2		0.77		0.26				0.13	
CO_2		0.05		0.04				0.00	
P_2O_5	0.14	0.16	0.15	0.31	0.21	0.26	0.13	0.19	0.16
S		0.04		0.03				0.06	
F		0.08		0.14				0.05	
MnO	0.26	0.06	0.16	0.36	0.38	0.37	0.21	0.30	0.26
BaO		0.04		0.05				0.13	
Rare earths		0.14		0.20				0.05	

A: Aegirine-biotite-syenite (average of 2 analyses)
B: Aegirine-riebeckite-syenite (1 analysis).
C: Average of A and B.
D: Aegirine-riebeckite-quartz-syenite (average of 6 analyses).
E: Riebeckite-quartz-syenite (average of 3 analyses).
F: Average of D and E.
G: Aegirine-granite (1 analysis).
H: Riebeckite-granite (1 analysis).
I: Average of G and H.

Process of Fenitization

(i) Original rocks

The original rocks are mainly fine-grained garnet-muscovite-biotite-schist and muscovite-biotite-schist, composed of quartz, potash-feldspar, biotite and muscovite, with or without garnet.

(ii) The first step

The first sign of alkali metasomatism is a marked decrease of quartz and muscovite, associated with an increase of microcline and with appearance of albite in the rocks. Then, muscovite and garnet

Table 18. Mineral composition of average syenite of series E_2

Oxides	wt. %	Apatite	Zircon	Biotite	Riebeckite	Aegirine	Magnetite	Titanite	Or	Sericite	Zeolite	Ab	Quartz	Residue
SiO_2	62.29		0.4	2.1	0.4	4.8		0.4	15.6	0.8	0.6	34.2	3.0	
Al_2O_3	15.96			0.9					4.4	0.7	0.3	9.7		
Fe_2O_3	4.30			0.3	0.1	2.9	1.0							
FeO	2.00			1.3	0.1	0.1	0.5							
MgO	0.67			0.6		0.1								
CaO	0.65	0.2				0.2		0.3						
Na_2O	7.21					1.1					0.2	5.9		
K_2O	4.86			0.6					4.1	0.2				
H_2O-	0.27													+0.27
H_2O+	0.71			0.2						0.1	0.3			+0.1
TiO_2	0.56			0.1				0.5						
ZrO_2	(0.77)		0.8											
CO_2	(0.05)													(+0.05)
P_2O_5	0.15	0.2												
S	(0.04)													(+0.04)
F	(0.08)													(+0.08)
MnO	0.16			0.2										
BaO	(0.04)													(+0.04)
Rare earths	(0.14)													(+0.14)
		0.4	1.2	6.3	0.6	9.2	1.5	1.2	24.1	1.8	1.4	49.8	3.0	

Bulk molecular composition of modal feldspars: $Or_{31\cdot3}$ $Ab_{68\cdot7}$

Table 19. Mineral composition of average quartz-syenite of series E_2

Oxides	wt. %	Apatite	Zircon	Riebeckite	Aegirine	Magnetite	Titanite	An	Or	Ab	Quartz	Residue
SiO_2	63.33		0.1	5.2	1.7		0.4	0.2	17.2	30.3	8.2	
Al_2O_3	15.36			0.1				0.2	4.9	8.6		+1.6
Fe_2O_3	3.88			1.0	0.9	2.0						
FeO	3.10			2.0	0.1	1.0						
MgO	0.52			0.5								
CaO	1.03	0.3		0.1	0.1		0.4	0.1				
Na_2O	6.07			0.5	0.4					5.2		
K_2O	4.46			0.2					4.5			
H_2O-	0.17											+0.17
H_2O+	0.57			0.2								+0.4
TiO_2	0.56						0.6					
ZrO_2	(0.26)		0.3									
CO_2	(0.04)											(+0.04)
P_2O_5	0.26	0.3										
S	(0.03)											(+0.03)
F	(0.14)											+0.14
MnO	0.37			0.2								+0.2
BaO	(0.05)											(+0.05)
Rare earths	(0.20)											(+0.20)
		0.6	0.4	10.0	3.2	3.0	1.4	0.5	26.6	44.1	8.2	

Bulk molecular composition of modal feldspars: $Or_{36\cdot0}$ $Ab_{63\cdot3}$ $An_{0\cdot7}$

Table 20. Mineral composition of average granite of series E_2

Oxides	wt. %	Apatite	Zircon	Riebeckite	Aegirine	Limonite	Or	Ab	Quartz	Residue
SiO_2	73.62		0.1	4.5	3.5		16.8	15.7	33.0	
Al_2O_3	10.60			0.3	0.1		4.8	4.4		+1.0
Fe_2O_3	3.59			1.0	2.3	0.3				
FeO	1.17			1.2						
MgO	0.36			0.4						
CaO	0.30	0.2		0.2						−0.1
Na_2O	4.06			0.5	0.9			2.7		
K_2O	4.53			0.1			4.4			
H_2O-	0.16			0.1						+0.1
H_2O+	0.34			0.3						
TiO_2	0.38			0.2						+0.2
ZrO_2	(0.13)		0.1							
CO_2	(0.00)									
P_2O_5	0.16	0.2								
S	(0.06)									(+0.06)
F	(0.05)									(+0.05)
MnO	0.26			0.1						+0.2
BaO	(0.13)									(+0.13)
Rare earths	(0.05)									(+0.05)
		0.4	0.2	8.9	6.8	0.3	26.0	22.8	33.0	

Bulk molecular composition of modal feldspars: $Or_{51.8}\ Ab_{48.2}$

disappear, while large porphyroblasts of microcline-perthite appear, giving rise to a rock which may be called biotite-quartz-syenite.

(iii) The second step

The next step of fenitization is marked by the production of green amphibole, first sporadically scattered and then uniformly distributed throughout the rocks. The amphibole is probably riebeckitic in composition, having $\alpha=1.681$. Biotite sometimes disappears and sometimes changes to a darker variety. Albite increases markedly in amount. Thus the rocks become practically identical with those of series E_2.

Chemical Variations

Table 21 shows the chemical compositions of original mica schists, fenite, and syenites of series E_2. The migration of materials during the fenitization is clarified by comparison of compositions of the same volume of original and resultant rocks. As was pointed out by Barth (1948), the same volume of rock usually contains nearly the same number of oxygen atoms. Then the analyses were recalculated to atomic proportions on the basis of 160 oxygen atoms in accordance with Barth's proposal.

The first step of fenitization, represented by the change from A to B of Table 21, is characreterized by introductuon of K and Na into the original schists. The second step, represented by the change

Table 21. Chemical compositions of mica-schists and fenites

	Analyses (wt. %)			Recalculated atomic number (O=160)			
	A	B	C		A	B	C
SiO_2	70.48	60.30	62.29	Si	60.8	54.8	57.7
Al_2O_3	12.14	16.27	15.96	Al	12.3	17.4	17.5
TiO_2	0.50	1.16	0.56	Ti	0.3	0.9	0.4
Fe_2O_3	3.57	4.95	4.30	Fe^{+3}	2.3	3.4	3.0
FeO	3.22	3.32	2.00	Fe^{+2}	2.3	2.5	1.5
MgO	4.21	4.12	0.67	Mg	5.4	5.6	1.0
MnO	0.11	0.06	0.16	Mn	0.1	0.04	0.1
CaO	1.57	3.46	0.65	Ca	1.4	3.4	0.7
Na_2O	0.12	1.12	7.21	Na	0.2	2.0	12.9
K_2O	2.50	4.52	4.86	K	2.7	5.2	5.8
H_2O+	1.58	0.74	0.71				
H_2O-	0.22	0.10	0.27				
P_2O_5	0.08	0.13	0.15	P	0.1	0.1	0.1
F	0.08	0.06	0.08				
	100.38	100.31	99.87	Total	87.9	95.3	100.7
O=F	0.03	0.03	0.03				
Total	100.35	100.28	99.84				

A: Composite analysis of 6 mica-schists (Specimen No. AM 440706–10,12, 14, 17, 19 and 23). Anal. by T. MIYASHIRO.

B: Amphibole-biotite-quartz-syenitic fenite (Specimen No. AM 440706–27). Anal. by T. MIYASHIRO.

C: Average composition of syenites of series E_2

from B to C, is characterized by the remarkable increase of Na, while the content of K remains nearly constant. (Here the end product of the fenitization is assumed to be identical to the syenites of series E_2.)

Fenitization and the Origin of the Rocks of Group E

It is difficult to determine the areal extent to which the rocks were subjected to fenitization, for the final product of this process is similar to the rocks of series E_2. So far in this paper, fenitization has been supposed to be limited to rocks of rather extraordinary compositions occurring in a small area adjacent to the contact with the igneous mass. This supposition has, however, no sufficient ground. The writers have no conclusive evidence to preclude the possibility that not only the fenites but also all the rocks of series E_2, or even all the rocks of group E, have been produced by intense fenitization. If such be the case, what has been called fenites in this paper represents a product of a less advanced stage of fenitization, which leads eventually to the production of rocks of group E in more advanced stages.

8. Characteristics of Pegmatites

Detailed description of many pegmatites of this complex is not given in this paper. Only a few remarkable characteristics will be summarized below:

(1) The mineral assemblages of pegmatites are generally similar to those of the surrounding rocks. For example, the pegmatites cutting nepheline-syenites are nepheline-syenite-pegmetites or cancrinite-syenite-pegmatite, while the pegmatites cutting quartz-syenites and granites are quartz-bearing ones. The pegmatites cutting rocks with hastingsite, also contain hastingsitic amphibole, while the pegmatites cutting rocks with riebeckite, also contain riebeckitic amphibole (though the compositions of the amphiboles in the pegmatites differ slightly from those in the surrounding rocks).

(2) The relative proportions of the constituent minerals in pegmatites differ from those of the surrounding rocks. For instance, nepheline is usually more abundant than sodalite and cancrinite in nepheline-syenite, while the former is less abundant than the latter in the associated pegmatites. Further the minerals of pegmatites differ in composition somewhat from those of the surrounding rocks,

as will be shown later.

9. Inclusions in the Alkalic Rocks

In the rocks of series W_2, E_2 and the monzonitic syenite series, the following types of inclusions were found:

A) Crystalline schists such as mustcovite-biotite-schists with or without garnet (Fig. 6 in Plate III).

B) Rocks of basic compositions. The original rocks are evidently amphibolite in some cases but are unknown in others. They show various stages of progressive digestion (Fig. 5 in Plate III).

10. Chemical Characteristics of the Alkalic Rocks

The nepheline-syenites, syenites, and quartz-syenites of group W have lower SiO_2, Fe_2O_3, and Na_2O and higher Al_2O_3, CaO, and K_2O

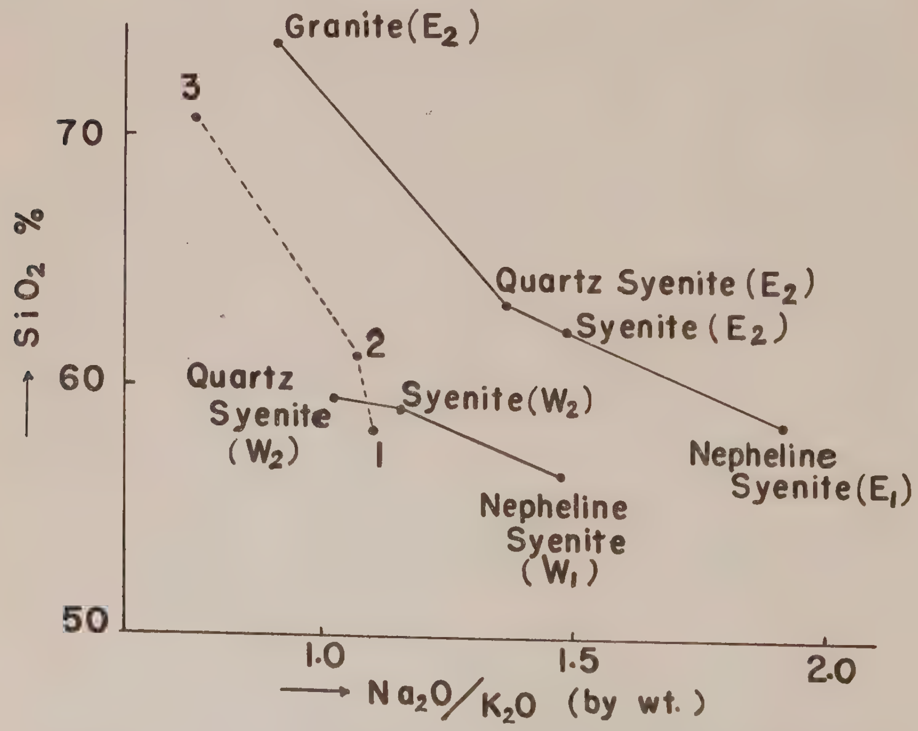

Fig. 4. Chemical characteristics of groups W and E, and of the monzonitic syenite series. (1, monzonitic syenite; 2, quartz-monzonitic syenite; 3, granite of the monzonitic syenite series.)

than the corresponding rock types of group E. Hence the ratio Na_2O/K_2O is lower in the rocks of group W than in the rocks of group E with the similar SiO_2 (Fig. 4).

The Fukushin-zan plutonic complex does not have any basic igneous rock in the proper sense. The sum of the Na_2O and K_2O contents of the rocks present is larger than the CaO contents in all cases. Therefore it is impossible to determine the PEACOCK's (1931) alkali-lime index of the rock series of this complex. The writers use an index, called *saturation index* in this paper, as a substitute for the alkali-lime index.

It is a general tendency in a rock series that the rocks oversaturated with silica have higher silica percentages than the rocks undersaturated with silica. The silica percentage of a rock just saturated with silica differs in different rock series. It is small in subalkalic series, but is larger in alkalic series. Therefore this value can be used as an index characterizing rock series.

Thus the saturation index is obtained by the following way: if the amounts of normative quartz and the total amounts of normative undesaturated minerals (such as olivine and nepheline) of the rocks of a series are plotted against SiO_2% (by wt.) and curves are drawn

Table 22. Comparison of rock series by means of the saturation index

Rock series	Saturation index	Alkali-lime index
The average volcanic rocks of Japan	43	63
Mull normal magma series	48	59
Katmai	50	64
San Franciscan volcanic field	50	56
Lassen Peak	51	62
Jan Mayen	54	51
Circum-Japan Sea alkalic province	57	53
Fukushin-zan district, series W_2	59	—
Oslo	61	52
Mull alkalic magma series	62	51
Fukushin-zan district, series E_2	62	—
Crazy Mountains	63	(48)
Teneriffe	66	47

Note: The upper five rock series are subalkalic, and the remaining ones alkalic

for these points, the curve for quartz and that for the undersaturated minerals shouls intersect the zero line at the same point. The $SiO_2\%$ corresponding to this point is called the saturation index of this series.

Table 22 shows the saturation indices of various rock series of the world. Thus the value 53 is the boundary between the subalkalic and alkalic rock series. Alkalic rock series have higher saturation indices than the subalkalic ones, while the former have lower alkali-lime indices than the latter.

11. Distribution of Elements among the Constituent Minerals

In order to know approximately the proportion of each element contained in particular minerals, the writers calculated the mineral compositions of the principal rock types from their average chemical compositions, as stated before. The results will be reviewed below:

Si: The bulk of silicon is contained in feldspars and quartz. The remaining small part is contained in nepheline, biotite, amphibole and other silicate minerals.

Al: The bulk of aluminium is contained in feldspars and feldspathoids. The remaining part is contained in biotite, amphibole, epodote, garnet, etc.

Fe and *Mg*: The bulk of iron and magnesium is contained in biotite, amphibole, pyroxene, and opaque minerals.

Ca: The distribution of calcium is worthy of special attention. Calcium is distributed, by little quantities, among apatite, titanite, calcite, garnet, epidote, amphibole, pyroxene, cancrinite, and albite. Generally none of these minerals contains dominant part of calcium present. In the calculation of C. I. P. W. norm, however, the bulk of Ca is allotted to anorthite molecule. For this reason the composition of normative feldspar differs so remarkably from that of modal feldspar that the norm is not useful in this case.

Na: The bulk of sodium is contained in feldspars and, if present, in felspathoids. The quantities of sodium contained in aegirine and amphibole are usually very small as compared with those contained in feldspars and feldspathoids.

K: The bulk of potassium is contained in feldspars, and the remaining small part is in biotite, muscovite, amphibole and nepheline, if present.

H: Some quantity of water above 105°C is contained in cancrinite, sodalite, biotite, muscovite, and amphibole, as a constituent. The water content of these minerals, however, are too small to explain all the water content of the rock above 105°C with. Hence, some part of the water in the rocks must be contained in fluid inclusions in minerals. Under the microscope fluid inclusions are abundant in quartz.

Ti: The bulk of titanium seems to be contained in titanite, and the remaining small part mainly in biotite.

Zr: The bulk of zirconium is perhaps contained in zircon, though this statement has not been ascertained.

CO_2: Carbon dioxide is a component of cancrinite and carbonate in nepheline syenite, and probably a component of carbonate alone in quartz-bearing rocks.

P: Practically all phosphorous is contained perhaps in apatite.

S: The distribution of sulphur is not evident, because the writers have not examined the rocks under the reflection microscope.

F: The fluorine contents of the rocks of this complex is so large that only a small part of it can be considered to be contained in apatite, even if we suppose that the apatite has the highest fluorine content possible. Thus a large part of fluorine must be contained in biotite, amphibole and also fluorite.

Mn: The bulk of manganese is contained in biotite. The analysed biotites of this complex show very high manganese contents.

Ba: The distribution is not evident.

Rare earths: The distribution is not evident, though some part of them is contained in allanite.

IV. Mineralogy

1. Feldspars

Practically all the rocks of this complex contain feldspars in quantities ranging from 45 to 80%. The feldspars are very clear and xenomorphic in all cases, except turbid plagioclase in the rocks of the monzonitic syenite series. The optical data are shown in Table 23.

A) Albite Grains (Low Albite)

Albite occurs abundantly as small clear, equidimensional, xeno-

Table 23. Optical properties of feldspars

Series	Specimen No.	Microcline-perthite		Albite grains	Microcline grains
		Albite blebs	Microcline host		
W_1	11419	2V 90°	n. d.	2V(+)70°	absent
	11453	2V(+)87°	2V(−)70°	2V(+)77°	absent
W_2	11423	2V(+)84°	n. d.	n. d.	absent
	11429	2V(+)74°	n. d.	2V(+)72°	n. d.
	11500	n. d.	n. d.	2V(+)80°	absent
	11465	2V(+)83°	n. d.	2V(+)76°	absent
Monzonitic syenite series	18909	2V 90°	n. d.		
	18911	2V 90°	2V(−)80°		
E_1	AM 431201-17a	2V(+)84°	2V(−)87°	2V(+)78°	2V(−)79°
	AM 431201-17b	2V(+)78°	2V(−)80°	2V(+)77°	2V(−)74°
	AM 431201-19	2V(+)80°	2V(−)87°	2V(+)77°	2V 90°
			α 1.519	α 1.528	α 1.519
			β 1.522	β n. d.	β 1.522
			γ 1.526	γ 1.531	γ 1.525
	AM 431205-13	2V(+)80°	2V(−)81°	2V(+)80°	2V(−)72°
			α 1.520	α 1.531	α 1.519
			β 1.522	β 1.534	β 1.522
			γ 1.526	γ n. d.	γ n. d.
	AM 440627-5	2V(+)84°	2V(−)85°	2V(+)78°	2V(−)86°
E_2	AM 431207-2	n. d.	n. d.	2V(+)70°	2V(−)88°
	AM 440628-1	absent	absent	2V(+)78°	2V(−)84°
	AM 431207-1	n. d.	n. d.		2V(−)70°-(+)80°
				α 1.529	α 1.520
				β 1.532	β 1.524
				γ n. d.	γ 1.528
	AM 440705-5	absent	absent	n. d.	2V(−)83°
	AM 440521-13	2V 90°	n. d.	2V(+)86°	n. d.
Fenites	AM 440706-20	2V(+)75°	2V(−)77°	2V(+)74°	2V 90°
	AM 440706-30	2V(+)75°	2V(−)64°	2V(+)70°	2V(−)80°
			α 1.521	α 1.530	α 1.521
			β 1.525	β 1.534	β 1.524
			γ 1.527	γ n. d.	γ 1.527

morphic grains in almost all the rocks. The optical angle about Z is 70°–80° and α_D is 1.529–1.531 in most cases. From these values the composition is estimated to be 0–8% An. The composition of modal plagioclase, calculated from the bulk chemical analyses of the rocks, are also 0–5% An, except in the rocks of the monzonitic syenite series having turbid plagioclase. Thus, the optical determination and chemical analyses are well in harmony with each other.

Very rarely "albite" grains with optical angles about Z of 80°–86° were found. These may be richer in the An molecule than ordinary albite.

Systematic difference in composition of albite in different rock types was not noticed.

B) Microcline Grains

Microcline occurs abundantly as small clear, equidimensional, xenomorphic grains in the rocks of group E, while it is absent or very scanty in the rocks of group W. The refractive indices are as follows:

$$\alpha_D = 1.519\text{–}1.521$$
$$\gamma_D = 1.525\text{–}1.528$$

When we adopt SPENCER'S (1937) diagram showing the relation between the composition and optical properties, the composition is estimated to be about $Or_{90}Ab_{10}$—$Or_{70}Ab_{30}$.

The optical angle of the microcline differs in different grains even in a single slice. Usually it is 70°–90° about X. In some grains the quadrille structure is observed throughout the grains, and in others only in parts.

C) Microcline-Perthite Crystals

Microcline-perthite occurs in almost all the rocks. It is so-called bleb- or patch-perthite. It occurs in large porphyritic xenomorphic crystals, up to 30 sq. mm. in thin sections. Some crystals are relatively intricate in form, filling the interstices between small microcline and albite grains (Fig. 1 in Plate IV).

The ratio in quantity of albite blebs to microcline host is variable, generally ranging from 1:1 to 1:3. When the perthite is twinned on the Carlsbad law, the blebs and host are twinned with a composition plane in common. Albite-blebs or patches are always twinned polysynthetically on the albite law. The mirocline host usually shows the quadrille structure in parts.

Optical angle 2V about Z of the albite bleb is 74°–90°. Albite blebs have a little larger optical angle than the albite grains of the same rock (Fig. 5). It may be assumed that this difference is due to the difference in composition between the two; thus, the albite blebs are richer in the An molecule than the albite grains of the same rock.

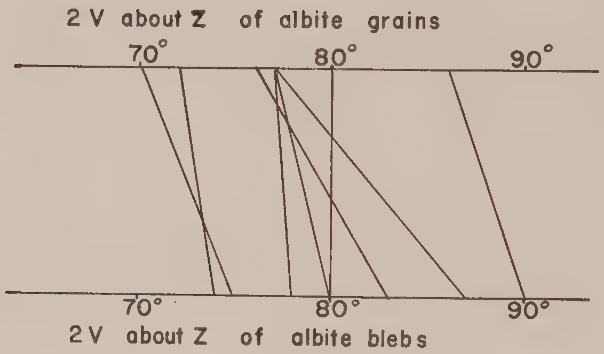

Fig. 5. The relation between the optical angles of albite grains and of the associated perthitic albite blebs in rocks of the Fukushin-zan district.

No definite relation was found in the optical angle between microcline grains and microcline hosts of the same rock.

Microcline-perthite includes poikilitically almost all kinds of minerals present in the rock, except microcline grains.

D) Crystallization of Perthite

From the proportion of the albite blebs to the microcline host in perthite, the bulk chemical compositions of most of the perthites are estimated as $Or_{10}Ab_{60}$—$Or_{60}Ab_{10}$. A perthite, whose analysis is shown in column 1, Table 24, falls within this range.

As will be discussed later, the rocks of this complex appear to have crystallized at too low temperatures for homogeneous alkali feldspars of such compositions to form. The writers consider that the microcline hosts and albite blebs crystallized probably simultaneously directly from magma, or from the disperse phase of fenitization. The difference in composition between the albite blebs and albite grains suggests that the stage of crystallization of the microcline-perthite differs from that of the albite grains in the groundmass.

Table 24. Chemical compositions of feldspar and feldspathoids

	1	2	3	4	5
SiO_2	65.58	41.94	37.42	36.85	35.22
Al_2O_3	19.58	34.26	31.14	30.93	29.79
TiO_2	n. d.	n. d.	n. d.	n. d.	n. d.
Fe_2O_3	0.21	0.55	tr.	0.52	tr.
FeO	n. d.	n. d.	n. d.	n. d.	n. d.
MgO	0.12	0.30	0.39	0.37	0.05
MnO	n. d.	n. d.	n. d.	n. d.	n. d.
CaO	0.49	0.28	0.93	0.29	8.17
Na_2O	5.90	15.82	21.68	22.01	18.16
K_2O	7.88	6.04	0.13	0.48	0.17
H_2O+	0.23	1.32	2.46	2.82	2.73
H_2O-	0.14	0.25	0.45	0.36	
F	n. d.	n. d.	n. d.	n. d.	n. d.
Cl	n. d.	0.09	7.12	6.98	0.03
SO_3	n. d.	n. d.	0.00	n. d.	0.08
CO_2	n. d.	n. d.	n. d.	n. d.	5.88
Total	100.13	100.85	101.72	101.61	100.28
Less O		0.02	1.60	1.57	
		100.83	100.12	100.04	
Refr. ind.		ε 1.537 ω 1.541	1.4827		ε 1.5015 ω 1.5238

1: Microcline-perthite from nepheline-syenite (series W_1), Fukushin-zan. Spec. gr. 2.587. Anal. by H. Yoshizawa (Chikyu, 19, 432–458, 1033).

2: Nepdeline from nepheline-syenite-pegmatite (series E_1), Shinjô-zan. Anal. by N. Saito (Jour. Chem. Soc. Japan, 64, 1152, 1943).

3: Sodalite from sodalite-syenite-pegmatite (series W_1), Fukushin-zan. Spec. gr. 2. 298. Anal. by K. Haraguchi (Chikyu, 10, 262–265, 1928).

4: Sodalite frsm nepheline-syenite-pegmatite (series E_1), Shinjô-zan. Anal. by N. Saito (Jour. Clem. Soc. Japan, 64, 1152, 1943).

5: Cancrinite from cancrinite-syenite-pegmatite (series W_1), Fukushin-zan. Spec. gr. 2. 44. Anal. by K. Seto and S. Tsurumi (Jour. Jap. Assoc. Min. Petr. Econ. Geol., 5, 1–14, 53–68, 1931).

The textural relation shows that the albite grains were formed earlier than the microcline-perthite. The albite grains are richer in Ab than the albite blebs of microcline-perthite. Thus, plagioclase

became poorer in Ab at later stages. Hence the trend of compositional variation of plagioclase with the advance in crystallization is reverse to that in ordinary cases (Fig. 6).

The stage of crystallization of microcline grains is not evident. They appear to have crystallized earlier than the microcline-perthite, judging from the fact that marginal parts of the microcline-perthite fill the interstices of them, but they appear to have crystallized later than the microcline-perthite, judging from the fact that they never occur as inclusions in the microcline-perthites.

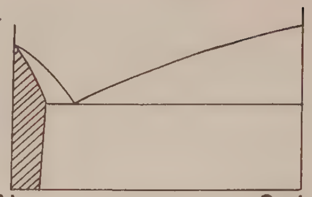

Fig. 6. Schematic diagram showing the crystallization of albite soloid solution and Ca-bearing minerals (garnet and epidote). The composition range of albite solid solution is very limited under the physical conditions concerned. Albite and Ca-bearing minerals are in eutectitc relation. Thus, the trend of the compositional variation of albite solid solution is reverse to the ordinary trend, as shown in the figure.

E) Plagioclase of the Monzonitic Syenite Series

All the rocks of the monzonitic syenite series contain turbid plagioclase besides clear albite. The turbid plagioclase is sometimes albite in composition, but is commonly oligoclase. It occurs as large crystals, more or less showing tendency towards idiomorphism. It shows various stages of progressive digestion.

2. Nepheline

Nepheline occurs in xenomorphic grains in nepheline syenites of series W_1 and E_{II}, occupying about 9% of the rock on the average. Usually it occurs in porphyritic crystals, though rarely it forms small grains of the groundmass.

Nepheline is easily recognized under the microscope by the abundance of characteristic needle-shaped inclusions of a zeolitic mineral with lower refractive indices and weaker birefringence. The inclusions are generally 0.02–0.04 mm. in length and 0.005 mm. in width. They are arranged roughly parallel to the c-axis of the nepheline host, and are distributed nearly evenly throughout the host.

As is shown in Table 25, the refractive indices of nepheline vary within very limited ranges:

Table 25. Optical properties of nepheline

Series	Specimen No.	ω	ε
W_1	11410	1.539	
	11443	1.542	
	11447	1.543	
	11449	1.542	
	11450	1.540	
	11451	1.543	
	11453	1.540	
	11479	1.539	
	11487	1.540	1.536
	11489	1.541	1.537
	11501	1.540	
	11503	1.539	
E_1	AM 431202-3	1.543	
	AM 431202-5	1.541	1.537
	AM 440627-5	1.541	1.537

Note: Nepheline AM 431202-5 is from nepheline-syenite-pegmatite, and all the others are from nepheline-syenites.

$$\omega_D = 1.539\text{–}1.543\,.$$

No systematic difference in refractive indices of nepheline between series W_1 and E_1 was noticed, though there is a small systematic difference in Na : K ratio of the rocks between the two series (Fig. 4).

A nepheline with $\omega = 1.541$, $\varepsilon = 1.537$, $a_0 = 10.01$ A, and $c_0 = 8.39$ A from a nepheline syenite pegmatite associated with rocks of series E_1 was analyzed as is shown in column 2 of Table 24. It has the following molecular composition

$$(Na_2Al_2Si_2O_8)_{71.4}(K_2Al_2Si_2O_8)_{17.9}(CaAl_2Si_2O_8)_{1.4}(Si_2Si_2O_8)_{9.3}$$

A part of the nepheline crystal is frequently replaced by sericite, sodalite or cancrinite.

3. Sodalite and Cancrinite

These minerals occur only in nepheline-syenites and associated pegmatites. They never occur in quartz-bearing rocks. Sometimes they are in isolated grains and sometimes they replace nepheline from the margin. In pegmatites, purplish sodalite sometimes replaces

greenish grey nepheline in vein- or network-like form. The chemical compositions of two sodalites and a cancrinite are shown in Table 24.

Some rocks of series W_1 and E_1 contain much cancrinite instead of nepheline, and may be called cancrinite-syenite, though the rocks are very similar to the associated nepheline-syenite in other respects.

4. Quartz

Quartz occurs in small irregular grains in rocks of series W_2 and E_2 and also of the monzonitic syenite series.

Quartz grains usually contain innumerable fluid inclusions, especially in the central part of the grains.

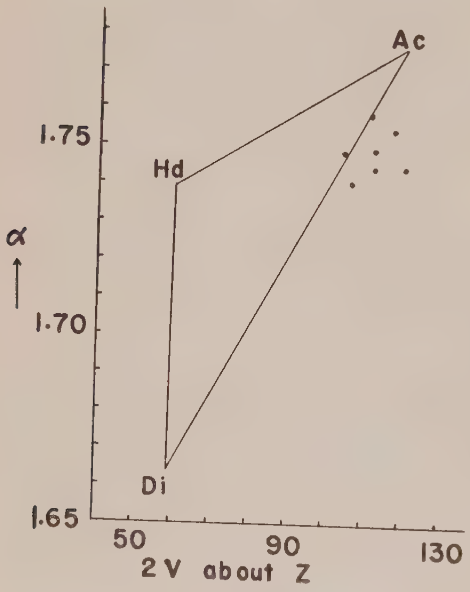

Fig. 7. The α-index and optical angle of aegirines from the Fukushin-zan district. Ac, Di, and Hd represent the points of end members of acmite, diopside, and hedenbergite respectively. The dots represent aegirines form the Fukushin-zan.

5. Aegirine

Aegirine occurs commonly in rocks of series E_1 and E_2, and sometimes in rocks of series W_1. Usually it does not show any zonal structure. However, when it is zoned, its margin is paler in colour than the interior. The pleochroism is usually as follows:

X=Y=yellowish green
Z=pale brownish yellow

The optical data are shown in Table 26 and Fig. 7. An aegirine was analysed as shown in column 7, Table 27*. Though Fig. 7 may give an impression that the aegirines have compositions intermediate between acmite and diopside, actually the analysis shows that the aegirine is intermediate between acmite and hedenbergite. The acmite molecule (Ac) amounts to nearly 90% in the analysed aegirine.

* It is to be noted that the aegirine in column 6 and the riebeckite in column 9 of Table 27 were separatee from one and the same rock specimen.

Table 26. Optical properties of aegirine

Series	Specimen No.	$c\wedge X$	2V	α	γ
W_1	11449	16°	(−) 88°		
	11453	21°	(+) 88°		
W_2	11465		(−) 82°		
E_1	169101	9°	(−) 80°		
	169110	4°	(−) 72°		
	169119	13°	(−) 80°		
	169124	3°	(−) 70°		
	169132	5°	(−) 66°		
	169136	2°	(−) 66°		
	169140	1°	(−) 65°		
	169705	3°	(−) 66°		
	AM 431205-13	n. d.	n. d.	1.74	1.78
	AM 431201-17a	7°	(−) 68°	1.744	
	AM 431201-17b	7°	(−) 60°	1.744	
	AM 440627-5	10°	(−) 74°	1.740	
E_2	AM 431207-2	4°	(−) 69°	1.758	
	5994	19°	(+) 86°		
	11536	n. d.	(−) 64°-80°		
	AM 431207-1	n. d.	(−) 76°	1.748	
	AM 440702-10	n. d.	(−) 60°-66°	1.754	1.805
Fenite	AM 431209-12	4°	(−) 68°	1.749	

Very rarely aegirinaugite, poorer in the acmite molecule, was found in certain rocks of group E.

6. Amphiboles

A) Hastingsite in Rocks of Group W

Hastingsite occurs commonly in rocks of group W. It shows so strong absorption that reliable optical measurement was not possible. Thin sections of the mineral cut in some directions do not extinguish at all between crossed nicols even when monochromatic light is used.

Frequently it shows zonal structure with brownish green-blue interior and clear green-blue border. (This statement refers to the colour of an exteme tint observed in a direction of 15° from the c-axis.) With high magnification, it is recognized that the brownish

tinge of the interior is due to innumerable minute, brownish, ascicular inclusions arranged parallel to the c-axis of the crystal. It may

Table 27. Chemical compositions of aegirine and amphiboles

	6	7	8	9	10	11
SiO_2	50.17	37.33	39.28	52.41	47.60	49.82
Al_2O_3	0.93	12.78	11.73	0.61	3.49	0.51
TiO_2	0.57	1.32	0.73	0.45	1.09	0.90
Fe_2O_3	31.13	8.58	6.77	14.37	11.06	16.57
FeO	2.27	21.65	22.85	14.82	18.79	21.53
MgO	0.19	1.48	2.78	5.07	4.56	1.09
MnO	0.58	1.36	0.20	1.46	0.99	0.53
CaO	1.24	9.46	11.62	1.33	2.56	0.76
Na_2O	12.07	3.49	0.50	4.94	4.72	6.54
K_2O	tr.	1.89	1.69	2.10	1.42	0.57
H_2O+	0.52	0.81	1.97	2.02	2.84	2.03
H_2O-	n. d.	0.22	0.12	0.10	0.74	n. d.
F	n. d.	n. d.	0.52	0.30	n. d.	0.45
Total	99.67	100.37	100.76	99.98	99.86	101.30
Less O			0.22	0.13		0.21
			100.54	99.85		101.09
α	1.754	1.706	1.688		1.680	1.701
β	n. d.	1.723	1.707		1.687	1.711
γ	1.805	1.724	1.716		1.691	n. d.
2V	(−) 60°–66°	(−) 20°	(−) 46°			

6: Aegirine from aegirine-rebeckite-quartz-syenite (series E_2), Kogan-zan. Specimen No. AM440702–10 of MIYASHIRO. Anal. by J. ITO (Min. Jour., 1, 1955).

7: Hastingsite from aegirine-hastingsite-biotite-nepheline-syenite (series W_1), Fukushin-zan. Spec. gr. 3.458. Anal. by H. YOSHIZAWA (Chikyu, 20, 354–361, 1933).

8: Hastingsitic hornblende from hornblende-biotite-quartz-monzonitic syenite, southwestern foot of Fukushin-zan. Specimen No. AM 440618–8. b=Y, $c \wedge Z=21°$, X=pale yellow, Y=brownish green, Z=brownish green (interior) and green blue (margin) in zonal arrangement, Y>Z>X. Anal. by T. MIYASHIRO.

9: Riebeckite from aegirine-riebeckite-quartz-syenite (series E_2), Kogan-zan. Specimen No. AM 440702–10. Refractive index for the direction of the least absorption=1.686. Anal. by T. MIYASHIRO.

10: Riebeckite from quartz-syenite-pegmatite (series E_2), Kozan-zan. Anal. by S. KOMATSU (Z. HARADA, Jour. Geol. Soc. Japan, 46, 290–292, 1939).

11: Riebeckite from granitic pegmatite (series E_2), Saiho-ri. Specimen No. AM 440521–8 of MIYASHIRO. Anal. by J. ITO (Min. Jour., 1, 1955).

have been formed by unmixing from the hastingsite.

A chemical analysis of a hastingsite of group W is shown in column 7, Table 27, and the optical data in Table 28.

Table 28. Optical properties of amphiboles

Varieties	Series	Specimen No.	α	β	γ	2V	SiO_2 contents of host-rocks
Hastingsite	W_1	11450	n. d.	1.709	n. d.	n. d.	
		11451	n. d.	1.709	n. d.	n. d.	
	W_2	AM 440606-2	n. d.	1.703	n. d.	n. d.	
Hornblende and Hastingsite	Monzon. syenite series	18907	1.687	1.695	1.699	(−)58°	60.69%
		18908	n. d.	n. d.	n. d.	(−)37°	62.19
		18910	n. d.	n. d.	n. d.	(−)60°–55°	60.93
		18915	n. d.	1.710	1.712	(−)5°	71.16
		18916	n. d.	1.710	1.712	(−)5°	70.09
		18918	1.691	n. d.	1.712	(−)44°	60.73
		11524	1.686	n. d.	1.703	(−)50°	63.71
		AM 440618-8	1.688	1.707	1.716	(−)46°	n. d.
Riebeckite	E_2	AM 431207-2	1.69	n. d.	n. d.		
		AM 440628-1	1.68	n. d.	n. d.		
		AM 440705-5	1.869	n. d.	1.697		
		AM 440529-5	n. d.	1.72	n. d.		
		AM 440529-7	n. d.	1.70	n. d.		

B) Hornblende and Hastingsite of the Monzonitic Syenite Series

Beautiful blue amphibole occurs in rocks of the monzonitic syenite series (INOUE, 1950). Its absorption is not so strong that reliable optical measurement was easy. It extinguishes between crossed nicols as is usually the case with ordinary minerals.

The amphibole in monzonitic syenite and quartz-monzonitic syenite has larger optical angles and lower refractive indices than that in granite of the same series. The former is common hornblende, while the latter is probably a variety of hastingsite, though the latter differs in optical properties from the above-described hastingsite of group W. Where the amphibole shows zonal structure, the interior is larger in optical angle and more brownish in colour than the margin. Thus, with the progressive variation of the host rocks from

monzonotic syenite, through quartz-monzonitic syenite, to granite, the amphibole changes from common hornblende to hastingsite as shown in Fig. 8.

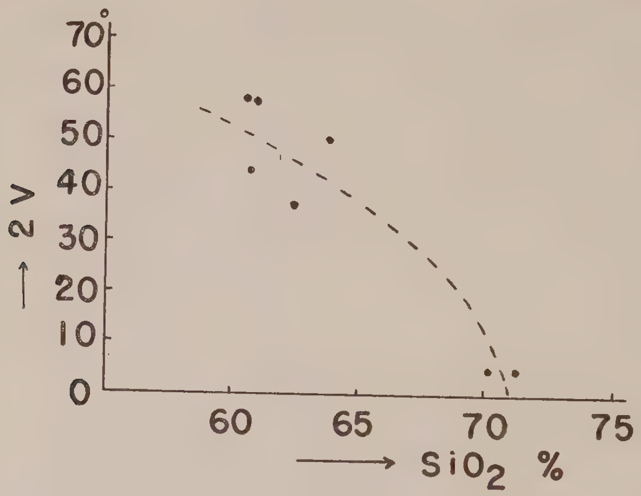

Fig. 8. The relation between the optical angle about X of amphiboles and the SiO_2 contents of their host rocks in the monzonitic syenite series. The dots represent amphiboles under consideration.

A chemical analysis of an amphibole of this series is shown in column 8, Table 27. Its low alkali content and high K/Na ratio are remarkable.

C) Biebeckite in Rocks of Group E

Riebeckite occurs in rocks of series E_1 and E_2. It shows so strong absorption that reliable optical measurement was not possible. Thin sections of the mineral cut in some directions do not extinguish between crossed nicols, even with monochromatic light.

The chemical compositions of the riebeckites are shown in columns 9–11, Table 27. Column 9 shows the composition of a riebeckite from quartz-syenite of Kogan-zan, while column 10 shows the composition of a riebeckite from quartz-syenite-pegmatite of the same hill. The difference between the two may represent a progressive variation in composition of amphibole with the variation of the host rocks from the ordinary facies to the associated pegmatite. As the riebeckite of column 10 is a little different in composition from the

typical riebeckite, it was given a new variety name *heikolite* after the town Heikô by Y. KINOSAKI (1935).

7. Biotite

Biotite is the most common coloured mineral of this complex. It is always rich in iron, and may be classified into the following four groups:

A) The most common variety, characterized by strong absorption and higher refractive indices:

γ_D=1.687–1.656

X=yellow or pale yellow

Y=Z=dark green, dark brownish green, or dark brown

In ordinary thin sections, X and Y are nearly opaque.

B) Light coloured variety of limited occurrence, characterized by weaker absorption and lower refractive indices:

γ_D=1.655–1.637

X=pale yellow

Y=Z=deep green or deep brownish green

This variety occurs locally in rocks of series W_1 and E_1, and may be a product of late- or post-magmatic alteration.

C) Biotite occurring in nepheline (or cancrinite)-syenite-pegmatites is similar to the variety (A) except that the former is generally more deeply greenish in colour than the latter:

γ_D=1.688–1.672

X=yellow or pale yellow

Y=Z=dark green

D) Reddish biotite: characterized by a peculiar reddish brown colour. It occurs in granite and granitic pegmatite of series E_2.

γ_D=1.679

Three samples of the variety (A) and one of the variety (C) were analyzed as shown in Table 29. All these biotites are low in MgO and high in FeO and Fe_2O_3. The MnO contents of the biotites are also relatively high as compared with biotites from ordinary igneous and metamorphic rocks. In Table 29, the analyses are arranged in the order of decreasing MgO contents. With the decrease in MgO contents, the SiO_2 and Al_2O_3 contents also decrease, while the Fe_2O_2 and total iron contents increase, and the refractive indices become higher. Judging from the fact that the pegmatite-biotite is

Table 29. Chemical compositions of biotites and vesuvianite

	12	13	14	15	16
SiO_2	32.43	32.24	31.45	29.21	34.83
Al_2O_3	18.64	15.54	15.01	13.48	19.12
TiO_2	1.10	1.97	1.04	0.70	2.58
Fe_2O_3	4.53	8.53	12.45	20.22	2.77
FeO	19.92	21.94	21.02	16.03	2.75
MgO	6.86	5.32	4.19	1.37	0.19
MnO	2.33	2.08	2.01	2.00	0.67
CaO	0.41	0.30	0.32	0.10	32.77
Na_2O	0.52	0.46	tr.	1.99	0.85
K_2O	9.20	8.13	9.21	8.29	0.23
H_2O+	3.66	3.35	3.48	4.27	2.25
H_2O-	0.45	0.24	0.30	2.26	0.04
F	0.16	0.13	0.14	n. d.	0.97
P_2O_5	0.00	0.00	0.00	0.00	n. d.
Total	100.21	100.23	100.62	99.92	100.02
Less O	0.07	0.06	0.06		0.41
	100.14	100.17	100.56		99.62
α	1.600	1.600	1.602	1.616	ε 1.722
γ	1.656	1.668	1.670	1.679	ω 1.730
2V	0°	0°	0°	0°	

12: Biotite from aegirine-biotine-nepheline-syenite (series E_1), Shachô-zan. Specimen No. AM 431205-13. X=vero pale yellow, Y=Z=deep green. Anal. by T. MIYASHIRO.

13: Biotite from aegirine-biotite-nepheline-syenite (series E_1), Shinjô-zan. Specimen No. AM 431201-19. X=pale yellow, Y=Z=opapue ordinary thin section) and dark browhish green (extremely thin section) Anal. by T. MIYASHIRO.

14: Biotite from biotite-nepheline-syenite (series W_1), Fukushin-zan. Specimen No. AM 440619-13. X=pale yellow, Y=Z=opaque (ordiary thin section) and dark brownish green (extremely thin section). Anal. by T. MIYASHIRO.

15: Biotite from cancrinite-syenite-pegmatite (series W_1), Fukushin-zan. Specimen No. AM 440617-14 X=pale yellow, Y=Z=opaque (ordinary thin section) and green (extremely thin section). Anal. by T. MIAYSHIRO.

16: Vesuvianite from cancrinite-syenite-pegmatite (series W_1), Fukushin-zan. Specimen No. AM 440617-1. Anal by T. MIYASHIRO.

lowest in MgO, the trend of decreasing MgO probably represents the progressive variation of biotite in composition with advancing crystallization of their host rocks.

Table 30. Optical properties of biotite

Series	Specimen No.	α	γ
W_1	11450		1.667
	11451		1.666
	11453		1.658
	11483		1.666
	AM 440619-13	1.602	1.670
	AM 440617-14	1.616	1.679
W_2	AM 440606-2		1.668
	AM 440614-22		1.667
	AM 440619-9		1.654
	AM 440619-12		1.645
	11465		1.687
Monzonitic syenite series	18907		1.667
	18909		1.676
	18910		1.681
	AM 440618-8		1.674
E_1	AM 431201-19	1.600	1.668
	AM 431205-13	1.600	1.656
	AM 440627-5	1.607	1.670
	AM 431204-3	1.585	1.637
	AM 431205-12	1.600	1.655
E_2	AM 440705-5		1.679

The four analyzed biotites were examined by A. A. LEVINSON and E. Wm. HEINRICH (1954) by means of the single-crystal X-ray method, and were found to belong to the 1-layer monoclinic variety.

8. Muscovite and Sericite

Muscovite occurs frequently in syenites of series W_2. It was probably formed by deuteric action. The optical angle 2V ranges from 22° to 30°.

White mica in small scaly habit, called sericite in this paper, is produced not uncommonly by the secondary alteration of nepheline.

9. Garnets

A) Grandite (garnet of the grossularite-andradite series)

Most of the garnets of this complex are grandite. They are usually pale yellow or colourless in thin sections, but rarely deeper in colour. They are isotropic in all cases (Fig. 2 in Plate IV).

Grandite is common in nepheline syenite of series W_1 and E_1, while it is rare in rocks of series W_2 and E_2. It does not occur in the rocks of the monzonitic syenite series.

The refractive index (n_D) and the edge length of the unit cube in kX (a_0) of two grandites from vesuvianite-bearing garnet-biotite-nepheline-syenite of series E_1 are as follows:

Specimen no.	n_D	a_0	Estimated composition
AM 431204-3	1.792	11.89	$Gr_{61}And_{34}Others_5$
AM 440628-11	1.783	11.84	$Gr_{59}And_{26}Others_{15}$

These values are plotted in Fig. 9.

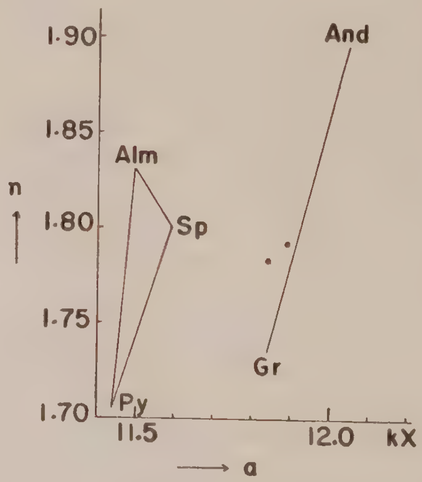

Fig. 9. The unit cell dimension and refractive index of garnets from the Fukushin-zan district. The dots represent two grandites from rocks of series E_1. And, Gr, Sp, Alm, and Py represent end members of andradite, grossularite, spessartine, almandine and pyrope respectively.

B) Garnet in rocks of the monzonitic syenite series is pale pink or colourless in thin sections. It is always isotropic. It is probably a member of the almandite-pyrope series.

$$n_D = 1.774$$

10) Vesuvianite

Vesuvianite occurs at several localities in this district.

A) Vesuvianite from a vesuvianite-bearing garnet-biotite-nepheline-syenite of series E_1 at Shachô-zan, Kennai-men. The vesuvianite tends to form colourless idiomorphic crystals, smaller than 2 mm. in

diameter, with faces a(100), m(110), and c(001). Sometimes it shows zonal structure (Figs. 2 and 3 in Plate IV).

$$\omega_D = 1.719, \qquad \varepsilon_D = 1.715 .$$

B) Vesuvianite from a cancrinite-syenite-pegmatite vein cutting ordinary nepheline-syenite of series W_1 at the southern foot of Fukushin-zan (INOUE and MIYASHIRO, 1951). This vein is composed of microcline-perthite, microcline, albite, cancrinite, sodalite, biotite, vesuvianite, allanite, and opaque mineral. The crystals of vesuvianite are usually irregular, though rarely idiomorphic with faces a(100), f(210), m(110), c(001), and p(111). They are smaller than 2.5 cm in diameter (Fig. 4 in Plate IV). The chemical composition of a vesuvianite is shown in Table 29 with its optical constants.

C) Vesuvianite from vesuvianite-garnet-aegirine-hastingsite-biotite-nepheline-syenite of series W_1 at Fukushin-zan. The vesuvianite tends to form more or less idiomorphic crystals, up to a few mm in length. It is very pale yellow in ordinaay thin sections.

Vesuvianite in nepheline syenite or allied rocks were described from Almunge by QUENSEL (1915), from Bancroft by OSBORNE (1930) and from Seiland by BARTH (1927). Vesuvianite of such a mode of occurrence is characterized by higher contents of Al and Ti, and lower contents of Ca and Mg than vesuvianites from metamorphosed calcareous rocks.

11. Allanite and a Related Mineral

Allanite occurs sparingly in nepheline syenites of series W_1.

A brown radioactive mineral, apparently similar to allanite, occurs in some nepheline-syenite of series E_1 and in some nepheline-syenite pegmatites cutting through nepheline-syenite of series W_1. The brown mineral has higher refractive indices and stronger birefringence than ordinary allanite. It is not known whether it is a variety of allanite or another mineral—such as chevkinite.

The brown radioactive mineral occurs in prismatic or rounded crystals, and is often twinned (Fig. 5 in Plate IV). It has stronger pleochroism than ordinary allanite, showing the following optical properties:

$$\alpha_D = 1.784, \ \gamma - \alpha = \text{ca. } 0.04, \ 2V(-) = 74 ,$$

X = nearly colourless

Y = Z = dark reddish brown.

X-ray powder photographs showed a pattern with the following d-spacings in kX: 3.53(w), 3.22(w), 2.90(vs), 2.64(m), 2.14(s), 1.88(m), 1.63(s), 1.43(m), 1.28(m).

12. Epidote

A) Epidote in rocks of series W_2

Basic inclusions in rocks of series W_2 contain epidote which was formed, together with albite, by the recrystallization of more basic plagioclases. Epidote-biotite-syenite of series W_2 contains a large quantity of epidote, and probably represents digested basic inclusions.

These epidotes occur generally in idiomorphic crystals.

B) Epidote in rocks of the monzonitic syenite series

Epidote or clinozoisite is produced as a by-product of recrystallization and albitization of plagioclase, as was stated before.

13. Enigmatite

As was described before, a subordinate rock type of series E_2 contain a large quantity of enigmatite. The mineral is prismatic or spindle-shaped, up to 1.3 mm. long and 0.3 mm. in diameter. It is deep reddish brown in some directions and is practically opaque in others.

14. Other Minerals

A) Apatite

Apatite occurs in minute irregular or prismatic crystals practically in all types of rocks.

B) Carbonates

A little carbonate is found sporadically in various kinds of rocks of this complex. It is not certain whether it is primary or secondary.

C) Fluorite

Fluorite occurs as small inclusions in feldspars and nephelines, and sometimes it fills interstices between other minerals.

D) Lessingsite

Y. KINOSAKI (1940) found a deposit of cerium mineral at Shôra-san. J. TAKUBO and T. KONDO (1942) identified the mineral as lessingsite. It occurs in a vein cutting through alkali syenite. According to KINOSAKI the vein is composed of riebeckite, lessingsite, fluorite, molybdenite, allanite, mica, potash feldspar, and quartz. An analysis

of the mineral by TAKUBO and KONDO is as follows: SiO_2 19.02, FeO 1.86, MnO 1.79, Al_2O_3 0.36, ThO_2 0.00, Ce_2O_3 30.71, the other Ce group oxides 27.76, Y group oxides 2.80, CaO 12.47, MgO 0.15, P_2O_5 0.87, H_2O+ 0.57, H_2O- 0.04, F 2.51, Total 100.91%, Less O for F 1.06. (A part of F may be due to the admixed fluorite in the analyzed sample.)

E) Opaque Minerals

Opaque minerals are widely but sparingly present in various rocks.

In a nepheline-syenite-pegmatite cutting through nepheline syenite at Shachô-zan, a large mass of ilmenite, amounting to one ton, was found.

F) Titanite

Titanite occurs in irregular grains or wedge-shaped crystals in various rocks.

Innumerable minute grains of titanite cluster around opaque minerals, forming rims, in rocks of the monzonitic syenite series.

G) Tourmaline

Tourmaline occurs very sparingly in some rocks of the monzonitic syenite series. Its pleochroism is as follows: $//$to c=pinkish, $\perp$ to c=purple-blue.

H) Zeolite

Zeolite occurs in some nepheline syenite as an alteration product from nepheline. However, minute zeolite-like inclusions in nepheline may be deuteric.

I) Zircon

Zircon occurs in idiomorphic or irregular grains. A fairly large quantity of zircon was found in some quartz-syenite-pegmatites at Kogan-zan, and was mined for some period.

V. Some Petrogenetical Problems

1. Preliminary Statement

The rocks of group W show the appearance of ordinary plutonic rocks, while those of group E show close resemblance to gneissose metamorphic rocks. Further, the rocks of group E are exposed in the area mainly surrounded by schistose metamorphic rocks. This fact might be regarded as suggesting that the gneissosity of the

rocks of group E was formed by regional metamorphism after the consolidation of magma. This interpretation is, however, impossible, because the regional metamorphism took place earlier than the intrusion of the alkalic rocks, judging from the fact that some schists occur as inclusions in alkalic rocks of group W.

These alkalik rocks may have been formed by consolidation of some magmas. However, it is also possible to explain the origin of these rocks on the assumption that they were formed by some processes of metasomatism of pre-existing rocks. No decisive evidence to prove or disprove their magmatic origin was found. Therefore in this chapter the writers will discuss the origin of the alkalic rocks on the basis of both the magmatic and metasomatic hypotheses.

The origin of the monzonitic syenite series and fenites was already discussed in Chapter III.

2. Origin of the Rock Series by Magmatic Hypothesis

Series W_1 and E_1 comprise undersaturated and nearly saturated rocks as regards silica, while the other two series (W_2 an E_2) comprise oversaturated and saturated rocks. Undersaturated and oversaturated rocks do not occur in one and the same rock series. The mutual relation between undersaturated and oversaturated rocks do not appear to be so close as to give us an impression that the one was derived from the other.

If we assume that various rocks of this complex were derived from a common parent magma, the magma had perhaps a nearly saturated composition, for saturated and nearly saturated rocks are comprised in all the rock series. (This parent magma is not necessarily identical in composition to any syenite now exposed in this district.)

The main course of crystallization differentiation of this parent magma may be summarized as follows:

The parent magma, though nearly saturated as a whole, was presumably rather heterogeneous in composition, being partly slightly undersaturated and partly slightly oversaturated. From this magma, small feldspar grains began to crystallize first, together with some coloured minerals. Then large porphyroblasts of microcline-perthite crystallized. Where the parent magma was slightly undersaturated, the residual liquid became more and more undersaturated by the

crystallization of feldspars. Where the parent magma was slightly oversaturated, the residual liquid became more and more oversaturated. Finally, nepheline or quartz began to crystallize depending upon the degree of saturation of residual magmas.

Separation of residual liquids from crystals at various stages of crystallization, produced varied rock types of each series.

3. Origin of the Rock Series by Metasomatic Hypothesis

The progressive metasomatism of the pre-existing rocks, especially schistose metamorphic rocks, by the action of alkalic emanation, may have produced various series of oversaturated and undersaturated igneous-looking alkalic rocks. The gneissosity of group E may be a relct fabric inherited from the pre-existing rocks.

If this hypothesis is valid, the "fenites" represent a less advanced stage of metasomatism, ordinary gneissose alkalic rocks of group E a more advanced stage, and the almost unfoliated rocks of group E the end product of metasomatism. The rocks of group W may also be considered to represent the highest grade in this progressive series of metasomatism, having become rheomorphic to be able to intrude into the solid rocks.

We have much less knowledge on the law and possible extent of metasomatism than on the law of crystallization differentiation. Hence it is difficult to depict the process more in detail.

4. Origin of a few Mineralogical Peculiarities

(A) Albite-Epidote Association

In epidote-biotite-syenite of series W_2 and certain basic inclusions included in rocks of the same series, epidote-clinozoisite occurs in association with albite, instead of basic or intermediate plagioclase. This fact suggests that probably the temperature of crystallization of series W_2 was too low to form basic or intermediate plagioclase, similarly as in the case of albite-epidote association in metamorphic rocks of the epidote-amphibolite and greenschist facies. Unfortunately there is no rocks of such basic compositions in the other series.

(B) Reverse Trend in Crystallization of Plagioclase

The albite blebs in porphyritic microcline-perthite are more calcic than the albite grains in the groundmass of the same rock, as was stated before. If we accept that the porphyritic microcline-perthite

crystallized later than albite grains as their textural relations suggest, we are lead to the conclusion that the composition of crystallizing plagioclases changed progressively from sodic to more calcic one. This is reverse to the ordinary trend of crystallization of this mineral (Fig. 6). Conceivably it may be an event characteristic of such low temperature type of alkalic rocks.

(C) Occurrence of Grandite (Lime-Garnet) and Vesuvianite.

Rock of this complex frequently contain small quantities of grandite. The Ca contents of these rocks, however, are usually so small that we have no special reason to postulate contamination of the magma by calcareous rocks. The writers regard them as a product of, either ordinary crystallization from magma or metasomatism of non-calcareous rocks, under a certain peculiar pysical and chemical conditions.

In the rocks of this complex there occur three constituents mainly composed of CaO, Al_2O_3 and SiO_2: namely grandite garnet, epidote-clinozoisite, and the An molecule in plagioclase. If we compare their compositions with one another, grandites contain the smallest amounts of Al and Si of the three, combined to the equal amount of Ca, as follows:

Grandites	$Ca_3(Al, Fe)_2Si_3O_{12}$	$=Ca_6(Al, Fe)_4Si_6O_{24}$
Epidote-clinozoisite	$Ca_2(Al, Fe)_3Si_3O_{12}(OH)$	$=Ca_6(Al, Fe)_9Si_9O_{36}(OH)_3$
An molecule	$Ca\ Al_2Si_2O_8$	$=Ca_6Al_{12}Si_{12}O_{48}$

This fact suggests that grandites may be relatively easily produced in nepheline-syenite which is most undersaturated with SiO_2. Indeed, grandites occur mainly in nepheline syenites and rarely in syenites, but extremely rarely, if any, in quartz-bearing rocks of this complex. Grandite occurs frequently in biotite-nepheline-syenites which are relatively rich in Al_2O_3. Hence Al appears to have a less important influence on the formation of grandites than Si.

Vesuvianite-bearing garnet-biotite-nepheline syenite, occurring at Shachô-zan (series E_1), and garnet-nepheline-syenite (series E_1) are extraordinarily rich in Ca. Hence they may have been produced by the assimilation of limestone. The stable occurrence of vasuvianite and grandite itself, however, may be attributed to a deficiency in Si, as in the above case. Another possible explanation of these Ca-rich rocks is that they may have been produced by segregation and concentration of Ca-rich materials from some parts of the nepheline-

syenite mass, just as in the case of epidote veins in metamorphosed basic rocks. The occurrence of garnet-nepheline-syenite as pockets and veins may support the latter view.

VI. Physical Conditions Prevailing During the Formation of Alkalic Plutonic Rocks

1. Diversity in Temperature of Formation

It has frequently been considered in the petrological literature that the alkalic rocks are produced generally at lower temperatures than most other igneous rocks. Such a view came probably from a commonly accepted hypothesis that the alkalic rocks represent the last residual solution in crystallization differentiation. The present writers, however, in the course of their study, were deeply impressed by the fact that there is no sound ground for this view. The petrological evidences show that some alkalic rocks crystallized at high temperatures, while other alkalic rocks such as those in the Fukushin-zan district, were formed at much lower temperatures. The diversity in temperature of formation of alkalic plutonic rocks is an important fact which has never been fully appreciated. The writers consider that the diversity is closely connected with the diversity in their origin.

The physical conditions under which an alkalic plutonic mass was formed, are revealed in the following two ways. First, the temperature at the time of emplacement are revealed in the mineral compositions of the contact metamorphic rocks associated with the mass, only if the recrystallization was advanced sufficiently. Secondly, the temperatures of crystallization are revealed in the mineral compositions of the alkalic rocks themselves.

If there is no large amount of superheat in the magma, the two kinds of temperatures should be in parallel. Actually some alkalic rocks, which show evidences of crystallization at high temperatures, caused little thermal metamorphism to the country rocks, as is exemplified by the alkalic masses of the Morotsu district (YAGI, 1953). In such cases probably the condition was not favourable for recrystallization of the country rocks, though the temperatures may have reached relatively high values.

2. Contact Metamorphism Caused by Alkalic Plutonic Masses

The alkalic plutonic masses of the Oslo district produced various contact metamorphic rocks, which have become well known by a classic study by V. M. GOLDSCHMIDT (1911). The inner aureole is composed of hornfelses of the pyroxene-hornfels facies.

Usually the occurrence of rhombic pyroxene in rocks of the contact aureole is characteristic of the pyroxene-hornfels facies. It is interesting to note that the occurrence of rhombic pyroxene in contact metamorphic rocks was noticed for the first time in a hypersthene-cordierite-rock in the aureole of a nepheline-syenite mass at Umptek by RAMSAY (1894) and also in the aureole of an essexite mass at Sölvsberget by BROGGER (1894). The aureole of the alkalic mass at Monzoni contains monticellite and melilite, which both indicate a condition of high temperature.

These facts suggest that these alkalic rocks were intruded at higher temperatures than most of calc-alkalic granitic masses, which usually produce metamorphic rocks of the amphibolite facies even in the innermost aureole. Accordingly, these alkalic rocks, at least, can not have been produced by some processes of crystallization differentiation or assimilation of ordinary calc-alkalic granitic rocks.

On the other hand, the alkalic masses of the Haliburton-Bancroft district in Canada, intruded into limestones and other kinds of rocks to produce diopside, amphiboles, vesuvianite, and other metamorphic minerals. Though many investigators studied the district, rhombic pyroxene and wollastonite were not found in any rocks there (ADAMS and BARLOW, 1910; GUMMER and BURR, 1946). Therefore the contact metamorphic rocks of the district did not attain the grade of pyroxene-hornfels facies, but belong to the amphibolite and lower facies. The rocks of the Fukushin-zan plutonic complex also appear to have been emplaced at relatively low temperatures. Where the rocks come in contact with pre-existing metamorphic rocks of the amphibolite facies at the Saiho-ri area, any appreciable textural change owing to the thermal effect of the mass was not noticed.

Thus these evidences show the existence of diversity in the temperature of alkalic masses at the time of emplacement.

3. Mineral Compositions of Alkalic Plutonic Rocks

It is interesting to note that the alkalic plutonic rocks, associated with contact metamorphic rocks of the high temperature type, such

as those in the Oslo district, contain such minerals that appear to have crystallized at high temperatures, while the alkalic plutonic rocks, associated with contact metamorphic rocks of the low temperature type, such as those in the Haliburton-Bancroft district or the Fukushin-zan district, contain such minerals that appear to have crystallized at lower temperatures. For example, the Oslo rocks contain anorthoclase or cryptoperthite formed by unmixing of high temperature alkali feldspers, while the Haliburton-Bancroft and Fukushin-zan rocks contain low albite and microcline. Especially in rocks of series W_2 of the Fukushin-zan district, the temperature of crystallization was so low that intermediate or basic plagioclase was not stable.

One of the writers (A. MIYASHIRO, 1951a) found that nephelines associated with anorthoclase or sanidine in alkalic plutonic rocks show a wider range in chemical composition than those associated with common orthoclase or microcline, and this fact is probably due to the enlargement of the composition range in nepheline in response to the increase in temperature (or decrease in pressure) of crystallization.

4. Genetical Classification of Alkalic Plutonic Rocks

The diversity in physical condition during the formation of alkalic plutonic rocks must be closely related with diversity of their origin. The alkalic plutonic rocks of the high temperature type are frequently associated with volcanic rocks, and appear to constitute subvolcanic masses, while those of low temperature type are not generally associated with volcanic rocks. Conceivably the former represents differentiates from basaltic parent magma, while the latter does not.

References cited

ADAMS, F. D. and BARLOW, A. E. (1910): Geology of the Haliburton and Bancroft areas, Province of Ontario. Canad. Geol Surv. Mem. No. 6, 419 pp.

BARTH, TOM. F. W. (1927). Die Pegmatitgänge der Kaledonischen Intrusivgesteine im Seiland-Gebiete. Skr. utgitt. av Det Norske Vid.-Akad. Oslo, I Mat.-naturv. Kl. No. 8, pp. 1-123.

—— (1948): Oxygen in rocks: a basis for petrographic calculations. Jour. Geol. Vol. 56, pp. 50-60.

BRÖGGER, W. C. (1894): The basic eruptive rocks of Gran. Quart. Jour. Geol. Soc. Vol. 50, pp. 15-38.

—— (1921): Das Fengebiet in Telemark, Norwegen. pp. 150-179.

ECKERMANN, H. von (1948): The alkaline district of Alnö Island. Sverig. geol. undersökning, Ser. Ca, No. 36.

GOLDSCHMIDT, V. M. (1911): Die kontaktmetamorphose im Kristianiagebiet. Vidensk. Skrift. I. Mat.-Naturv. Klasse, No. 1, 483 pp.

GUMMER, W. K. and BURR, S. V. (1946): Nephelinized paragneisses in the Bancroft area, Ontario. Jour. Geol. Vol. 54, pp. 137–168.

INOUE, T. (T. MIYASHIRO at present) (1950): Amphiboles and biotites from the Fukushin-zan alkaline complex, Korea. Jour. Geol. Soc. Japan. Vol. 56, pp. 71–77.

INOUE, T. (T. MIYASHIRO at present) and MIYASHIRO, A. (1951): Occurrence of vesuvianite in nepheline-syenitic rocks of the Fukushin-zan district, Korea; with general consideration of the relation between the composition and occurrence of vesuvianite. Jour Geol. Soc. Japan, Vol. 57, pp. 51–57.

KINOSAKI, Y. (1935): Miscellaneous notes on the minerals recently found in Korea. Jour. Mining Assoc. Korea, Vol. 18, pp. 167–193.

KINOSAKI, Y. (1940): A preliminary report on the cerium ore deposit at Shôra-san, Temba-ri, Nan-men, Heikô-gun, Kôgen-dô. Chôsen-kôgyô, Vol. 7, pp. 1–3.

LEVINSON, A. A., and HEINRICH, E. Wm. (1954): Studies in the mica group: single crystal date on phlogopites, biotites and manganophyllites. Amer. Min. Vol. 39, pp. 937–945.

MIYASHIRO, A. (1951 a): The ranges of chemical composition in nepheline and their petrogenetic significance. Geochim. Cosmochim. Acta. Vol. 1, pp. 278–283.

MIYASHIRO, A. (1951 b): Kyanites in druses in kyanite-quartz-veins from Saiho-ri in the Fukushin-zan district, Korea. Jour. Geol. Soc. Japan. Vol. 57, pp. 59–63.

OSBORNE, F. F. (1930): The nepheline gneiss complex near Egan Chute, Dungannon Township, and its bearing on the origin of the nepheline syenite. Amer. Jour. Sci. Vol. 20, pp. 33–60.

PEACOCK, M. A. (1931): Classification of igneous rock series. Jour. Geol. Vol. 39, pp. 54–67.

QUENSEL, P. (1915): Vesuvian und Hastingsit aus dem Nephelinsyenit von Almunge. Gentralbl. Min. usw. pp. 201–208.

RAMSAY, W. (1894): Das Nephelinsyenitgebiet auf der Halbinsel Kola, I. Fennia, Vol. 11, No. 2, 225 pp.

ROSENBUSCH, H. (1910): Elemente der Gesteinslehre. 3. Aufl.

SPENCER, E. (1937): The potash-soda feldspars, I. Thermal stability. Min. Mag. Vol. 24, pp. 453–494.

TAKUBO, J. and KONDO, T. (1942): Lessingsite from Ryozo Mine, Kogen-do, Korea. Sci. Rep. Geol. Min. Inst., Kyoto Imp. Univ., Vol. 1, pp. 21–25.

YAGI, K. (1953): Petrochemical studies on the alkalic rocks of the Morotu district, Sakhalin. Bull. Geol. Soc. Amer. Vol. 64, pp. 769–810.

YOSHIZAWA, H. (1932): Some observations at Fukushinzan, Korea. Chikyu, Vol. 17, pp. 75-84.

Plate I

Explanation of Plate I

Fig. 1. Biotite-nepheline-syenite of series W_1 from the southern slope of Fukushin-zan. (Lower nicol only, ×7.) Glomeroplasmatic clusters of biotite are set in the matrix of colourless minerals. (Specimen No. 11515)

Fig. 2. Aegirine-hastingsite-biotite-nepheline-syenite of series W_1 from the summit of Fukushin-zan (Lower nicol only, ×7.) Glomeroplasmatic clusters (g), composed of biotite, aegirine, garnet, hastingsite, and zircon, are set in the matrix of clear alkali feldspars (f) and rather turbid nepheline (n). (Specimen No. 11449)

Fig. 3. Hastigsite-biotite-nepheline-syenite of series W_1 from the southern slope of Fukushin-zan (Between crossed nicols, ×7.) Large crystals of microcline-perthite (p) are set in the matrix (n) which contains small grains of nepheline, partly altered to sericitic aggregates. (Specimen No. 11503)

Fig. 4. Aegirine-hastingsite-biotite-nepheline-syenite of series W_1 from the summit of Fukushin-zan. (Between crossed nicols, ×7.) Microcline-perthite (p) and nepheline (n). (Specimen No. 11449)

Fig. 5. Biotite-syenite of series W_2 from the southeastern slope of Fukushin-zan. (Lower nicol only, ×7.) Biotite (lack,), muscovite (turbid), and alkali feldspars (clear). (Specimen No. 11527)

Fig. 6. Epidote-biotite-syenite of series W_2 from the southern slope of Fukushin-zan. (Lower nicol only, ×7.) Microcline-perthite (p) and glomeroplasmatic clusters (g), composed mainly of small epidote grains and biotite flakes. (Specimen No. 11426)

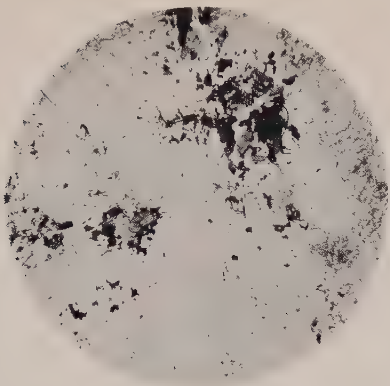

Fig. 1

Fig. 2

Fig. 3

Fig. 4

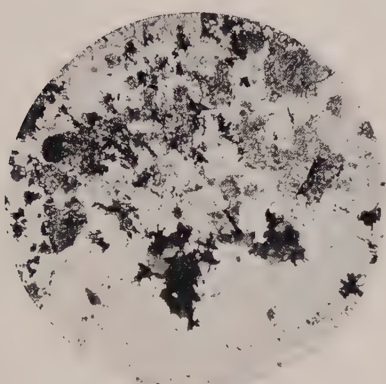

Fig. 5

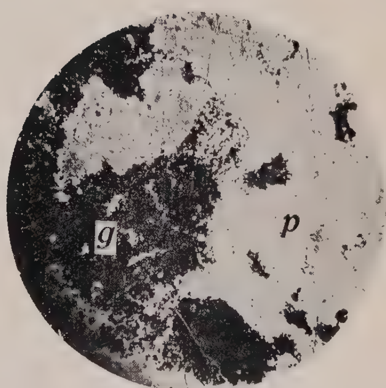

Fig. 6

Plate II

Explanation of Plate II

Fig. 1. Hornblenbe-biotite-quartz-monzonitic syenite of the monzonitic syenite series from Shôji. (Lower nicol only, ×7.) Glomeroplasmatic clusters (g), composed of biotite and hornblende, are set in the matrix of alkali feldspars and quartz (fq), together with plagioclase (pl, turbid). (Specimen No. 18911)

Fig. 2. Hornblende-biotite-quartz-monzonitic syenite of the monzonitic syenite series from Shôji. (Between crossed nicols, ×7.) The crystals of plagioclase (pl, black) are idiomorphic against quartz (q, white), which the latter shows undulatory extinction. Symbol "p" denotes microcline-perthite, and "h" hornblende with many minute poikilitic inclusions of biotite. (Specimen No. 18909)

Fig. 3. Hornblende-biotite-quartz-monzonitic syenite of the monzonitic syenite series from Shôji. (Lower nocol only, ×7.) Biotite and hornblende (dark); plagioclase (turbid); alkali feldspar (clear), (Specimen No. 18912)

Fig. 4. Hornblende-biotite-quartz-monzonitic syenite of the monzonitic syenite series from Daison. (Lower nicol only, ×7.) Poikilitic crystals of hornblende include many minute granules of quartz, together with small numbers of apatite and albite. (Specimen No. 18918)

Fig. 5. Aegirine-riebeckite-biotite-nepheline-syenite of series E_1 from Shinjô-zan. (Between crossed nicols, ×7.) Porphyritic microcline-perthite (right) and nepheline (left) are set in the fine-grained groundmass, the former showing the Carlsbad twinning. (Specimen No. 169119)

Fig. 6. Aegirine-riebeckite-biotite-nepheline-syenite of series E_1 from Shinjô-zan. (Lower nicol only, ×7.) Glomeroplasmatic clusters are in parallel elongation. (Specimen No. 169124)

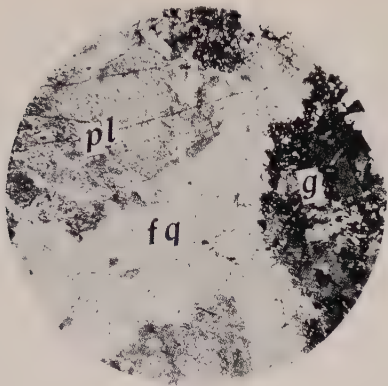

Fig. 1

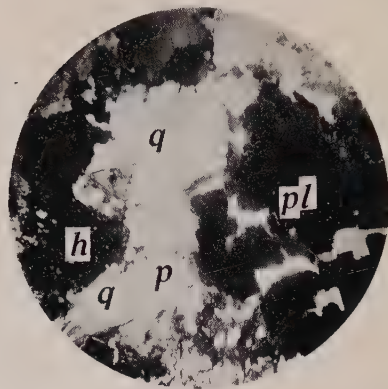

Fig. 2

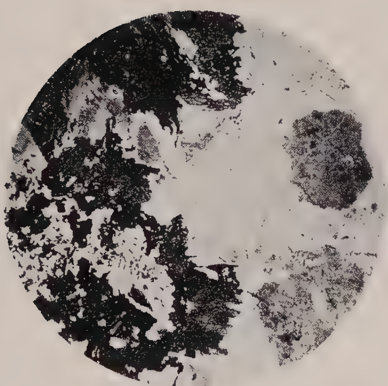

Fig. 3

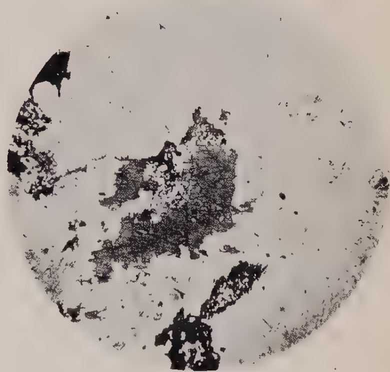

Fig. 4

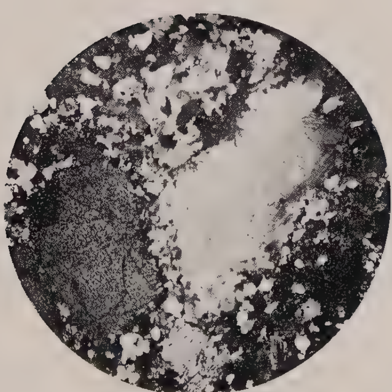

Fig. 5

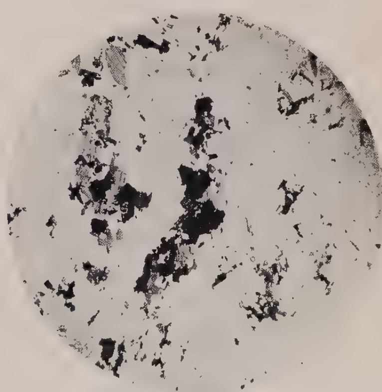

Fig. 6

Plate III

Explanation of Plate III

Fig. 1. Aegirine-biotite-syenite, with gneissose structure, of series E_2 from Shôra-san. (Lower nicol only, $\times 7$) (Specimen No. 11589)

Fig. 2. Aegirine-riebeckite-quartz-syenite of series E_2 from Shôra-san. (Lower nicol only, $\times 7$)

Fig. 3. Alkali granite showing post-crystalline deformation, of series E_2 from Saiho-ri. (Between crossed nicols. $\times 24$) (Specimen No. AM 440528-7)

Fig. 4. A country rock, probably sheared by the intrusion of the alkalic mass at Saiho-ri. (Between crossed nicols, $\times 24$) Elongated crystals of quavtz in parallel arrangement show strongly wavy extinction. (Specimen No. AM 440522-6)

Fig. 5. Basic inclusion, composed mainly of barkevikite and plagioclase, in rocks of series W_2. from Teidô-ri. (Lower nicol only, $\times 24$) (Specimen No. AM 440606-11)

Fig. 6. Inclusion of garnet-chlorite-sericite-schist in quartz-monzonitic syenite from Gyokudô-ri. (Lower nicol only, $\times 24$) (Specimen No. AM 440624-14)

Fig. 1

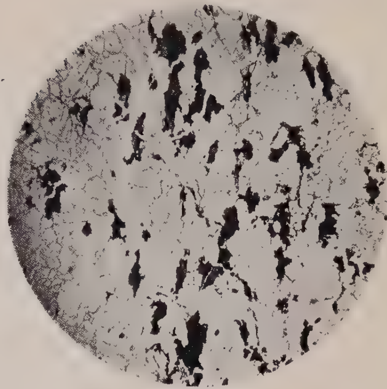

Fig. 2

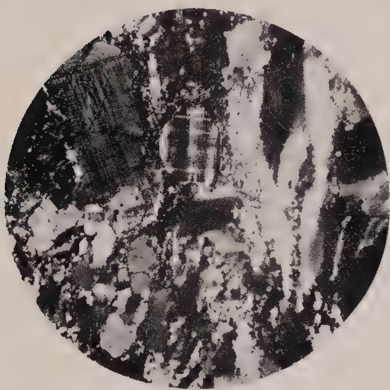

Fig. 3

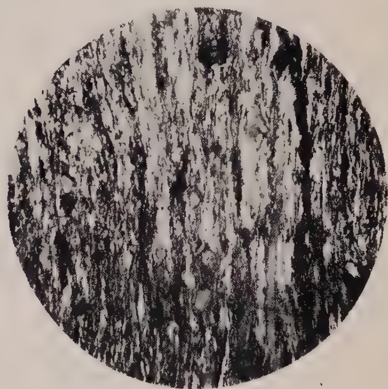

Fig. 4

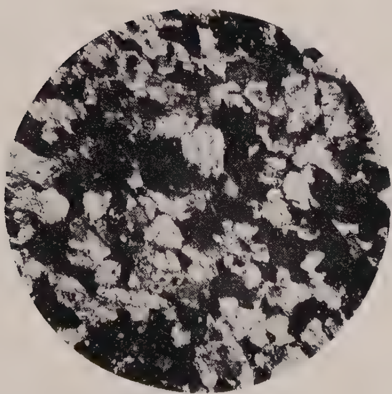

Fig. 5

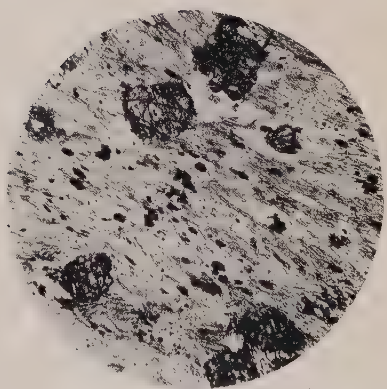

Fig. 6

Plate IV

Explanation of Plate IV

Fig. 1. Porphyritic microcline-perthite, twinned on the Carlsbad law, in aegirine-riebeckite-biotite-nepheline-syenite of series E_1 from Shinjô-zan. (Between crossed nicols. $\times 7$) (Specimen No. 169101)

Fig. 2. Vesuvianite and garnet in nepheline-syenite of series E_1 from Shachô-zan. (Lower nicol only, $\times 9$) More or less prismatic crystals are vesuvianite, the other dark minerals are garnet and biotite. (Specimen No. 440628-11)

Fig. 3. An idiomorphic crystal of vesuvianite in nepheline-syenite of series E_1 from Shachô-zan. (Lower nicol only, $\times 36$) Faces of the prism zone, (100) and (110), are observed, together with cleavage (110). (Specimen No. AM 431204-4)

Fig. 4. Vesuvianite embedded in cancrinite from cancrinite-syenite-pegmatite associated with rocks of series W_1 from the southern slope of Fukushin-zan. $\times 0.7$ (Specimen No. AM 440617-1e)

Fig. 5. Well-formed crystals of allanite or chevkinite in nepheline syenite of series E_1 from Shinjô-zan. (Lower nicol only, $\times 82$) (Specimen No. AM 431203-11)

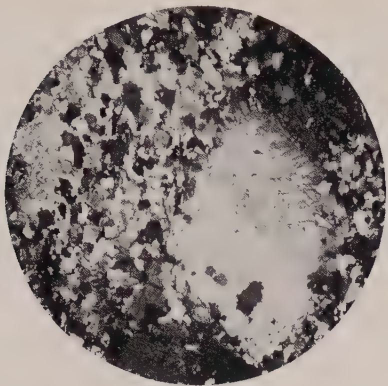
Fig. 1

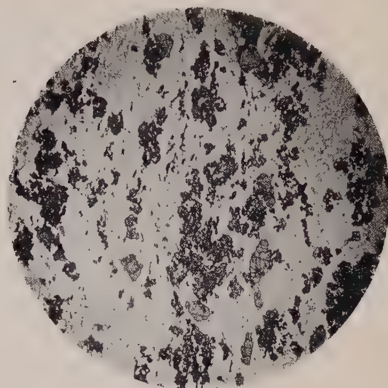
Fig. 2

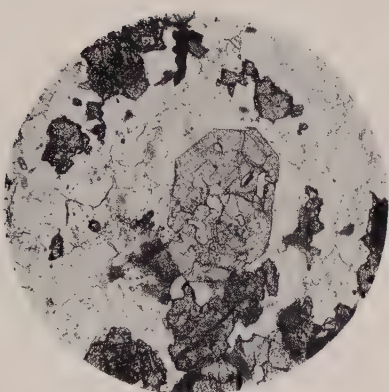
Fig. 3

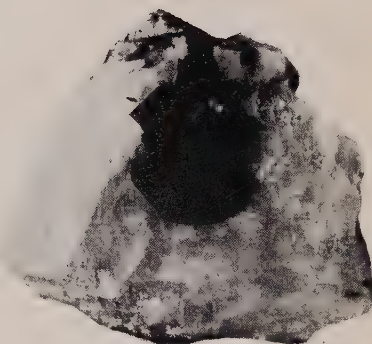
Fig. 4


Fig. 5

Particle Size Distribution in the Vicinity off Sagami River Mouth
(The Processes Forming Beach and Dune Sands)

By

Noriyuki Nasu

Geological Institute, Faculty of Science, University of Tokyo

Abstract

The separation or sorting of modern sediments into sand and mud fractions is quite common in nature. For example, sediments in the vicinity of the Sagami River mouth in Japan fall naturally into two groups separated by the twelve meter depth contour; the well sorted sandy materials occurred shoreward of this line, and muddy sediments were found in deeper water. The transition between these two areas was quite sharp. The significance and cause of this separation is interpreted here in terms of hydrodynamics using the results of particle size distribution analyses of sediments.

As can be shown by well-known principles of hydrodynamics, the settling velocity for sand size fraction is distinctly faster than that for the finer mud fraction; therefore, sand is rapidly settled to the bottom when the water loses its transporting power, while the mud fractions remain in suspension for a long period of time. Also, the critical threshold velocity for the transportation of sediments is minimal for the fine sand size and thus fine sand is most easily transported as bed load along the bottom. These characteristics of the fluid motion accelerate the sorting of sediments into sand and mud fractions.

Table of Contents

Introduction

In 1947 while studying the coastal formations at Ikeshinden in the Shizuoka Prefecture of Japan (Fig. 12), the writer observed that coast dune sands as well as beach sands had fairly constant median diameters and showed good sorting. The abundance of uniformly sorted sand aroused the author's interest in the mechanism by which wind and waves were able to perform this feat. Later, alternate layers of sand and silt with relatively sharp boundaries were also observed in the Miocene Shidara formations in the vicinity of Mt. Horaiji, Aichi Prefecture surveyed in 1948, and in the Zushi formation among the Miura group studied in 1949 on the Miura Peninsula, Kanagawa. The boundaries between each layer were sharp and distinct rather than gradational.

It was thought that the occurrence of uniformly well sorted material as in dunes and beaches, as well as the alternation of layers of sand and silt with relatively sharp boundaries, could be explained on a basis of general hydrodynamic principles operating during the transportation of the sediments (Nasu, 1951, 1954, 1955). Because of basic differences in settling velocity and critical tractive velocity which depend principally upon sediment size, source sediments are sorted into sand and mud fractions during transportation, and upon deposition this will tend to cause a relatively sharp transition be-

tween layers of sand and silt. The same principles are thought to apply to the formation of beach sands, only in this case the fine material has been removed and deposited elsewhere.

To better understand the processes involved in the sorting of sediments an investigation involving both ancient and modern sediments was decided; the modern being used as an analogue to aid in understanding the older formations. Accordingly, a study was made of the sediments of the marine Pliocene Miura group, and a systematic series of samples were obtained from the various types of sand and silt layers within the group (NASU, 1956). Two modern environments were studied in detail: (a) the area off the Sagami River mouth, which is exposed to the open ocean and includes sediments from a beach and narrow continental shelf; and (b) the vicinity of Obitsu Delta, a small river delta in Tokyo Bay.

Later the writer found the general principles relating sorting and particle size distribution of sediments to the fluid mechanics of the transporting medium had been treated theoretically by INMAN (1949). However, it was felt that the application of these principles to certain phase of ancient sediments and to certain specific modern environments was warranted. Considerable time was spent in the present study in investigating the relationship between particle size distributions and the transporting processes in dune and beach sands, along with such features as the steep marginal slope of the small scale delta of the Obitsu River, and in older sediments where relatively sharp boundaries between sandy and silty materials occur.

Coast dunes in the Ikeshinden were resurveyed and also coast dunes in the Mera, Chiba, were surveyed in 1951. A modern sample at Adak, Aleutian Island, and dune samples in the vicinity of Hakodate, Hokkaidō, Japan, were collected in the autumn of 1953. Inland dune sands in the Yuma desert, California, were obtained during 1954. Beach and dune sands in the vicinity of Pismo Beach and Morro Bay, California, were added to the data during 1954 (Fig. 12).

Three different sedimentological occurrences: the characteristically uniformly sorted material of beach and dune sands, the steep marginal slope of small scale delta, and sand and silt alternations in older sediments, are controlled by the same principles which result in the separation of sand and mud fractions during the process of transportation and deposition. The main purpose of this paper is to

interprete the occurrence of beach and dune sands. The other two occurrences will be discussed in another papers (NASU, 1956; NASU and SATO, in preparation).

Since the size, shape, and the specific gravity of sediment components are directly related to the mechanics of transportation, this paper is concerned primarily with the results of particle size distributions of the sediments.

Needless to say, it is very important to check constituents of the sediments including the macro and micro organisms, mineral species, etc., to know the influence of the environment on the sediments. However, this part of the problem is left for fufure investigation and is not treated in detail in this paper.

Acknowledgments

This study was initiated at the Geological Institute, University of Tokyo, and completed at the Scripps Institution of Oceanography, University of California.

The writer is sincerely indebted to Professors Takao SAKAMOTO and the late Yanosuke OTUKA in the Geological Institute, University of Tokyo, and to Professors Robert S. Arthur, Milton N. Bramlette, Douglas L. Inman and Francis P. Shepard of the Scripps Institution of Oceanography, for their guidance and assistance.

Also, the writer is indebted to Messrs. Isamu MURAI and Yoshiaki SATO of the University of Tokyo and to Mr. Gene RUSNAK of the Scripps Institution of Oceanography for their assistance and criticism.

Appreciation is also expressed to Dr. Mashito NAKANO and Mr. Masami KOIZUMI of the Central Meteorological Observatory, and to the Hydrographic Department of Japan for their assistance during this study.

This research has been partly supported by a Grant in Aid for Fundamental Scientific Research from the Department of Education of Japan.

Methods

Sampling

The field survey and the sampling of sediments in the vicinity of the Sagami River mouth were undertaken by R/V Asashio of the

Central Meteorological Observatory of Japan during August 22, 23, and 25, 1950, along three radiating ranges from the river mouth and trending southeast, south, and southwest. The very mouth and the inside of the river were surveyed by a small fishing boat on September 4, 1950. The section between the areas surveyed in August and September, 1950, was completed on October 28, 1950 also by using a small boat. There were 55 samples collected from 54 locations, and designated as Series A samples (Fig. 3).

Because it was impractical to collect all samples at the same time, the only thing that could be done was to collect these over as short a period of time as possible.

In order to get a representative particle size distribution, it is usually advisable to obtain approximately 40 to 50 grams of sediment for each analysis (TWENHOFEL and TYLER, 1941, p. 46). An effort was made to obtain at least 125 grams for each sample, because it is recommended that an extra amount be reserved for other purposes (KRUMBEIN and PETTIJOHN, 1938, pp. 31–33). However, it was sometimes difficult to obtain this quantity of sample with the snapper-type sampling devices used in this study.

Samples were obtained in glass bottles directly from beaches and dunes, while those from shallow water bottoms were obtained by skin diving. The deeper bottom samples were collected by the Marukawa type snapper sampler from a boat (Cent. Meteo. Observatory, 1956).

The depth of water varies due to tides and waves in shallow water where both affect the distribution of sediments. Therefore, the depth at each station was corrected for tide and for the inclination of the line to the bottom sampler, so that the recorded depths all corresponded to the standard reference level (Indian Spring Low Water, or approximately lowest low water) for the area studied. Since the depth variations caused by waves were difficult to measure, they were counted as a part of the measurement error. The reason for such corrections is due to the basic concept that the bottom sediments might reflect the long term processes of the water movement and would be more related to the mean depth of the water than to the depth at the time the samples were collected.

Particle Size Distribution Analyses

Curves showing the weight distribution as a function of the logarithm of particle size for sediments from a certain locality are usually similar to normal distribution, when a sufficient amount of sediment is analyzed (KRUMBEIN, 1939a, p. 584; INMAN, 1952, p. 126). The word "sufficient," as used above, means that this amount will fulfill the basic condition of statistics.

For convinience, the diameter of a particle "d", in millimeters, is replaced here by ϕ as expressed in equation (1) (KRUMBEIN, 1939a,

p. 566).

$$(1) \qquad d=\frac{1}{2^{\phi}}=2^{-\phi} \qquad \text{or} \qquad \log_{10}d=-\phi\log_{10}2$$

The logarithmic scale of d corresponds to the linear scale of ϕ. One example of the weight distribution according to size variation is illustrated in Figure 1A. If the total weight S of fractions coarser than a certain size ϕ in Figure 1A is plotted on the ordinate, Figure 1A will be converted into the curve shown in Figure 1B. This is called a cumulative frequency curve (KRUMBEIN, 1939a, p. 563). If a curve is drawn through certain points, for example, n points based on the actual measurements, and n is large, the curve so constructed will give a close approximation to the true cumulative frequency curve. Then, an approximate frequency curve can be constructed from this cumulative curve by using a graphic differenciating technique (KRUMBEIN, 1934). To facilitate comparison of one sample with

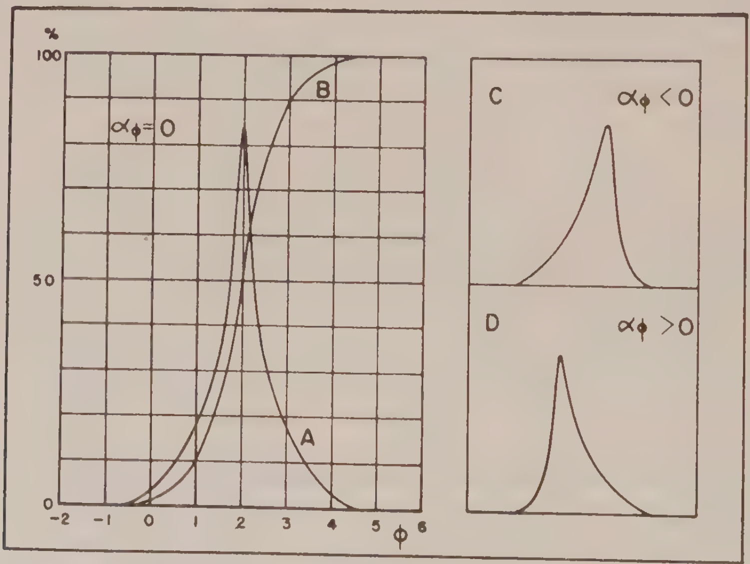

Fig. 1. Erequency Distribution Curves

A. Normal frequency distribution curve.

B. Cumulative frequency curve of the above normal frequency distribution curve.

C. Skewed (negative) frequency distribution curve.

D. Skewed (positive) frequency distribution curve.

another, the total weight of each sample should always be counted as an unit or 100 percent. Therefore, the total area of the frequency curve is 1 or 100 percent in Figure 1A.

The mean value M, standard deviation (or sorting) σ, skewness α_3 and kurtosis β_2, of the frequency distribution curve in Figure 1A are expressed in the following epuations from the viewpoint of statistics (Krumbein, 1936):

(2) $$M=\int\phi\cdot r\cdot d\phi/\int r\cdot d\phi=\int\phi\cdot r\cdot d\phi \qquad (\because \int r\cdot d\phi=1)$$

(3) $$\sigma=\sqrt{\int r\cdot(\phi-M)^2\cdot d\phi/\int r\cdot d\phi}=\sqrt{\int r\cdot(\phi-M)^2\cdot d\phi}$$

(4) $$\alpha_3=\int r\cdot(\phi-M)^3\cdot d\phi/\sigma^3\int r\cdot d\phi=\int r\cdot(\phi-M)^3\cdot d\phi/\sigma^3$$

(5) $$\beta_2=\int r\cdot(\phi=M)^4\cdot d\phi/\sigma^4\int r\cdot d\phi=\int r\cdot(\phi-M)^4\cdot d\phi/\sigma^4$$

Here r is the weight of fraction at any point on the curve in Figure 1A. M indicates the ϕ value at the center of gravity of the frequency distribution curve. Standard deviation σ, shows the horizontal scattering of the frepuency curve. When σ is small, it indicates good sorting, and when the sorting is poor, σ shows a large value. Skewness α_3 shows the degree of asymmetry: the larger the absolute value of α_3, the stronger the degree of asymmetry. If the frequency curve is skewed as shown in Figure 1C, and 1D, the value of α_3 will be negative or positive. If the curve has perfect symmetry with respect to M, then α_3 equals to zero. Kurtosis β_2, is a measure of the sharpness or peakedness of the distribution curve. Furthermore, the ϕ value at S equal to 0.5 or 50 percent in Figure 1B is the median diameter expressed by the notation Md. The projection of the value of the median divides the frequency distribution curve into two equal areas.

Because the calculation of the above measures becomes quite involved, an approximate method (INMAN, 1952) which gives the required accuracy is applied in this study. According to the method, ϕ_5, ϕ_{16}, ϕ_{50}, ϕ_{84}, and ϕ_{95} are defined as the ϕ values for which the cumulative percent of sediment by weight is coarser than 5%, 16%, 50%, 84%, and 95%, respectively.

The phi mean diameter M_ϕ, the phi median diameter Md_ϕ, the phi deviation measure (a measure of standard deviation or sorting) σ_ϕ, the phi skewness measures α_ϕ, $\alpha_{2\phi}$, and the phi kurtosis measure β_ϕ are obtained from the following relations:

(6) $$M_\phi=\frac{1}{2}(\phi_{16}+\phi_{84})$$

(7) $$\sigma_\phi=\frac{1}{2}(\phi_{84}-\phi_{16})$$

(8) $$\alpha_\phi=\frac{M_\phi-\phi_{50}}{\sigma_\phi}$$

(9) $$\alpha_{2\phi}=\frac{\frac{1}{2}(\phi_5+\phi_{95})-\phi_{50}}{\sigma_\phi}$$

(10) $$\beta_\phi=\frac{\frac{1}{2}(\phi_{95}-\phi_5)-\sigma_\phi}{\sigma_\phi}$$

(11) $$Md_\phi=\phi_{50}$$

The equations to calculate ϕ_5, ϕ_{16}, ϕ_{50}, ϕ_{84}, ϕ_{95} values reversely from known values of Md, σ_ϕ, α_ϕ, $\alpha_{2\phi}$, β_ϕ, Md_ϕ were described by Inman (1952, p. 130), so that they will not be described here. The values of ϕ_5, ϕ_{16}, ϕ_{84} and ϕ_{95} are not tabulated in this paper to simplify the case, but if desired, these values can be recalculated using the relation given in Inman's paper.

The values obtained from equations (6) through (10) present approximations or measures of the true values defined by equations (2) to (5).[1] The modal diameter may be the most significant measure of central tendency in the interpretation of the distribution patterns of sediments. However, since the mode is difficult to obtain, the phi median diameter, Md_ϕ, will be used in this study as the measure of central tendency because it more closely approximates the mode than does the mean diameter, M_ϕ (INMAN and CHAMBERLAIN, 1955). The phi deviation measure, σ_ϕ, is a measure of spread or dispersion of sizes, and is used to study the patterns of sorting. The phi skewness measure, α_ϕ, is a measure of asymmetry of the size distribution. Among those six measures, three measures, i. e., Md_ϕ, σ_ϕ, and α_ϕ are used in this paper to illustrate the size distribution of sediments. The values of M_ϕ, β_ϕ, $\alpha_{2\phi}$ are tabulated in Table II and III in the appendix for future references.

The size classification of sediments used in this study is defined in Table I and is an adaptation of systems proposed by Wentworth and Krumbein.

Modern sediments, which were unconsolidated, required little preparatory treatment before analyses. In a few cases for the finest sediments, a 0.025 normal solution of sodium hexametaphosphate,

1) Inman discussed the order of the approximation in the appendix of his paper by choosing several cases. Namely, Normal, Gram-Charlier curves and Pearson Type I and III curves were illustrated which are generally similar to the size frequency distribution curves of sediments.

$Na_6(PO_3)_6$, was used to minimize the effects of flocculation (INMAN, 1953).

Sieving technique (KRUMBEIN and PETTIJOHN, 1938, pp. 135–143) or settling tube method[2] (EMERY, 1938; POOLE et al., 1951) was applied to sandy sediments. For silt and clay size sediments, the pipette method was used (KRUMBEIN and PETTIJOHN, 1938, pp. 166–172). Mixed sediments of sand and silt size were divided into sands and silts by wet sieving; then sieving and pipette methods were applied to each fraction.

Table I. Size Classification of Sediments Used in This Study[3]

Class Range in mm.	Class Range in phi units	Terminology	
d>2	$\phi<-1$	Gravel	
2>d>1	$-1<\phi<0$	Very coarse	Sand
1>d>1/2	$0<\phi<1$	Coarse	Sand
1/2>d>1/4	$1<\phi<2$	Medium	Sand
1/4>d>1/8	$2<\phi<3$	Fine	Sand
1/8>d>1/16	$3<\phi<4$	Very fine	Sand
1/16>d>1/256	$4<\phi<8$	Silt	Mud
1/256>d	$8<\phi$	Clay	Mud

Since the range of particle sizes in any one sample often exceeds any single Wentworth class, the following nomenclature will be applied to sediment aggregates:

Median Diameter coarser than	-1ϕ	Gravel
Median Diameter ranging from	-1ϕ to 4ϕ	Sand
Medirn Diameter finer than	4ϕ	Mud

Sediments off the Sagami River Mouth

Topography

The sand beach along the coast of the Gulf of Sagami extends about forty kilometers between Kamakura and Odawara, except where interrupted by a few minor headlands (Fig. 2). The Ōiso

2) The results by settling tube analysis differ slightly from those obtained by sieve analysis; for example, as discussed by INMAN (1953, pp. 22–23); but it was felt that this discrepancy could be neglected for the purpose of this paper. INMAN (1953) compared the results by two methods on the same sediments and found that the difference became significant when the content of heavy minerals or micaceous materials exceed fifteen percents of the total sample.

3) Classification modified from Krumbein (1939, p. 566) and Wentworth (1922, p. 384).

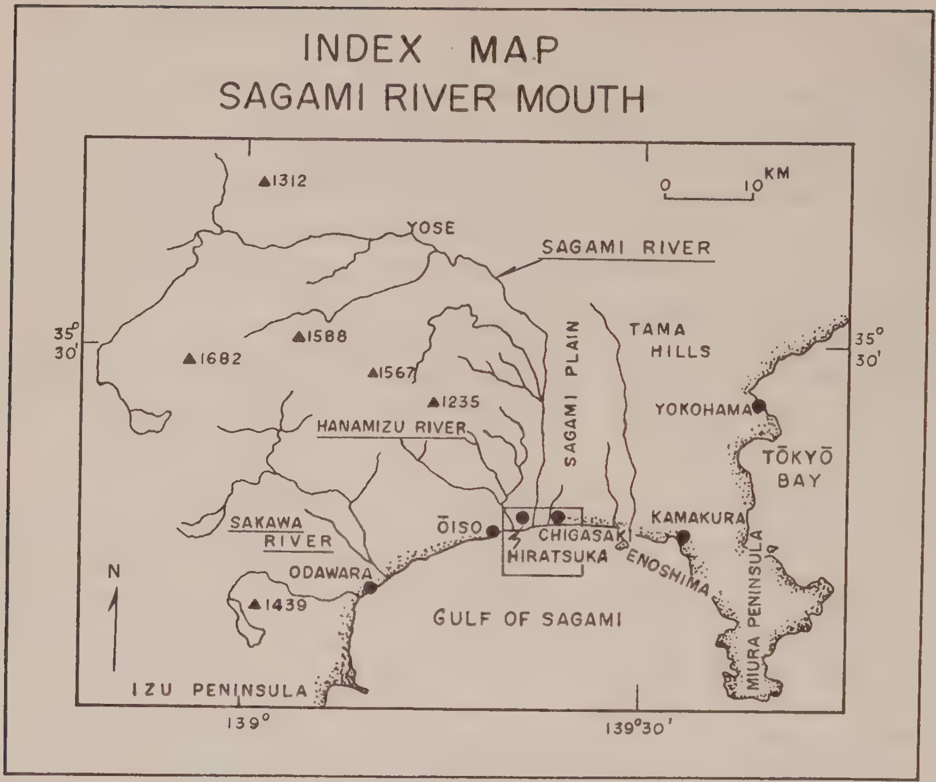

Fig. 2

Tertiary hills extend to the gulf at Ōiso, but the beach continues east of this point where the broad, flat, alluvial Sagami Plain borders the coast. The western half of the gulf coast is bordered by the alluvial plain of the Sakawa River. The Sagami Plain has been cultivated with the exception of a few sand dune areas which have developed especially close to the shore. The latter results in a slightly hilly configuration.

At times in the past the expression "Sagami Bay" has been used for this area, but only the "Gulf of Sagami" will be used here in order to distinguish a coast line exposed to the open sea as opposed to that along a bay with narrow entrance, such as Tokyo Bay.

The Sagami River runs through the Sagami Plain from north to south and joins the gulf between Hiratsuka and Chigasaki. The River has a fairly steep gradient (0°40′ in average) in its upper and

middle reaches, but low gradient (0°08′ in average) over the Sagami Plain.

So far there are no data available about the rate of discharge of the River. Sea water flows inland through the river mouth during periods of high tide at the surface by the writer's observation, but this condition is changed by precipitation which raises the water level of the river. In is not known whether salt water flows inland along the bottom.

The Hanamizu River circles the eastern outskirt of the Ōiso Tertiary hills which mark the western margin of the Sagami Plain, and pours into the sea 3500 meters west of the Sagami River mouth. However, the discharge is far less than that of the Sagami River.

The submarine topography of the surveyed area is shown in

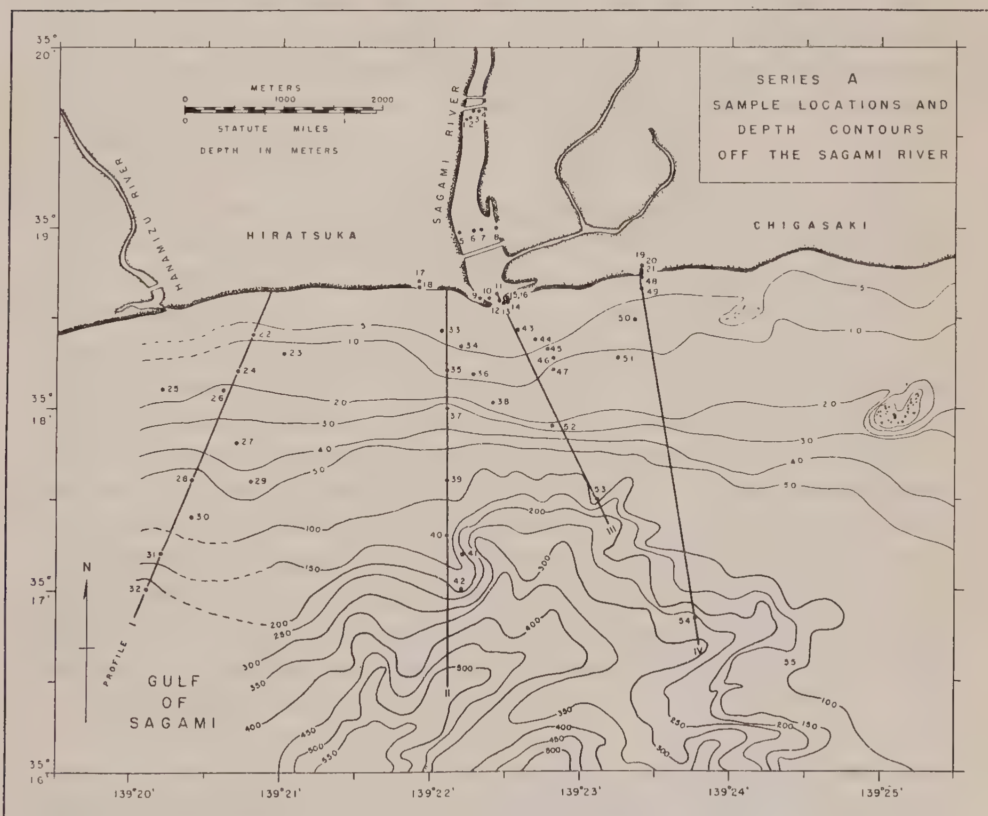

Fig. 3

Fig. 3. Down to depths of 50 meters, the contour lines are almost parallel to the shore, but at the depth of 100 meters, the contours become irregular due to the existence of a submarine canyon of which the head is approximately 1700 meters from the river mouth.

The contour lines in the vicinity of the Sagami River mouth are based upon the detailed echo sounding chart of the Hydrographic Department of Japan, surveyed during 1949 to 1950 (Surv. Hydro. Depart. Japan, 1950). To the west off the Hanamizu River, there was no detailed chart available except No. 80 (Surv. Hydro. Depart. Japan, 1941) and No. 3001 (Surv. Hydro. Depart. Japan, 1955).

There is no deltaic topography at the Sagami River mouth. Approximately ten years ago a dam was constructed at Yose, which is about forty kilometers inland and along the main stream of the river. Prior to this construction, it is possible that a deltaic configuration was present, but, as there was no evidence of this topographical feature according to a chart of that time, the dam apparently had no marked effect upon the topography at the river mouth.

There are two reefs east of the Sagami River mouth, the first being at an approximate distance of 2000 meters and closer to the shore than the other, which is approximately 4000 meters from the river mouth. These reefs are said to be layered sedimentary rocks and are thought to be the western extension of the Neogene Miura group. The results of a boring along the coast at Hiratsuka show a thickness of the alluvial deposits of 84.5 meters covering the consolidated Neogene sediments. (OTUKA, 1937, p. 977).

Since the Ōiso Hills consist also of Neogene sediments, it seems probable that the unconformity between the consolidated late Tertiary rocks and the unconsolidated Quarternary deposits is near the surface off the coast of Chigasaki as indicated by the reefs, then slopes down to the depth of 84.5 meters at Hiratsuka, and comes up again to the surface at Ōiso. The Sagami River or the Paleo-Sagami River might fill the valley between the Ōiso and the Miura-Tama Tertiary Hills, with its alluvial plain now extending to the present coast line.

Field Observations

When the inner river mouth was surveyed on September 4, 1950, the following observations were made:

(1) The river water was a little muddy and the water level was higher than the average. This may have been the result of heavy precipitation upstream, accompanying " Typhoon Jane " centered around the Kansai District (350 kilometers west) on the preceding day.

(2) The bottom sediments consisted only of coarse materials, i. e., gravels and sands; mud was not found. This might indicate that mud which caused the turbidity of the water, was carried in suspension and was not present in appreciable quantity in the bottom sediments.

(3) Sample location A–13, situated at the very mouth of the river at a depth of 6 meters, had a few fresh as well as old bamboo leaves in the sediments. These leaves might have been swept into the river, or the bottom erosion might have exposed older sediments.

(4) The right and the left bank of the river mouth consisted of sand containing gravel. The gravel on the left bank at the river mouth formed a steep slope which extended into the water and some of these gravels were agitated by wave motion.

The conditions observed during the survey on October 28, 1950, were as follows:

(5) Turbid water emanated from the river mouth into the sea. Upon entering the sea the turbid mass expanded to the width of several hundred meters, a width much greater than that of the river. There was a distinct boundary between turbid water and clear sea water.

(6) Cusps were formed along the beach having wave length of several tens of meters. In the vicinity of Sample No. A–21, east of the river mouth, the concave area of the cusp facing the sea was occupied by sand, while the convex points or apices consisted of a mixture of sand and gravel. At sample location A–21, which is situated at the concave portion of a cusp, a vertical section 30–40 centimeters deep showed an alternation downward of fine sand, pebbles, fine sand and coarse sand. This sequence might be an indication of lateral migration of cusps along the beach.

(7) Waves were comparatively low on this particular day so that it was possible to land through the breaker zone and onto the beach at location A–21 in a small fishing boat. However, during the survey in August the breakers were higher, perhaps, about 1.5 meters.

(8) It appeared that the particle sizes of beach sands and dune sands were fairly consistent. The content of gravels increased in the vicinity of the river mouth. Sample A-19 and A-20 were dune sands, and Sample A-18 and A-21 were beach sands. Sample A-17 was taken in the transition area between beach and dunes.

(9) It appeared that well sorted sands were collected from depths shallower than approximately twelve meters. In the samples collected from greater depths the mud content increased. The transition of these two areas was quite sharp. This fact was also observed during the survey in August.

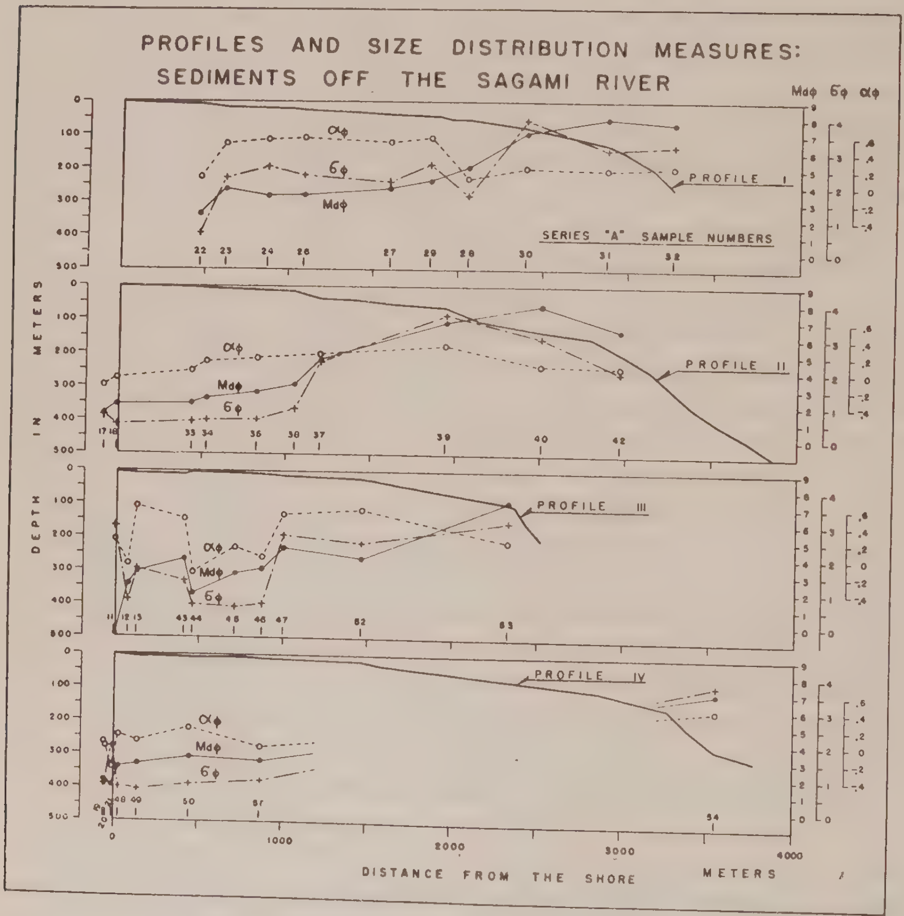

Fig. 4

(10) In the vicinity of the river mouth there was a marked difference in the distribution of sediments. Sand and mud mixtures were collected at depths even shallower than ten meters.

Particle Size Distributions

The phi median diameter Md_ϕ, the phi deviation measure σ_ϕ, and the phi skewness measure α_ϕ for each location are plotted in Fig. 4 with bottom profiles based on Section I, II, III, IV in Fig. 3. The significant aspect of the data from the area, as plotted in Fig. 4, can be summarized as follows:

(1) The median diameters of the beach and dune sands are all within a range of 1ϕ to 2ϕ, and the sorting, as measured by σ_ϕ, is less than 1.0. This indicates the predominance of medium sand on beaches and dunes in this area.

(2) In general, the sorting becomes worse, i. e., σ_ϕ increases in value with the distance from the shore.

(3) In general, the median diameter becomes finer, i. e., Md_ϕ increases in value with distance from the shore.

(4) Some exceptions to the above generalities occur near the river mouth and along the Profile III extending seaward from the river, possibly due to the insufficient sorting of sediments.

(5) Inside the river the sediment is somewhat coarser and the sorting is poor.

In Fig. 5, the phi median diameters as well as the phi deviation measures and the phi skewness measures are plotted as functions of the depth of water. The followings are the major sequences synthesized from this Figure:

(6) Md_ϕ values increase as the depth increases.

(7) The sorting is good and σ_ϕ values are concentrated around 0.5 when the depth is shallower than 12 meters. At depths slightly greater than 12 meters, the values of σ_ϕ suddenly jumps to approximately 2. This result agrees with the visual observation mentioned previously, and has a direct relation to the processes forming beach and dune sands as described in a latter section.

(8) α_ϕ plots are concentrated between −0.4 and zero in shallow water, then change to plus values at the twelve meter depth. In the deeper portions it is difficult to establish a tendency because of the paucity of data.

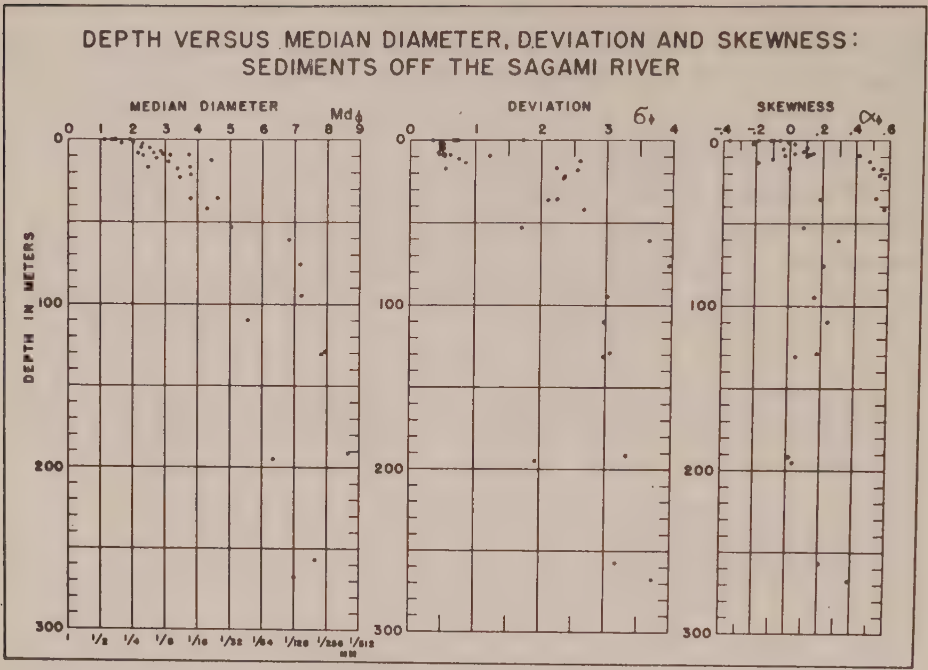

Fig. 5

The phi deviation measure as well as the phi skewness measure are plotted as a function of the phi median diameter in Fig. 6. This figure illustrates the following conclusions:

(9) σ_ϕ values are minimal at median diameter Md_ϕ ranging from 1ϕ to 3ϕ, then increase continuously with both increasing and decreasing values of the median, in general.

(10) For median diameters in the range of -1ϕ to 3ϕ, the skewness as indicated by α_ϕ is concentrated near zero. As the median increases from 3ϕ to 4.5ϕ, the skewness jumps to positive values of about 0.6, then gradually decreases with increasing values of Md_ϕ.

Constituents

A few representative samples (A-7, A-18, A-28, and A-50) were chosen from each area of the investigation, and their constituents coarser than 4ϕ were studied. The same method of visual estimation described by SHEPARD and MOORE (1954) was applied here. The

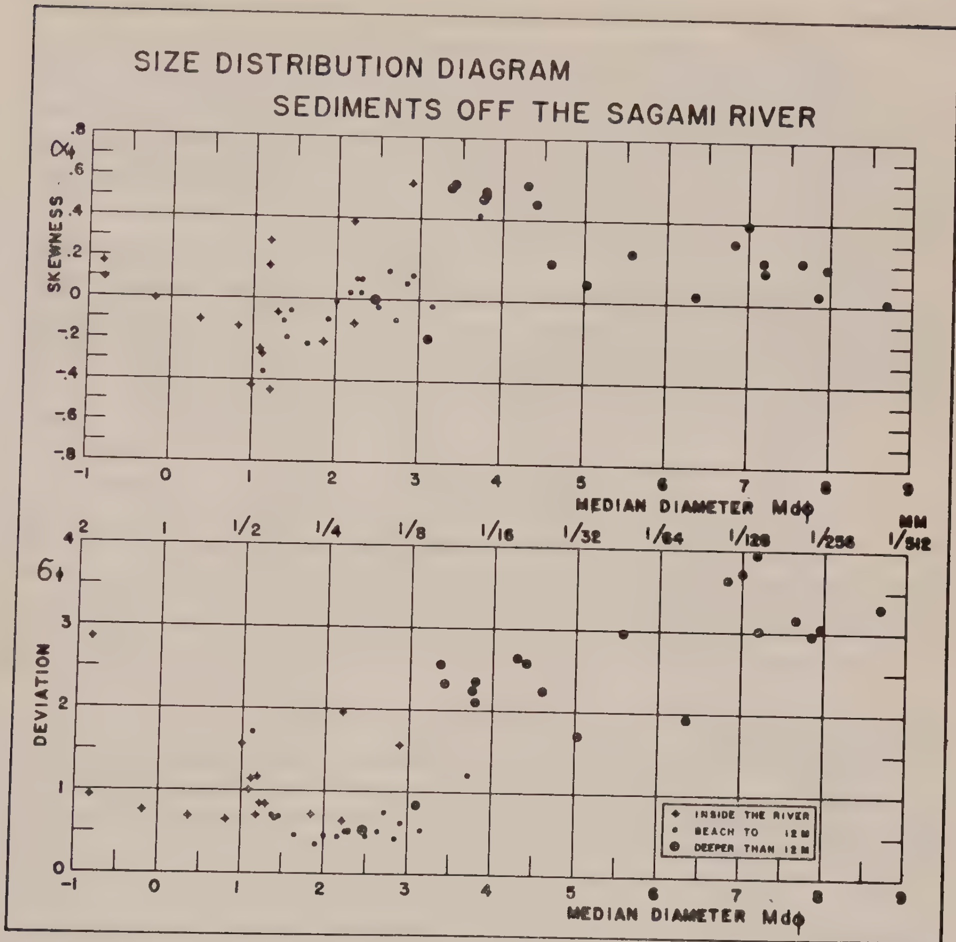

Fig. 6

results as shown in the Table IV in the appendix indicate that the terrigenous materials are more than 99% except Sample A-28 which includes 1.5% of plant fibers.

The same samples for which visual estimation of coarse fraction were made, were divided into heavy and light minerals. Percentage of areas occupied under the microscope for monominerals, rock fragments and other constituents were estimated for each heavy and light part of samples. The mineral grain analyses were based upon the principles described by KRUMBEIN and PETTIJOHN (1938, pp. 320–340).

The results show that light minerals are dominant (about 90%) except in one sample (A-18: 50%) which was located along the beach.

The constituents of each sample suggest that the source of sediment supply might not consist of metamorphic rocks but igneous and sedimentary rocks, because the heavy minerals are predominantly augite, hornblende, hypersthene, olivine and miscellaneous opaque minerals.

Igneous rocks, Tertiary and Mesozoic sedimentary rocks outcrop along the drainage basin of the river except along the Sagami Plain which consists of Quarternary deposit of the river. Metamorphic rocks are rarely seen in this area (FUJIMOTO, 1951; YAMASHITA et al., 1955).

Hydrodynamics

It will be necessary to discuss briefly a few known principles of hydrodynamics because of their importance to the present problem before entering into the interpretation of the sediment distributions in the area, previously mentioned.

Settling Velocity of Particles

The patterns of fluid motion in two geometrically similar situations are identical when the REYNOLDS' number "R" are epual, and the flow changes from laminar to turbulent at the same value of R regardless of the size of flow and features of the fluid (HAGEN, 1839; 1854, p. 17; REYNOLDS, 1883). The definition of R is given by:

(12) $$R=dw/\nu, \qquad \nu=\mu/\rho$$

The symbols are defined as: d: dimension of a particle; w: velocity of the main flow; ν: kinematic coefficient of the viscosity of the fluid μ: dynamic viscosity coefficient of the fluid; ρ: density of the fluid.

When the resistance force "f" of the fluid on a sphere is as expressed in equation (13), the relation between the resistant coefficient C_D in the same equation and the REYNOLDS' number R obtained by various experiments is as illustrated in Figure 7 (PRANDTL-TIETJENS, 1931, pp. 115–116, 130–134; WIESELSBERGER, 1914; WADELL, 1934a; ALLEN, 1900; LIEBSTER, 1927; LADENBURG, 1907; ARNOLD, 1911).

(13) $$f=\frac{1}{2}C_D\,\rho\,w^2\,\pi(d/2)^2$$

Stokes introduced equation (14) when the resistance force f is due only to the viscosity of the fluid and not to the form drag (LAMB, 1932, pp. 597–604).

(14) $$f=3\pi\,\mu\,w\,d$$

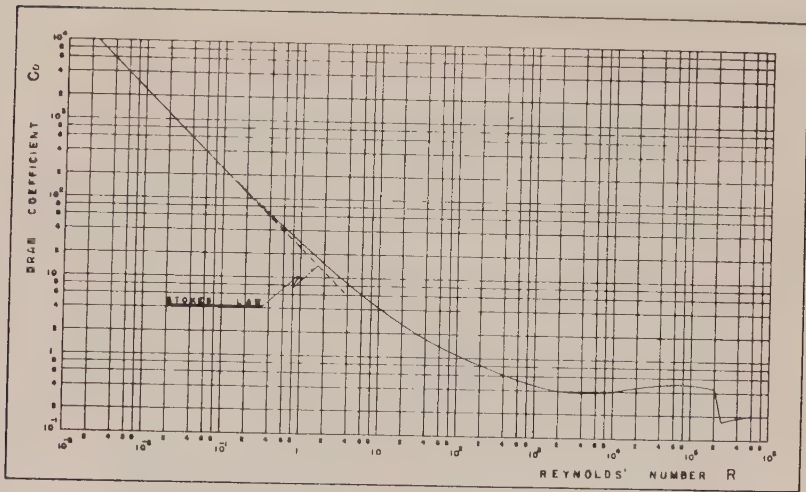

Fig. 7. Drag Coefficient of a Sphere in Terms of Reynolds Number (after Wadell, 1934a, et al.)
Solid curve presents the experimental results.

Combination of (13) and (14) gives

(15) $$C_D R = 24$$

which plots as a straight line in Figure 7. Experimental values shown in this figure (solid line) coincide with this theoretical line up to values of R equal to about 0.2. This straight part of the curve is defined here as the "Stokes law range." On the contrary, when the force f is assumed only due to form drag instead of viscosity, then C_D takes on a constant value regardless of R in equation (13). Infact, in a range of $10^3 < R < 2\times10^5$ the experimental values satisfies this relation, which will be here called "Form drag range." In a range of $0.2 < R < 10^3$ the experimental values show gradual transition from "Stokes law range" to "Form drag range". Finally, the range of $R > 2\mathrm{x}10^5$ can be defined as "Range exceeding the critical Reynolds' number. Here, relation between C_D and R will be converted into that between settling velocity w and particle diameter ϕ or d.

When a sphere falls through a fluid maintaining constant velocity, the force caused by the gravity is balanced with those by the buoyancy and resistance. Thus,

(16) $$\frac{\pi}{6}(\sigma_s - \rho)\, g d^3 = \frac{1}{2}\rho\, C_D\, w^2\, \pi\, \frac{d^2}{4} \qquad \text{(c. g. s. units)}$$

(17) $$\therefore w = \sqrt{\frac{4(\sigma_s - \rho) g d}{3\rho C_D}} \quad \text{or} \quad w = \sqrt{\frac{4(\sigma_s - \rho) g}{30\, C_D \rho \cdot 2^{\phi}}} \qquad (\because 10d = 2^{-\phi})$$

here, σ_s: density of the sphere, ρ: density of a fluid, g: acceleration of gravity. On the other hand.

(18) $$R = \frac{wd}{\nu} = \frac{w}{10\nu \cdot 2^{\phi}}$$

Therefore, from equations (17) and (18)

$$(19) \qquad d=\sqrt[3]{\frac{3\rho\nu^2 C_D R^2}{4(\sigma_s-\rho)g}} \qquad \text{or} \qquad 2\phi=\frac{1}{10}\sqrt[3]{\frac{4(\sigma_s-\rho)g}{3\rho\nu^2 C_D R^2}}$$

$$(20) \qquad w=\sqrt[3]{\frac{4(\sigma_s-\rho)g\nu R}{3\rho C_D}}$$

For each pair of values C_D and R from the curve of Figure 7, there exists a corresponding pair d or ϕ and w which can be computed from epuations (19) and (20). By repeating this process, the R and C_D curve can be converted into ϕ(or d) and w curve. The left half of Figure 8 shows a few representative curves of this relation in different fluid temperatures and sphere densities. The relation between particle size and the time to fall a distance of one centimeter is shown in the right half of the same figure. Among the curves in Figure 8, one case is selected and redrawn in Figure 9 by changing the vertical scale to the logarithmic. Furthermore, two straight lines corresponding to the Stokes law and the Form drag law are inserted in the same figure. Figure 9 follows the original by RUBEY (1933) with a slight change of factors.

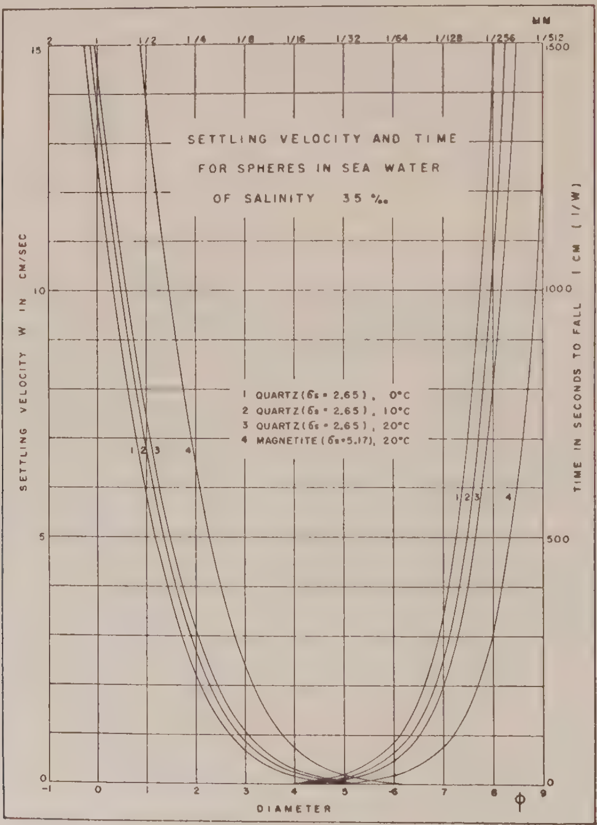

Fig. 8

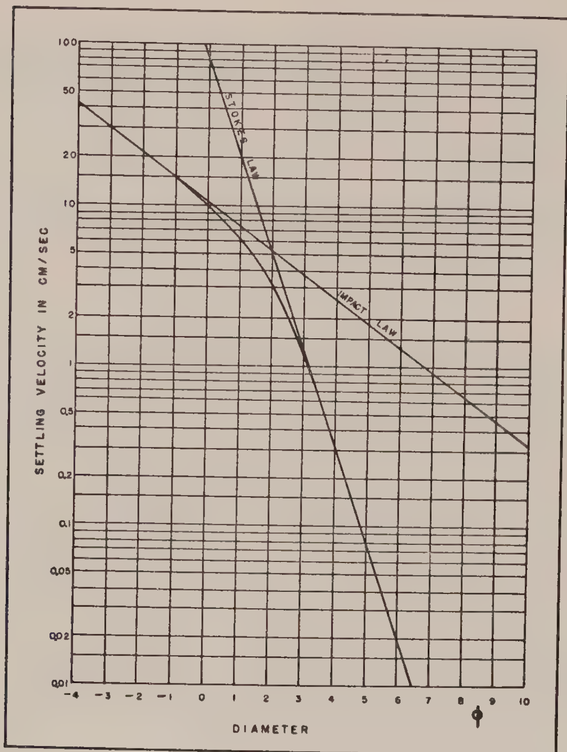

Fig. 9. Settling Velocity of Quartz Spheres in 20°C Sea Water of Salinity 35°/00 in Terms of Their Diameter ("Impact" here means "Form drag" in this paper.)

The range of ϕ values for each curve in Figure 8, corresponding to the transition range ($0.2<R<10^3$) in Figure 7, is as follows:

1	$3.4>\phi>-2.1$
2	$3.7>\phi>-1.8$
3	$4.0>\phi>-1.6$
4	$4.4>\phi>-1.1$

The above range of values approximately corresponds to "sand."

Generally, the specific gravity of quartz can be utilized for sediments (KRUMBEIN and PETTIJOHN, 1938, pp. 101–102). Since individual particles of sediments are not perfect spheres, the influence of shape deformation on the settling velocity must be considered even though this influence is much less in "Stokes law range" (WADELL, 1934b). Inasmuch as the major focus of this paper is the boundary between sands and muds (Stokes law range), the ensuring discussion will assume that all particles are spherically shaped.

In Figure 9 it is observed that sands occupy the particle range from -1ϕ to 4ϕ, which corresponds to the transition range of the Stokes law to the Form drag law. The settling

velocity of silt-clays corresponds to the Stokes law. Note that the original definition of sand and mud is not based upon the hydrodynamical reasons described here but upon the natural distribution of sediments. If it were assumed that the settling velocity is in accordance with the Form drag law through the whole range of ϕ in Figure 9, then the velocity at $\phi=3$ would be shifted to at $\phi=6.4$. The range of the ϕ-scale in Figure 8 is limited to particle sizes of ordinary sediments in nature. Settling velocity is high in the sand range but decreases quickly in the silt-clay range. In a range of sand, settling time is so short that size differences are minimized, but upon entering the silt-clay range the deviation of settling time is immediately increased.

Suspension

The above statements are based upon the situation when a particle falls in stagnant fluid. However, when flow is involved, there is a certain amount of turbulence which is associated with mass exchange in the fluid. Here, vertical mass exchanges will be considered. The difference in turbidity of two water domains will be decreased if the water mass exchange exists between them.

The gravity force compels suspended particles to settle to the bottom, and the vertical component of turbulence inclines to equalize the density of suspended particles from the surface to the bottom. Namely, the turbulence interferes with the settling tendency of suspended particles. Therefore, particles in suspension on the average take a longer time to settle to the bottom in turbulent fluid than in a stagnant one.

Because the stronger the turblence, the longer the settling time, silt-clay will take much longer to settle in a turbulent flow than in a stagnant fluid. Sand and gravel will not be influenced by the turbulence to the extent of silt-clay because of their primary faster settling velocities; therefore, the turbulence in a fluid will accelerate the separation of silt-clay from sand and gravel during transportation.

Threshold Velocity of Bottom Sediments

When the velocity of a fluid rises above zero, the uniform bottom particles will start to move where the current excerts a certain critical tractive force or drag on the bottom. The "friction velocity" which has the dimensions of a velocity and is defined as the square root of the tractive force divided by the density of the fluid, is often used in hydrodynamics in phase of tractive force or drag. The critical value of the friction velocity which causes a certain size sediment to begin motion is called "Threshold velocity" (BAGNOLD, 1954, p. 86; INMAN, 1949, p. 57). Since friction velocity is proportional to the velocity of the fluid at any given height above the bottom according to the von KARMAN-PRANDTL equation for boundary current over a rough surface, the fluid velocity can be related to the friction velocity and hence the drag.

The fluid velocity at some stated height above the bottom for a given threshold velocity will be referred to as the "Threshold mean flow velocity" and should not be confused with the threshold velocity which is a friction velocity. To be rigorous, the threshold mean flow velocity should always include the height at which it was measured.

The result of HJULSTRÖM (1935; 1939, p. 10) who experimented to obtain a relation between the threshold for the mean current in rivers and particle size of sediment is illustrated here in Figure 10 by changing the particle size in ϕ-scale. A curved band A as the results indicates that sand in a range from 0ϕ to 3ϕ starts to move at a velocity of 15 cm/sec. for the particular depths and conditions. The further the particle size

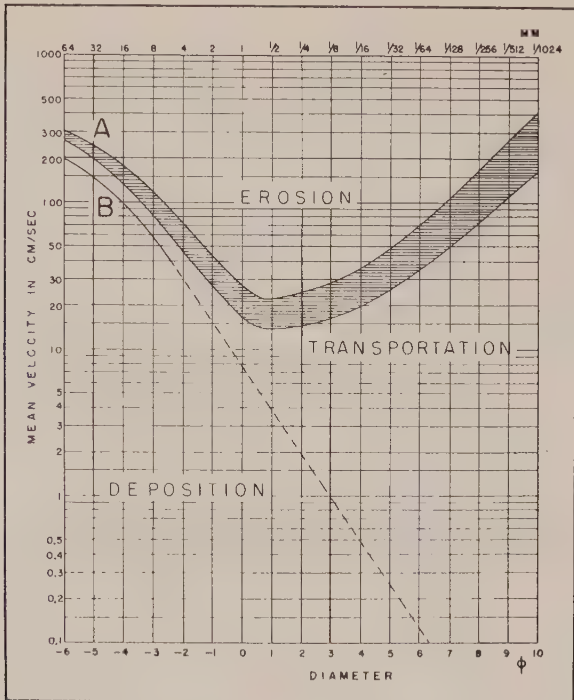

Fig. 10. Threshold Mean Flow Velocity for Particles in Water (after HJULSTRÖM, 1939)

departs from this range, the larger the velocity becomes. Once the motion starts, the particles do not cease their movement at the threshold mean flow velocity, but at a little lower velocity which is expressed by the B line in the figure. MENARD (1950, pp. 150–151) repeated the same type of experiment in a flume, and obtained similar results.

The above mentioned phenomenon has been observed not only in water but also in air. Figure 11 presents the same kind of relation between particle size and threshold velocity in air observed by BAGNOLD (1954, p. 88) and CHEPIL (1945, p. 405). In this figure particles start to move in the impact threshold velocity, and a sheet flow of bottom sediments is caused in the fluid threshold velocity. The minimum threshold velocity in air also in the medium to fine sand range.

It is not so easy to understand that threshold mean flow velocity for silt-clay is larger than that for fine sand. HJULSTRÖM suggested that it might be due to the cohesion of clay minerals. RUBEY (1938) synthesized, on the other hand, the results obtained by GILBERT (1914) and HJULSTRÖM (1935), and interpreted these as the consequence of the bottom boundary laminar layer: namely, there exists a thin laminar layer along the very bottom in a turbulent boundary layer, and small particles hidden in this film have only a rare chance to be plucked into suspension by turbulence.

According to the increase of the velocity, the intensity of turbulence becomes stronger

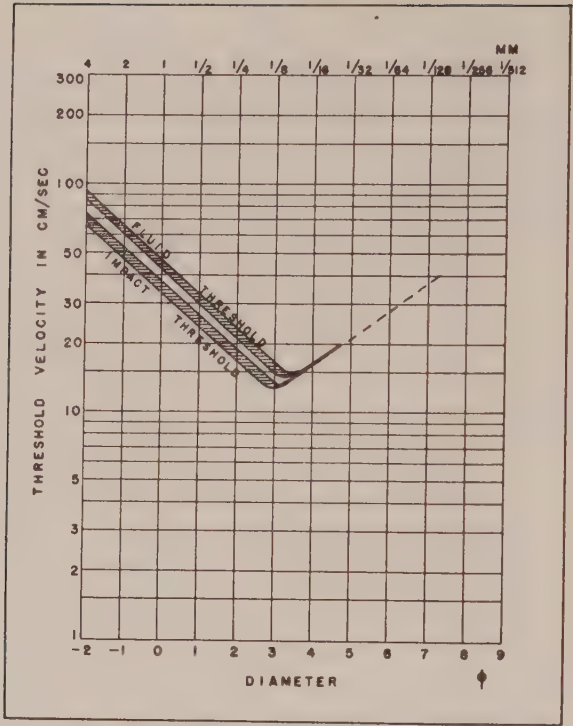

Fig. 11. Threshold Velocity for Particles in Air Flow (after Bagnold, 1954, and Chepil, 1945)

causing disturbance to reach the very bottom more frequently, thus the finer particles start to move.

The existence of the bottom laminar boundary layer is assured when the bottom surface is smooth, but is doubtful when it is rough. LESSER (1951) used three types of sediments and measured the vertical variation of horizontal velocity in a boundary layer in each case. The sediment types were: (1) gravel-sand ($Md\phi=0.18$, sorting poor), (2) mud-sand ($Md\phi=0.88$, sorting poor), and (3) mud ($Md\phi=4.32$, sorting good). The velocity distributions above the former two types satisfied the PRANDTL's equation for rough bottom surface, and the latter fulfilled not only this equation, but also von KARMAN's equation for smooth surface. Therefore, the existence of a laminar film is possible when the bottom consists of silt-clay size fractions.

Sediments and Flows (Summary)

The conclusions drawn of the settling velocity and the threshold velocity of sediments are as follows:

(1) Because settling velocities of sand and gravel are fast, the settling durations are short. In the silt-clay size, since the settling

velocity decreases very rapidly, the settling duration becomes much longer than that for the sand and gravel.

(2) The flow contains turbulence in general; due to this turbulence, vertical water mass exchange tends to postpone the duration of suspension of sediments. The stronger the turbulence is, the longer the duration will be when the particle size is constant. The smaller the size is, the stronger this influence will be when the intensity of turbulence stays constant. Therefore, silt-clays have more chences to be suspended in water.

(3) The threshold mean flow velocity of the bottom sediments is minimal at sand size. One possible cause of such an effect may be the existence of the bottom laminar boundary layer when the bottom surface consists of silt-clay materials. Because the bottom laminar boundary layer will keep the turbulence from reaching the very bottom, and the horizontal velocity will be very slight at this height, the particles small enough to be hidden in this layer will not be moved so easily.

(4) Therefore, settled silt-clays do not start to move at the velocity in which sands initiate their motion. With the increase of the velocity, the finer sediment will be plucked into the water because of the increase of turbulent intensity which reaches the bottom more often than before. Once being in suspension, silt-clays will stay in water for long durations due to their slow settling velocity emphasized by the vertical mass exchanges of water caused by the turbulence. If there is any horizontal advection, they will be transported very easily for a long distance.

(5) Though sands are the easiest to shift, the settling velocity is so fast that they settle back to the bottom quickly and the influence caused by the turbulence will not be as strong as in silt-clays. Therefore, they will tend to stay close to the bottom. Their transportation will be in the form of saltation or bottom surface creep (INMAN, 1949, p. 61).

(6) Gravels are hard to shift and the settling velocity is large, so they will tend to stay within certain limited areas.

(7) The most important fact is that there is a tendency for gravels, sands and silt-clays to separate from each other during the processes of transportation due to the hydrodynamical reasons mentioned here, i.e., sorting will take place. This separation is not

depend upon a special kind of fluid movement, but is due to the common processes of fluid motion which are going on constantly. The motion type differs in different types of sediments; for example, sands may take the creeping style, while silt-clays may be in suspension.

The Processes Forming Beach and Dune Sands

INMAN (1949) gives an explanation concerning the occurrence of beach sands from the theoretical viewpoint in terms of hydrodynamics which also NASU (1951) briefly explained from the same viewpoint based upon his own field data discussed further in this paper and in addition, the occurrence of dune sand is explained.

Particle Size Distribution of Beach and Dune Sands

Sand beach are often well developed along a coast open to the ocean where high waves are generally washing the shore. Sand dunes are often formed just inland from these sand beaches. Between these sand beaches, the coast line may be occupied by gravel beaches or eroded cliffs. Beaches with silty sediments are rarely seen, along the open coast to the ocean, but are often seen near the shorelines inside of bays, lagoons and estuaries.

In general, beaches and coastal as well as inland dunes consist of well sorted sands having median diameters Md_ϕ ranging from 1ϕ to 3ϕ (CARROL, 1939; DAPPLES, 1941; EVANS, 1939; HUFFMAN, and PRICE, 1949; INMAN, 1953; MACCARTHY, 1935; MACCARTHY, and HUDDLE, 1938; MARTENS, 1935; PETTIJOHN, 1949; REED, 1930; SIDWELL, and TANNER, 1939; THOMPSON, 1937). These earlier reported results coinside with those from beach and dune sands along the Gulf coast of Sagami.

In addition, beach sands, coastal and inland dune sands were collected by the writer from several areas in Japan as well as in the United States, as shown in Fig. 12 which are designated here as Series D samples. Table III contains the locations, sampling dates, and results of analyses of these samples. Fig. 13 shows the relations between the phi median diameters and the phi deviation measures and between the phi median diameters and the phi skewness measures. This figure also contains the results of particle size analyses of beach and dune sands among Series A and B samples (NASU and SATO, in preparation). The median diameters of these sands range from 1ϕ to 3ϕ and are well sorted. Interpretation of this figure indicates the fol-

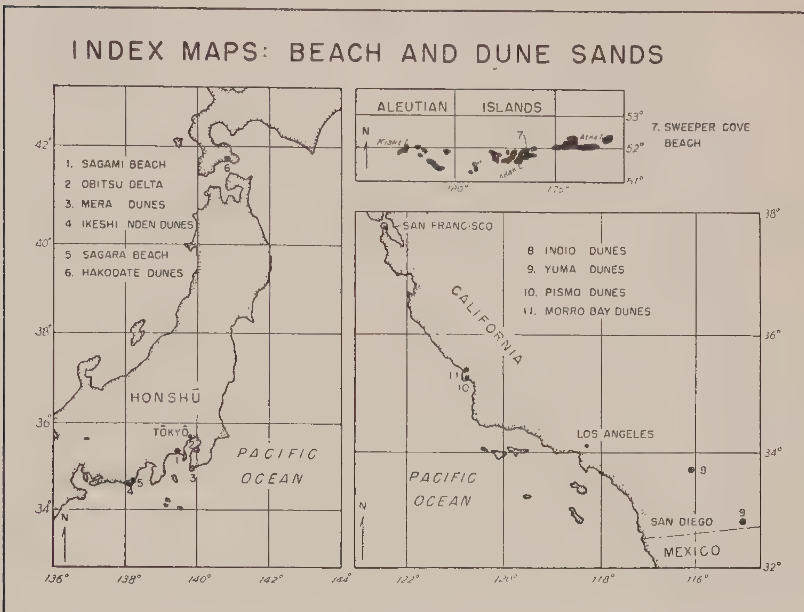

Fig. 12

lowing:

(1) Beach sands have the wider range of median diameters. The sorting is best when Md_ϕ is approximately 2ϕ. Skewness is almost always negative (in the sense that the distribution is skewed towards the coarser particle sizes) (Fig. 1C).

(2) The inland dune sands of the Yuma desert are well concentrated in a range of Md_ϕ between 2ϕ and 2.5ϕ; the sorting is a little poorer than that of the coast dunes; the skewness ranges from negative to positive.

The Effect of Waves in the Surf Zone

It is well known that some sand beaches show a cyclic variation in their profiles; for example, in general, along the coast of southern California the beaches extend seaward during the small waves of summer and are cut back during high waves of winter. This beach cycle is due to seasonal changes in wave characteristics (SHEPARD and LAFOND, 1940). GRANT (1943) suggested that the occurrence of this beach cycle is due to the difference in magnitude of the offshore and

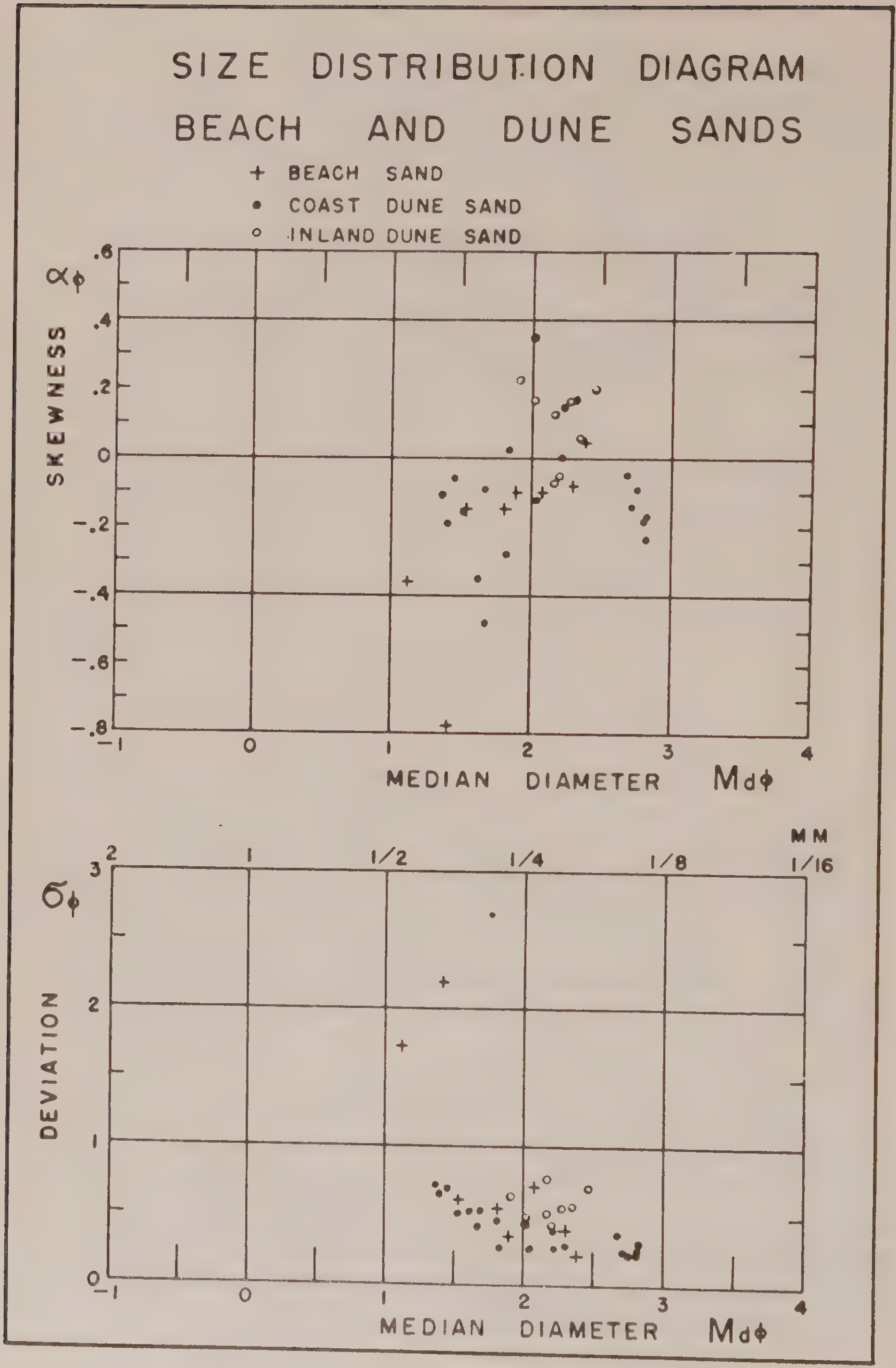
SIZE DISTRIBUTION DIAGRAM
BEACH AND DUNE SANDS
+ BEACH SAND
• COAST DUNE SAND
○ INLAND DUNE SAND
SKEWNESS α_ϕ
.6
.4
.2
0
−.2
−.4
−.6
−.8
−1
0
1
2
3
4
MEDIAN DIAMETER $Md\phi$
MM
2
1
1/2
1/4
1/8
1/16
σ_ϕ
DEVIATION
3
2
1
0
−1
0
1
2
3
4
MEDIAN DIAMETER $Md\phi$

Fig. 13

onshore velocity of water associated with wave motion near shore. MUNK (1949) explained this point later theoretically in his "Solitary wave theory." A brief summary will be presented here to synthesize these points.

At first, two cases will be assumed here to simplify the discussion: (a) wave profiles approaching the shore are sinusoidal having the same magnitude of size and duration of crest as well as trough, and (b) the profiles are trochoidal having steep crest of short duration and shallow trough of long duration. The solitary wave profiles are somewhat similar to the crest part of the trochoidal waves.

Onshore particle movement of water is associated with wave crest, and offshore one is associated with wave trough. During one cycle of sinusoidal waves, the water particle moving onshore with crest is a little more than that of the foregoing, or following trough, moving toward offshore; but the difference is small. On the other hand, since onshore particle movement of a trochoidal wave is larger than that of offshore, there is a considerable water mass movement toward shore. Due to this motion of water, the sea water piles up close to the shore; but when it exceeds a certain limit, it is compensated by the backward water movement such as rip currents (SHEPARD, EMERY and LAFOND, 1941).

The onshore velocity along the bottom is not so different from the offshore velocity in the case of sinusoidal profiles. For trochoidal profiles, the onshore velocities are greater in average than those of offshore. For this reason, in extreme cases, the bottom sediments in shallow water will be shifted only towards shore when the profiles are close to the trochoidal shape and the maximum offshore velocity does not exceed the threshold mean flow velocity of the sediments, while the latter is exceeded by the onshore maximum velocity. The duration of onshore motion or offshore motion does not matter at all in this case.

In general, the wave profiles having long wave lengths as well as long periods during the calm season of summer are actually far closer to the trochoidal shape than the sinusoidal one. During winter, waves are quite high, showing shorter lengths as well as shorter periods because of rough weather, and wave action can be considered somewhat similar to the case discussed in the sinusoidal profiles. Therefore, bottom sands are shifted to the onshore side during sum-

mer and are carried in the reverse direction during winter.

When waves approach shore diagonally, the normal component of wave forces will raise the surface level, and after reaching a certain point will be balanced by the offshore motion of water like rip currents. The parallel component to the shore causes the parallel currents along the shore. These currents called "longshore currents" are generally strongest at the surf zone and the zone slightly beyond the surf. Also, there are lateral components of the wave motion normal to the shore when waves attack the shore diagonally. Therefore, in this case, the bottom sediments are shifted not only normal to, but also parallel to the shore by the combined action of each cycle of waves and longshore currents (SHEPARD and INMAN, 1950; 1951; INMAN and QUINN, 1952; INMAN, 1954).

The Processes Forming Beach and Dune Sands

The orbital current velocities caused by waves have been measured by setting a current meter slightly beyond the surf along the Scripps Institution pier (INMAN and NASU, 1956). The results of these field data indicated that the orbital velocities along the bottom around the surf zone exceed 50 cm/sec. quite often and are occasionally more than 1 m/sec. It is obvious that the sediments of wide range of size will be stirred in the surf zone. KING (1951) mentioned that the depth of disturbance in the sand along the bottom correspond to the wave height. The orbital velocity normal to the shore generally decreases toward offshore because of increasing depth. The bottom sediments will not be disturbed any more beyond the depth where the maximum orbital velocity along the bottom becomes less than the threshold mean flow velocity for sandy sediments.

The movements of gravels, sands and muds near shore areas will be discussed here under the consideration of the above statements as well as the statement described in the section on hydrodynamics.

(1) Since gravels have high settling velocities and also their threshold mean flow velocities are high, rolling or sliding will be the only types of motion. Therefore, possibly, most of them will be distributed in limited areas of extent. For example, they will stay inside river mouths and contribute to expand their alluvial plains, or will stay close to the river mouth when they are brought out to sea. If the source of supply is the eroded sea shore cliffs, generally

speaking, they are also expected to stay close to the source.

(2) It was explained previously that the vertical components of the turbulence or the vertical water mass exchange, cause the sediment suspension, especially of silt-clays. In addition to these, there are horizontal components of the turbulence or horizontal water mass exchanges which cause the horizontal diffusion of suspended materials. Consequently, the suspended sediments are transported horizontally not only by the advections but also by the diffusion. Since the muds derived from the river mouths and cliffs are suspended in water for a long time, they will be scattered over a very wide area by the horizontal advections and the horizontal diffusions before they settle to the bottom. Some of them will be transported parallel to the shore because of longshore currents, but quickly they will be diffused toward offshore areas because of strong turbulence caused by surf waves which will very easily keep these silt-clays in suspension. If there is a plentiful supply of muddy sediments from the source, then the content of muddy deposits will increase suddenly beyond the depth where the bottom orbital velocities caused by waves become less than the threshold mean flow velocities for silt-clays.

(3) Sands have fast settling velocities and show minimum threshold velocities. Therefore, along the surf zone where the bottom velocities exceed the threshold mean flow velocity for sands, they are continuously in motion in form of saltation or creeping along the bottom. When the waves approach diagonally toward shore, the sands are shifted gradually parallel to the shore along the surf zone in the same direction of the longshore current. For this reason, sands migrate easily along the shore from their supply sources such as river mouths or sea shore cliffs and form sand beaches.

(4) Since the waves in the surf zone are rough enough, as along the Gulf coast of Sagami, to churn up the muddy fractions constantly along the open coasts to the ocean or sometimes along the coast of inner basins where winds are strong enough to maintain high waves, only the sandy sediments are able to remain along the shore. Because of grains ranging from 1ϕ to 3ϕ are most easily shifted, the beach sands commonly maintain the median diameters in this range of size and are well sorted. This forms beach sands which occupy long distance along coasts. Furthermore, it is easily understood that the median diameter will be shifted to the coarser fractions and the

sorting will become a little poorer when the waves are higher.

(5) As mentioned previously it has been observed along the Gulf coast of Sagami that there is a sharp boundary at approximately the depth of twelve meters. Well sorted sand occupies the area shallower than this depth and mud content suddenly starts to increase beyond this depth of water. This can be interpreted to show that sands which predominantly creep along the bottom in masses have a different type of motion prior to deposition than silt-clays which are transported in suspension; thus, the boundary between the areas occupied by these different types of sediments will not be gradual, but relatively sharp. This is the case especially along the shore where a great supply of source sediments can be expected. This rapid transition from sandy area to muddy area is not only in evidence in the Gulf of Sagami, but has been pointed out also by HOUGH (1935) at Southern Lake Michigan, and by TWENHOFEL and MCKELVEY (1939) at Devils Lake, Southern Wisconsin.

(6) The above statements are concerned with the action of water. The same process pertains to air as well as the relation between the threshold velocity and the particle diameter of bottom deposits is concerned as shown in Fig. 11. By coincidence, the threshold velocity also is at minimum around 3ϕ of particle size in the air. Therefore, beach sands already sorted by waves will be transported and sorted again by winds when they blow continuously; thus, sand dunes consisting of well sorted sands will be formed on the inland side of the sand beaches. The process will be the same in the interior, especially in desert dunes. The inland areas with strong winds and low precipitation like the deserts, for example, will have more chance to accumulate the wind-shifted sands to certain limited areas of extent and form sand dunes of which sands are well sorted and have fairly constant median diameters. The process forming the inland dune sands is essentially the same as that for coastal dune sands.

Relations Between Median Diameter, Sorting, and Skewness

The relations between Md_ϕ and σ_ϕ, as well as Md_ϕ and α_ϕ are very similar to each other throughout the results of particle size distribution analyses of the sediments along the Gulf of Sagami (Fig. 6 and 13), the Obitsu Delta (Fig. 14), and the Pliocene Miura group

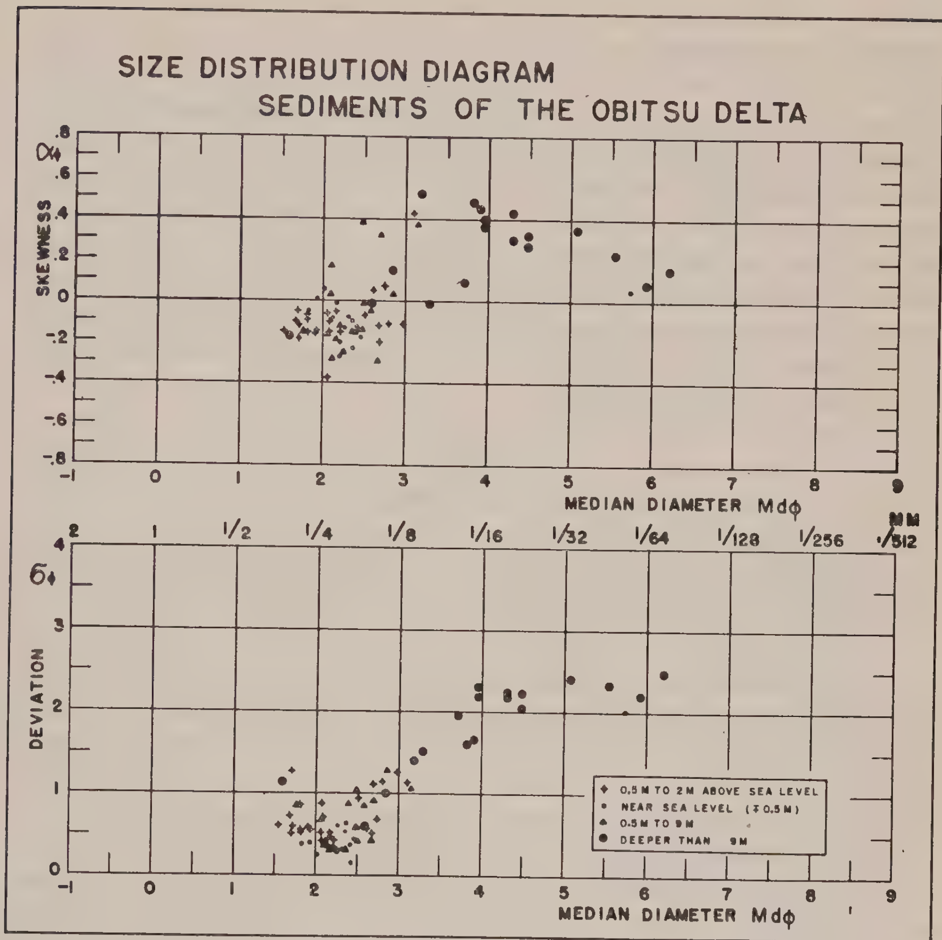

Fig. 14. Size Distribution Diagram of the Sediments of the Obitsu Delta, Chiba, Japan (after NASU and SATO, in preparation)

(NASU, 1956). These are not only seen in the cases of the writer's research, but also common among works cited previously (EMERY and STEVENSON, 1950; GRIFFITH, 1951; 1952; HOUGH, 1940; 1942; INMAN and CHAMBERLAIN, 1955; KRUMBEIN, 1939b; SHUKRI and HIGAZY, 1944; and TWENHOFEL, 1946).

The process resulting in the best sorting of median diameters in medium to fine sand ranges has already been interpreted from the viewpoint of hydrodynamics. Therefore, in sediments having a median

diameter apart from this range, the sorting will become poorer, because such sediments have larger threshold mean flow velocities.

Since the sediments tend to separate into sand and mud fractions during the common processes of transportation, source sediments having a wide range of size distribution will be separated into sands and muds in the course of time and distance. Therefore, the characteristic negative skewness of sediments having coarser median diameters than 3ϕ might be the result of the separation and escape of mud fractions from the source sediments (Fig. 1C). On the other hand, the large positive skewness at the finer median diameters around 4ϕ might be the evidence of the separation and escape of coarser materials from the source sediments (Fig. 1D).

Summary and Conclusions

As a result of a few established principles in hydrodynamics, sediments are commonly separated into sand and mud fractions during the common processes of transportation and deposition.

The significance and geologic importance of this separation reflected by the actual distribution of modern sediments in nature have been discussed in this paper. The area of the investigation was principally the nearshore area off the Sagami River mouth (Figs. 2 and 3). In addition, beach and dune sands were collected from different areas in Japan as well as in California. (Fig. 12).

The collected sediments were analyzed in various ways, but principally, the results of the particle size distribution of these samples have been used for the interpretation. Phi median diameters Md_{ϕ}, phi deviation measures σ_{ϕ}, and phi skewness measures α_{ϕ}, obtained from particle distribution curves, were the principal measures for the interpretation (Fig. 1).

In the vicinity off the Sagami River mouth, the topographic contours are parallel to the beach to a minimum depth of fifty meters. Well sorted sands occupy depths to approximately twelve meters and also cover beach and dune areas of the coast. In the samples collected from depths greater than twelve meters the mud content increased significantly. Thus, this approximate twelve meter depth contour can be considered as a narrow transition zone between sandy and muddy areas (Figs. 4 and 5).

The samples collected from different areas along the Pacific Ocean indicate that the beaches and coast as well as inland dunes consist in general of very well sorted medium to fine sands (Fig. 13).

Throughout these investigations of various areas, there existed always similar tendencies as seen in Figures 6, 13 and 14; namely, the sorting values are least when the phi median diameters are around 2ϕ, and the skewness values tend to be negative when the phi median diameters are less than 3ϕ, then suddenly increase toward large positive values when the phi median diameters approach 4ϕ. When the median diameters exceed 4ϕ, the phi skewness values in general decrease gradually toward zero.

Muds are suspended in water for a long period and are transported for a long distance by advection as well as the horizontal turbulence in water because of their slow rate of settling. On the contrary, the settling velocity of sand is very fast, though its tractive velocity, especially of fine sand is least compared with those for muds and gravels (Figs. 8 and 10). Gravels are not easily shifted due to their weight. Therefore, gravels, sands, and muds will be separated from each other during the common processes of transportation.

The orbital currents along the bottom are sometimes strong enough to churn up the sediments around the surf zone: The component of the orbital currents parallel to the shore, together with the longshore currents, will shift a part of the sediments from the river mouths along the shore when waves attack the shore diagonally. Thus, mud fractions on the bottom are put into suspension and scattered offshore by the horizontal water exchanges, and are not able to remain close to the shore. Only the well sorted medium and fine sands having fairly constant median diameters are able to stay along the shore and form sand beaches.

Under such a depositional environment as the Gulf of Sagami where the plentiful supply of muds, as well as sands, are expected during periods of precipitation, mud content increases abruptly beyond the limit of wave disturbances on the bottom, which was approximately twelve meters in case of the survey.

The threshold velocity in air is minimal when the median diameter is around 3ϕ. Therefore, winds select the fine sands from the beach sediments, which have already been sorted by the wave action, and form the coastal sand dunes inland of sand beaches. This is the case

not only near the coast but also in the further inland areas as in the Yuma desert dunes (Figs. 11, 12 and 13). This is the mechanism which form well sorted dune sands having fairly constant median diameters.

On the other hand, when the sediments supplied from river mouths exceed the scattering agency of waves and longshore currents, a delta may well be formed at the river mouth, for example, as seen in the Obitsu Delta in Tokyo Bay.

A sudden change of skewness measures from negative to positive in a range of median diameters from 3ϕ to 4ϕ is probably due to the separation of sand and mud during transportation.

References cited

ALLEN, H. S., 1900, The motion of a sphere in a viscous fluid: Phil. Mag., 5th Ser., v. 50, pp. 334–337.

ARNOLD, H. D., 1911, Limitations imposed by slip and inertia terms upon Stokes' Law for the motion of spheres through liquids: Phil. Mag., 6th Ser., v. 22, p. 762.

BAGNOLD, R. A., 1954 (or 1941, 1st Ed.), The physics of blown sand and desert dunes (2nd Ed.): Methuen & Co., London, 265 p.

CARROL, D., 1939, Beach sands from Bunbury, Western Australia: Jour. Sed. Petrol, v. 9, n. 3, pp. 95–104.

Cent. Meteo. Observ., Japan, 1956, Kaiyo kansoku shishin (6th Ed.): Oceanogra. Soc. Japan, 252 p.

CHEPIL, W. S., 1945, Dynamics of wind erosion: Soil Sci., v. 60, pp. 305–320; 397–411; 475–480.

DAPPLES, E. C., 1941, Surficial deposits of the deserts of Syria, Trans-Jordan, Iraq and western Iran: Jour. Sed. Petrol., v. 11, n. 3, pp. 124–141.

EMERY, K. O., 1938, Rapid method of mechanical analysis of sands: Jour. Sed. Petrol., v. 8, n. 3, pp. 105–111.

——, and R. E. STEVENSON, 1950, Laminated beach sands: Jour. Sed. Petrol., v. 20, n. 4, pp. 220–223.

EVANS, O. F., 1939, Sorting and transportation of material in the swash and backwash: Jour. Sed. Petrol., v. 9, n. 1, pp. 28–31.

FUJIMOTO, H., 1951, Nippon Chiho Chishitsushi-Kwanto Chiho: Asakura Book Co., Tokyo, 315 p.

GILBERT, G. K., 1914, Transportation of debris by running water: U. S. Geol. Survey Prof. Paper 86, 263 p.

GRANT, U. S., 1943, Waves as a sand-tranporting agent: Amer. Jour. Sci., v. 241, n. 2, pp. 117-123.

GRIFFITHS, J. C., 1951, Size versus sorting in some Caribbean sediments: Jour. Geol., v. 59, n. 3, pp. 211–243.

——, 1952, Grain-size distribution and reservoir-rock characteristics: Bull, Amer. Assoc. Pet. Geol., v. 36, n. 2, pp. 205–229.

HAGEN, G., 1839, Über die Bewegung des Wassers in engen zylindrischen Röhren: Pogg. Ann., Bd. 46, S. 423.

——, 1854, Abh. Akad. Wiss., Berlin, S. 17.

HJULSTRÖM, F., 1935, Studies of the morphological activity of rivers as illustrated by the River Firis: Geol. Inst. Upsala Bull. v. 25, pp. 267–270.

——, 1939, Transportation of debris by moving water: In Trask (ed.), Recent Marine Sediments, Tulsa, pp. 5–31.

HOUGH, J. L., 1935, The bottom deposits of southern Lake Michigan: Jour. Sed. Petrol., v. 5, n. 2, pp. 57–80.

——, 1940, Sediments of Buzzards Bay, Massachusetts: Jour. Sed. Petrol., v. 10, n. 1, pp. 10–32.

——, 1942, Sediments of Cape Cod Bay, Massachusetts: Jour. Sed. Petrol., v. 12, n. 1, pp. 10–30.

HUFFMAN, G. G., and W. A. PRICE, 1949, Clay dune formation near Corpus Christi, Texas: Jour. Sed. Petrol., v. 19,, n, 3, pp. 118–127.

INMAN, D. L., 1949, Sorting of sediments in the light of fluid mechanics: Jour. Sed. Petrol., v. 19, n. 2, pp. 51–70.

——, 1952, Measures for describing the size distribution of sediments: Jour. Sed. Petrol., v. 22, n. 3, pp. 125–145.

——, 1953, Areal and seasonal variation in beach and nearshore sediments at La Jolla, California: Beach Erosion Board Tech. Memo., n. 39, 82 p.

——, 1954, Beach and nearshore processes along the southern California coast: Geology of southern California. California State Division of Mines Bull. 170, 6 p.

——, and T. K. CHAMBERLAIN, 1955, Particle-size distribution in nearshore sediments: Soc. Econ. Paleo. & Mineral., Spec. Pub., n. 3, pp. 106–129.

——, and N. NASU, 1956, Orbital velocities associted with wave action near the breaker zone: Beach Erosion Board Tech. Memo. n. 79, 43 p.

——, and W. H. QUINN, 1952, Currents in the surf zone: Proc. 2nd Conf. on Coastal Engin., Houston, Texas, Nov., 1951, pp. 24–36.

KING, C. A. M., 1951, Depth of disturbance of sand on sea beaches by waves: Jour. Sed. Petrol., v. 21, n. 3, pp. 131–140.

KRUMBEIN, W. C., 1934, Size frequency distribution of sediments: Jour. Sed. Petrol., v. 4, pp. 65–77.

——, 1936, Application of logarithmic moments to size frequency distribution of sediments: Jour. Sed. Petrol., v. 6, pp. 35–47.

——, 1939a, Graphic presentation and statistical analysis of sedimentary data: In Trask (ed.), Recent Marine Sediments, Tulsa, pp. 558–591.

——, 1939b, Tidal lagoon sediments on the Mississippi delta: In Trask (ed.), Recent Marine Sediments, Tulsa, pp. 178–194.

——, and F. J. PETTIJOHN, 1938, Manual of sedimentary petrography: Appleton-Century-Crofts, Inc., New York, 549 p.

LADENBURG, R., 1907, Über die innere Reibung zäher Flüssigkeiten und ihre Abhängigkeit vom Druck: Ann. Physik, Bd. 22, S. 287.

LAMB, H., 1932, Hydrodynamics (6th ed.): Cover Pub. Inc., New York, 738 p.

LESSER, R. M., 1951, Some observations of the velocity profile near the sea floor: Trans. Amer. Geoph. Union, v. 32, n. 2, pp. 207–211.

LIEBSTER, H., 1927, Über den Wiederstand von Kugeln: Ann. Physik, Bd. 82, S. 541.

MACCARTHY, G. R., 1935, Eolian sands: a comparison: Amer. Jour. Sci,, 5th Ser., v. 30, n. 176, pp. 81–95.

——, and J. W. HUDDLE, 1938, Shape-sorting of sand grains by wind action: Amer. Jour. Sci., v. 35, n. 205, pp. 64–73.

MARTENS, J. H. C., 1935, Beach sands between Charleston, south Carolina, and Miami, Florida: Bull. Geol. Soc. Amer.,v. 46, n. 10, 1563–1596.

MENARD, H. W., 1950, Sediment movement in relation to current velocity: Jour. Sed. Petrol., v. 20, n. 3, pp. 148–160,

MUNK, W. H., 1949, The solitary wave theory and its application to surf problem: Annals. New York Acad. Sci., v. 151, Art. 3, pp. 376–424.

NASU, N., 1951, Interpretation of sedimentation phenomena in terms of fluid dynamics (Short communication): Jour. Geol. Soc. Japan, v. 57, n. 671, pp. 367–368.

——, 1954, Origin of sand and silt alternations (Discontinuous graded beddings) (Abstract): Bull. Geol. Soc. Amer., v, 65, n. 12, Part 2, p. 1290.

——, 1955, Significance of the separation of sediments into sand and mud fractions during common processes of transportation illustrated by modern and Tertiary sediments: unpublished dectoral dissertation, Scripps Institution of Oceanography, University of California, 161 p.

——, 1956, The origin of sand and silt alternations (Discontinuous graded beddings): Jour. Fac. Sci., Univ. Tokyo, Sec. II, v. 10, pp. 109–131.

——, and Y. SATO, (in preparation), Particle size distribution of the Obitsu Delta (The occurrence of the steep marginal slope of a small scale delta).

OTUKA, Y., 1937, Geolosic structure of the southern Kwanto region, Japan (in Japanese with English résumé): Bull. Earthquake Res. Inst., Tokyo Imp. Univ. v. 15, Part 4, pp. 974–1040.

PETTIJOHN, F. J., 1949, Sedimentary rocks: Harper and Brothers, New York, 526 p.

POOLE, D. M., W. S. BUTCHER, and R. L. FISHER, 1951, The use and accuracy of the Emery settling tube for sand analysis: Beach Erosion Board Tech Memo. n. 23, 11 p.

PRANDTL, L., and O. TIETJENS, 1931, Hydro-und Aerodynamik: Bd. 2, Julius Springer, Berlin, 299 p.

REED, R. D., 1930, Recent sands of California: Jour. Geol., v. 38, n. 3, pp. 223–245.

REYNOLDS, O., 1883, An experimental investigation of the circumstances which determine whether the motion of water shall be direct or sinuous, and of the law of risistance in parallel channels: Phlios. Trans. Roy. Soc. London.

RUBEY, W. W., 1933, Settling velocities of gravel, sand and silt particles: Amer. Jour. Sci., 5th Ser., v. 25, n. 148, pp. 325–338.

——, 1938, The force required to move particles on a stream bed; U. S. Geol. Survey Prof. Paper 189–E, pp. 121–141.

SHEPARD, F. P., K. O. EMERY, and E. C. LAFOND, 1941, Rip currents: a process of geological importance: Jour. Geol., v. 49, n. 4, pp. 337–369.

——, and D. L. INMAN, 1950, Nearshore water circulation related to bottom topography and wave refraction: Trans. Amer. Geoph. Union, v. 31, n. 2, pp. 196–212.

——, and D. L. INMAN, 1951, Nearshore circulation: Proc. lst Conf. on Coastal Engin., Long Beach, California, Oct., 1950, pp. 50–59.

——, and E. C. LAFOND, 1940, Sand movements along the Scripps Institution Pier: Amer. Jour. Sci., v. 238, n. 4, pp. 272–285.

——, and D. G. Moore, 1954, Sedimentary environments differenciated by coarse-fraction studies: Bull. Amer. Assoc. Pet. Geol., v. 38, n. 8, pp. 1792–1802.

Shukri, N. M., and R. A. Higazy, 1944, Mechanical analysis of some bottom deposits of the northern Red Sea: Jour. Sed. Petrol., v. 14, n. 2, pp. 43–69.

Sidwell, R., and W. F. Tanner, 1939, Sand grain patterns of west Texas dunes: Amer. Jour. Sci., v. 237, n. 3, pp. 181–187.

Surveys of Hydrographic Department of Japan, 1941, Chart of Nozima Saki to Omai Saki: Chart No. 80.

——, 1950, Sagami Bay (Part 1): unpublished original chart, surveyed between Sept. 1949 and Oct. 1950.

——, 1955, Sagami Bay: Chart No. 3001.

Thompson, W. O., 1937, Original structures of beaches, bars and dunes: Bull. Geol. Soc. Amer., v. 48, n. 6, pp. 723–752.

Twenhofel, W. H., 1946, Beach and river sands of the coastal region of southwest Oregon with particular reference to black sands: Amer. Jour. Sci., v. 9, n. 3, pp. 114–139.

——, and V. E. McKelvey, 1939, The sediments of Devil Lake, a eutropic-oligotropic lake of southern Wisconsin: Jour. Sed. Petrol., v. 9, n. 3, pp. 105–121.

——, and S. A. Tyler, 1941, Methods of study of sediments: McGraw-Hill Book Co., Inc., New York and London, 183 p.

Wadell, H., 1934a, Some new sedimentation formulas: Physics, v. 5, pp. 281–291.

——, 1934b, The coefficient of resistance as a function of Reynolds number for solids of various shapes: Jour. Franklin Inst., v. 217, n. 4, pp. 459–490.

Wentworth, C. K., 1922, A scale of grade and class terms for clastic sediments: Jour. Geol., v. 30, pp. 377–392.

Wieselsberger, C., 1914, Der Luftwiederstand von Kugeln: Z. F. M., Bd. 5.

Yamashita, N. et al., 1955, Geological map of the Kwanto region: Naigai Chizu Co. Inc., Tokyo.

Appendix

Table II. Data on Particle Size Distribution of Series A Samples
Sediments off the Sagami River Mouth

Sample No.	M_ϕ	Md_ϕ	σ_ϕ	α_ϕ	β_ϕ	$\alpha_{2\phi}$	% Sand	% Silt	% Clay	Sampling Date	Depth in Meters	Environment
A-1	0.83	1.08	1.01	−0.25	0.92	−0.85	92	0	0	1950-9-4	0.8	river
A-2	0.79	1.11	1.14	−0.27	0.64	−0.64	91	0	0	1950-9-4	0.8	river
A-3	0.73	0.82	0.65	−0.14	0.87	−0.44	96	0	0	1950-9-4	0.8	river
A-4	−0.73	−0.82	0.94	0.09	0.63	0.21	58	0	0	1950-9-4	0.7	river
A-5	1.69	1.84	0.72	−0.21	0.93	−0.63	99	0	0	1950-9-4	2.5	river
A-6	1.51	1.18	1.17	0.28	1.20	0.20	90	5	0	1950-9-4	1.4	river
A-7	0.31	0.99	1.57	−0.43	0.53	−0.47	79	1	0	1950-9-4	0.6	river
A-8	0.29	0.37	0.68	−0.11	1.01	−0.03	94	1	0	1950-9-4	0.3	river
A-9	1.23	1.29	0.84	−0.07	0.40	−0.02	99	0	0	1950-9-4		river bank
A-10	1.29	1.18	0.70	0.16	0.70	0.28	100	0	0	1950-9-4	1.7	river
A-11	−0.35	−0.83	2.84	0.17			51	1	0	1950-10-28	2.5	river
A-12	2.14	2.22	0.64	−0.12	1.62	−1.02	98	1	0	1950-9-4	2.7	river
A-13	3.77	2.89	1.56	0.57			71	19	9	1950-9-4	6.0	river
A-14	2.95	2.20	1.97	0.38	0.92	1.09	74	21	5	1950-10-28	3.0	river
A-15	0.84	1.22	0.85	−0.45	0.82	−0.84	95	0	0	1950-9-4		river bank
A-16	−0.18	−0.18	0.76	−0.01	0.63	−0.07	86	0	0	1950-9-4		river bank
A-17	1.27	1.40	0.67	−0.19	1.18	−0.81	97	0	0	1950-10-28		dune
A-18	1.86	1.90	0.35	−0.10	1.10	−0.72	100	0	0	1950-10-28		beach
A-19	1.41	1.45	0.69	−0.06	0.61	−0.13	100	0	0	1950-10-28		dune
A-20	1.29	1.37	0.71	−0.11	0.65	−0.32	99	0	0	1950-10-28		dune
A-21	0.50	1.12	1.72	−0.36	0.29	−0.43	80	0	0	1950-10-28		beach
A-22	2.35	2.30	0.53	0.10	1.03	0.21	98	2	0	1950-8-25	9.7	open sea
A-23	4.86	3.75	2.23	0.50	0.63	0.94	55	34	11	1950-8-25	16.7	open sea
A-24	4.75	3.36	2.55	0.55			58	29	13	1950-8-25	17.7	open sea
A-25	2.46	2.46	0.54	0.00	0.78	−0.09	99	1	0	1950-8-25	16.7	open sea
A-26	4.75	3.42	2.33	0.57	0.52	0.94	57	13	10	1950-8-25	22.8	open sea

A-27	4.89	3.79	2.10	0.52	0.88	1.16	56	33	11	1950-8-25	35.8	open sea
A-28	5.18	5.03	1.70	0.09	0.99	0.50	25	66	9	1950-8-25	52.6	open sea
A-29	5.80	4.29	2.64	0.57			43	39	18	1950-8-25	41.8	open sea
A-30	8.01	7.17	3.94	0.21			15	43	42	1950-8-25	75.8	open sea
A-31	8.49	7.95	3.06	0.18			1	50	49	1950-8-25	129.	open sea
A-32	8.30	7.65	3.16	0.21			2	52	46	1950-8-25	257.	open sea
A-33	1.95	2.00	0.46	−0.01	0.81	−0.30	99	0	0	1950-10-28	1.5	open sea
A-34	2.30	2.25	0.52	0.10	0.85	0.17	100	0	0	1950-10-28	4.6	open sea
A-35	2.71	2.64	0.52	0.14	0.79	0.29	97	2	0	1950-8-22	8.0	open sea
A-36	2.17	2.16	0.45	0.03	0.90	0.16	100	0	0	1950-10-28	8.1	open sea
A-37	5.02	4.69	2.24	0.19			40	48	12	1950-8-22	35.4	open sea
A-38	2.94	3.10	0.85	−0.19	0.31	−0.14	93	7	0	1950-10-28	13.1	open sea
A-39	7.91	6.82	3.64	0.30			13	45	42	1950-8-22	60.4	open sea
A-40	7.99	7.85	2.97	0.05			1	50	49	1950-8-22	130.	open sea
A-41	8.73	8.68	3.32	0.02			1	42	57	1950-8-23	191.	open sea
A-42	6.43	6.35	1.93	0.04	0.55	0.20	10	70	20	1950-8-22	194.	open sea
A-43	4.23	3.72	1.21	0.42	1.16	1.12	61	35	3	1950-10-28	9.1	open sea
A-44	1.55	1.65	0.46	−0.22	2.18	−1.93	95	0	0	1950-10-28	2.1	open sea
A-45	2.88	2.85	0.43	0.08	0.93	0.23	97	3	0	1950-10-28	7.2	open sea
A-46	3.13	3.15	0.53	−0.03	0.79	−0.07	94	6	0	1950-10-28	9.2	open sea
A-47	5.64	4.40	2.58	0.48			40	43	17	1950-10-28	12.2	open sea
A-48	2.30	2.29	0.51	0.03	1.01	−0.11	99	0	0	1950-10-28	2.2	open sea
A-49	2.48	2.50	0.46	−0.04	0.63	−0.15	100	0	0	1950-10-28	5.2	open sea
A-50	2.99	2.92	0.62	0.12	0.76	0.18	93	7	0	1950-10-28	8.7	open sea
A-51	2.64	2.72	0.74	−0.10	0.58	−0.22	98	2	0	1950-10-28	11.2	open sea
A-52	5.06	3.79	2.35	0.54			55	31	14	1950-8-23	21.3	open sea
A-53	7.67	7.20	3.02	0.16			3	55	42	1950-8-23	94.3	open sea
A-54	8.44	7.00	3.73	0.39			1	57	42	1950-8-23	267.	open sea
A-55	6.27	5.56	2.96	0.24			34	43	23	1950-8-23	110.	open sea

Note: The values of M_ϕ, β_ϕ and $\alpha_{2\phi}$ are also tabulated here in the interest of completness (cf. INMAN, 1953). The percentage of gravel is not indicated here, because it is easy to calculate by subtracting from 100% the total percentage of the sediments tabulated.

Table III. Data on Particle Size Distribution of Series D Samples
(Including a Part of Series B Samples of the Obitsu Delta)
Beach and Dune Sands

Sample No.	M_ϕ	Md_ϕ	σ_ϕ	β_ϕ	β_ϕ	$\alpha_{2\phi}$	% Sand	% Silt	% Clay	Sampling Date	Location (Fig. 12)	Environment
D-1	2.28	2.24	0.27	0.15	1.04	0.41	100	0	0	1950-11-4	Mera	coast dune
D-2	2.36	2.31	0.29	0.17	0.98	0.40	100	0	0	1950-11-4	Mera	coast dune
D-3	2.22	2.22	0.39	0.00	0.88	0.04	100	0	0	1950-11-4	Mera	coast dune
D-4	-0.29	1.42	2.19	-0.78	0.31	-0.91	65	0	0	1950-12-22	Ikeshinden	beach
D-5	1.63	1.67	0.43	-0.09	0.72	-0.30	100	0	0	1950-12-22	Ikeshinden	coast dune
D-6	2.02	2.05	0.26	-0.12	0.75	-0.48	100	0	0	1950-12-22	Ikeshinden	coast dune
D-7	1.85	1.84	0.28	0.02	0.85	0.00	100	0	0	1950-12-22	Ikeshinden	coast dune
D-8	2.40	2.39	0.22	0.05	0.77	0.09	100	0	0	1950-12-27	Sagara	beach
D-9	2.62	2.47	0.72	0.20	0.71	0.53	95	5	0	1952-2-22	Indio	inland dune
D-10	2.27	2.30	0.40	-0.08	0.63	-0.13	100	0	0	1953-8-24	Sweeper Cove	beach
D-11	1.44	1.62	0.52	-0.35	0.97	-0.99	99	0	0	1953-9-27	Hakodate	coast dune
D-12	1.42	1.68	0.54	-0.48	0.60	-0.77	100	0	0	1953-9-27	Hakodate	coast dune
D-13	1.44	1.52	0.51	-0.16	0.67	-0.39	100	0	0	1953-9-27	Hakodate	coast dune
D-14	1.68	1.81	0.46	-0.28	0.73	-0.62	100	0	0	1953-9-27	Hakodate	coast dune
D-15	2.24	2.17	0.52	0.13	0.76	0.38	100	0	0	1954-2-13	Yuma desert	inland dune
D-16	2.39	2.35	0.57	0.06	0.59	0.12	100	0	0	1954-2-13	Yuma desert	inland dune
D-17	2.07	1.92	0.64	0.23	0.77	0.37	100	0	0	1954-2-13	Yuma desert	inland dune
D-18	2.18	2.20	0.43	-0.05	0.69	-0.10	100	0	0	1954-2-13	Yuma desert	inland dune
D-19	2.19	2.02	0.49	0.35	0.76	0.80	100	0	0	1954-2-13	Yuma desert	inland dune
D-20	2.10	2.02	0.45	0.17	0.91	0.58	100	0	0	1954-2-13	Yuma desert	inland dune
D-21	2.38	2.28	0.56	0.17	0.75	0.45	99	1	0	1954-2-13	Yuma desert	inland dune
D-22	2.12	2.17	0.76	-0.07	0.65	-0.19	100	0	0	1954-2-13	Yuma desert	inland dune
D-23	2.66	2.68	0.38	-0.05	0.63	-0.11	100	0	0	1954-4-23	Pismo Beach	coast dune
D-24	2.76	2.82	0.26	-0.23	0.79	-0.33	100	0	0	1954-4-23	Pismo Beach	coast dune
D-25	2.77	2.82	0.29	-0.17	0.59	-0.38	100	0	0	1954-4-23	Pismo Beach	coast dune
D-26	2.76	2.80	0.22	-0.18	0.59	-0.45	100	0	0	1954-4-24	Morro Bay	coast dune
D-27	2.69	2.72	0.25	-0.14	0.63	-0.37	100	0	0	1954-4-24	Morro Bay	coast dune
D-28	2.73	2.75	0.23	-0.09	0.65	-0.22	100	0	0	1954-4-24	Morro bay	coast dune
B-23	1.73	1.82	0.55	-0.15	0.89	-0.49	99	0	0	1950-7-27	Obitsu Delta	beach
B-49	2.01	2.08	0.71	-0.10	0.96	-0.18	96	3	0	1950-7-29	Obitsu Delta	beach
B-50	1.45	1.54	0.61	-0.15	0.71	-0.39	100	0	0	1950-7-29	Obitsu Delta	beach

Table VI A. Composition of the Coarse Fraction of Representative Samples

Notes: Number for each constituent present the percentage in the entire sample. "tr." means trace.

Sample No. A-7

Size fraction, ϕ	<−2	−2 to −1	−1 to 0	0 to 1	1 to 2	2 to 3	3 to 4	<4
Fractional weight, %	6.5	13.5	10.0	20.0	37.0	9.2	2.7	98.9
Plant fibers	0	0	0	tr.	tr.	tr.	0.1	0.1
Terrigenous non-dark minerals	0	2.7	4.0	8.0	20.0	5.9	2.3	42.9
Terrigenous dark minerals	0	0	0.2	1.0	3.7	1.4	0.2	6.5
Terrigenous rock fragments	6.5	10.8	5.8	10.6	13.0	1.8	0.1	48.6
Terrigenous mica	0	0	0	0.4	0.3	0.1	tr,	0.8

Note: There are no shell fragments, Foraminifera, diatoms, ostracods, glauconite, and echinoid fragments.

Sample No. A-18

Size fraction, ϕ	<−2	−2 to −1	−1 to 0	0 to 1	1 to 2	2 to 3	3 to 4	<4
Fractional weight, %	0.0	0.0	1.0	4.7	56.3	37.9	0.1	100.0
Plant fibers	0	0	0	0	0	0	tr.	tr.
Terrigenous non-dark minerals	0	0	0	2.4	28.2	19.0	0.1	49.7
Terrigenous dark minerals	0	0	0	0.5	16.9	11.4	tr.	28.8
Terrigenous rock fragments	0	0	1.0	1.8	11.2	7.5	tr.	21.5
Terrigenous mica	0	0	0	0	0	0	0	0

Note: There are no shell fragments, Foraminifera, diatoms, ostracods, glauconite, and echinoid fragments.

Sample No. A-28

Size fraction, ϕ	<−2	−2 to −1	−1 to 0	0 to 1	1 to 2	2 to 3	3 to 4	<4
Fractional weight, %	0.0	0.0	0.2	0.7	1.2	8.3	14.6	25.0
Shell fragments	0	0	tr.	tr.	tr.	0	0	tr.
Foraminifera	0	0	0	tr.	tr.	0	0	tr.
Plant fibers	0	0	0.1	0.7	0.4	0.3	tr.	1.5
Terrigenous non-dark minerals	0	0	tr.	tr.	0.2	6.9	13.2	20.3
Terrigenous dark minerals	0	0	0	tr.	tr.	0.2	0.7	0.9
Terrigenous rock fragments	0	0	0.1	tr.	0.6	0.6	0	1.3
Terrigenous mica	0	0	0	tr.	tr.	0.3	0.7	1.0

Note: There are no diatoms, ostracods, glauconite, and echinoids.

Sample No. A-50

Size fraction, ϕ	<−2	−2 to −1	−1 to 0	0 to 1	1 to 2	2 to 3	3 to 4	<4
Fractional weight, %	0.0	0.0	0.1	0.3	5.6	51.0	35.5	92.5
Shell fragments	0	0	0	tr.	tr.	0	0	tr.
Foraminifera	0	0	0	0	tr.	0	0	tr.
Plant fibers	0	0	0	tr.	tr.	tr.	0	tr.
Terrigenous non-dark minerals	0	0	tr.	0.2	3.7	35.7	33.0	72.6
Terrigenous dark minerals	0	0	tr.	tr.	0.6	7.7	2.5	10.8
Terrigenous rock fragments	0	0	0.1	0.1	1.1	6.6	0	7.9
Terrigenous mica	0	0	0	tr.	0.2	1.0	tr.	1.2

Note: There are no diatoms, ostracods, glauconite, and echinoid fragments.

Sample No. D-6

Size fraction, ϕ	<−2	−2 to −1	−1 to 0	0 to 1	1 to 2	2 to 3	3 to 4	<4
Fractional weight, %	0.0	0.0	0.1	0.7	40.2	58.9	0.1	100.0
Shell fragments	0	0	0	0.1	0	0	0	0.1
Plant fibers	0	0	0	0	0	tr.	tr.	tr.
Terrigenous non-dark minerals	0	0	0	0.4	36.2	53.6	0.1	90.3
Terrigenous dark minerals	0	0	0	0.1	1.6	2.9	tr.	4.6
Terrigenous rock fragments	0	0	0.1	0.1	2.4	2.4	tr.	5.0
Terrigenous mica	0	0	0	tr.	0	tr.	tr.	tr.

Note: There are no Foraminifera, diatoms, ostracods, glauconite, and echinoid fragments.

Table IV B. Data on Mineral Grain Analyses of the Representative Samples

Sample No.	Size fraction ϕ	Heavy Minerals: % mono-minerals	Heavy Minerals: % rock frag-ments	Heavy Minerals: % Other consti-tuents	Light Minerals: % mono-minerals	Light Minerals: % rock frag-ments	Light Minerals: % Other consti-tuents	% Heavy minerals by wt.	% Light minerals by wt.
A-7	1-4	70	20	10	20	75	5	10.4	89.6
A-18	1-4	92	5	3	40	53	7	49.3	50.7
A-28	1-4	92	3	5	10	87	3	5.7	94.3
A-50	1-2	94	2	4	20	75	5	5.9	94.1
A-50	2-3	92	3	5	30	65	5	5.0	95.0
A-50	3-4	87	5	8	40	55	5	14.4	85.6
D-6	1-4	95	2	3	80	15	5	4.3	95.7

The Origin of Sand and Silt Alternations*
(Discontinuous Graded Beddings)

By

Noriyuki Nasu

Geological Institute, Faculty of Science, University of Tokyo

Abstract

There have been many discussions of the occurrence of thin-bedded alternations of sand and silt layers, and special emphasis has been given to abrupt change in texture at the base of graded beds. However, in many formations relatively abrupt changes also exist in the transition from coarse to fine sediments in a single unit. An interpretation of the abruptness of textural changes within a bedding unit is made here from hydrodynamic considerations, using examples from the Pliocene marine Miura group of Japan.

Because of basic differences in settling velocity and critical tractive velocity, source sediments are sorted into sand and mud fractions during transportation, and upon deposition this will tend to cause a relatively sharp transition between sand and silt. In addition to this vertical transition, sand and silt will also tend to show rapid transition zones in a horizontal direction.

Sporadic changes in the amount of source material and competency of the transporting agent will result in rapid horizontal migration of the transition zone between sand and silt and in this way certain submarine areas would be covered by sheets of sand and silt alternately, so that the resulting formation would exhibit both horizontal and vertical transitions.

Table of Contents

* This paper was presented at the annual meeting of the Geological Society of America, Los Angeles, November, 1954.

Introduction

When the sediments in the vicinity of Mt. Horaiji, Aichi Prefecture, Japan were surveyed in 1948, it was observed that the Miocene Shidara formations in this area included alternate layers of sand and silt, and that the boundaries between each layer were sharp and distinct rather than gradational (Fig. 7).

Alternate layers of sand and silt with relatively sharp boundaries were also observed in the Zushi formation among the Miura group studied in 1949 on the Miura Peninsula, Kanagawa, Japan. In the Miura group, the boundary between a silt layer and the overlying sand layer was always sharp, whereas there was some tendency for the sand layers to grade into the overlying silt layers, as seen in the Shidara formations.

It was thought that the alternation of layers of sand and silt with relatively sharp boundaries, could be explained on a basis of general hydrodynamic principles operating during the transportation of the sediments (NASU, 1951; 1954). Because of basic differences in settling velocity and critical tractive velocity which depend principally upon sediment size, source sediments are sorted into sand and mud fractions during transportation, and upon deposition this will tend to cause a relatively sharp transition between layers of sand and silt. The same principles are thought to apply to the formation of beach sands (NASU, 1956), and of small scale delta (NASU and SATO, in preparation), only in these cases the fine material has been removed and deposited elsewhere (NASU, 1955).

In order to better understand the processes involved in the sorting of sediments a study was made of the sediments of the marine Pliocene Miura group, and a systematic series of samples were obtained from the various types of sand and silt layers within the group.

An effort has been made since 1951 to add more data to the studies. Specifically, more samples were collected from the Pliocene

Miura group in 1951, and the sediments of the Sagara, Kakegawa Tertiary groups in Shizuoka, Japan were observed (Fig. 7).

The sand and silt alternations in the Pico formation near Ventura, north of Los Angeles, were observed during 1954.

The main purpose of this paper is to show that sand and silt alternations in older sediments are controlled by the same principles which result in the separation of sand and muddy materials during the process of the transportation and deposition. Since the size, shape, and the specific gravity of sediment components are directly related to the mechanics of transportation, this paper is concerned primarily with the results of particle size distribution of the sediments.

Acknowldgments

This study was initiated at the Geological Institute, University of Tokyo, and completed at the Scripps Institution of Oceanography, University of California.

The author is sincerely indebted to Professors Takao SAKAMOTO and the late Yanosuke OTUKA in the Geological Institute, University of Tokyo, and Professors Milton N. BRAMLETTE, Douglas L. INMAN, and Francis P. SHEPARD of the Scripps Institution of Oceanography for their assistance, criticism and guidance.

The writer also wishes to mention his deep appreciation to Messrs. Isamu MURAI and Takayasu UCHIO of the University of Tokyo for their assistance in the field survey as well as in the laboratory.

This research has been supported by a Grant in Aid for Fundamental Scientific Research from the Department of Education of Japan.

Methods

Sampling

Seventy-five samples from various types of sedimentary rocks were collected in 1949 and 1950 along a course which is approximately normal to the strikes of the Pliocene Miura group. The sampling locations are indicated in Fig. 1. These will be called as the Series C samples. Those which were collected in the same locality, but

from different beds, were differenciated from each other by naming them as C-6-1, C-6-2, etc.

Darticle Size Distribution Analyses

Since the statistical expression of particle size distribution has already been explained in detail by the author, it will not be repeated here (NASU, 1956, pp. 69-73). Only a few more informations will be discussed in addition.

Obviously, sediment grains should be disaggregated and sepatated from each other to obtain a realistic particle size distribution. Therefore, special treatment to disaggregate individual grains was necessary in the case of semi-consolidated sediments collected from the geologic formations. In this regard the sandy sediments were fairly easy to disaggregate, but silty sediments often caused difficulties. Both types of samples were kept in water for a long time and boiled, then separated by mechanical manipulation (KRUMBEIN and PETTIJOHN, 1938, pp. 43-75).

The sediments exposed on the earth's surface have been more or less weathered so that the size distribution curves obtained for them may be somewhat modified from their original shapes. Sandy sediments are usually less influenced by weathering than finer material from the same locality (KRUMBEIN and PETTIJOHN, 1938, p. 21). Sometimes flocculation occurs in the fine sediments during the process of mechanical analysis due to the chemical interaction of sediment and water.

As a result the particle size distribution curves will indicate a larger proportion of coarser material than actually occurred in the original sediment. For example, it is quite common to observe coagulation in sediments when they are brought into the sea from rivers. Therefore, in the analysis of sediments deposited in salt water it may be more realistic to use salt water for the mechanical analyses if the origianl distribution curves are desired. However, it is very difficult, if not impossible, to approximate the natural conditions in the laboratory.

Since the major focus of this paper was on the boundary between sand and silt, it was felt that results using the usual tap water (Tokyo) would be acceptable. Effects of varying degree of flocculation which occurred during analysis were in general accepted as part of laboratory experimental error. Thus the particle size distribution curves used here only approximate the natural distributions because of errors caused by flocculation, weathering and disintegrating processes. Sieving technique was applied to sandy sediments and the pipette method was used for silt-clay size sediments. (KRUMBEIN and PETTIJOHN, 1938, pp. 135-143; 166-172). Mixed sediments of sand and silt size were divided into sands and silts by wet sieving, then the sieving and pipette methods were applied to each fraction.

Sediments of the Pliocene Miura Group

Neogene and Quarternary sediments are exposed on the Miura Peninsula, between the Gulf of Sagami and Tokyo Bay, and along its

northern extension. The predominant strike of the formations is east southeast, and the southeasterly extension continues to the Bōsō Peninsula beyond Tokyo Bay. The western extension is buried under the Sagami alluvial plain, and the Tama alluvial plain conceals its northern extension. Among the Neogene sediments, a thick deposit called the "Miura group" occupies the area between the Zushi—Yokosuka line and the southern part of Yokohama. This group is reffered to the Pliocene Period (OTUKA, 1937), and shows a monoclinal dip (5°–15°) toward the north northeast. The base of the group overlies the Miocene Hayama group disconformally.

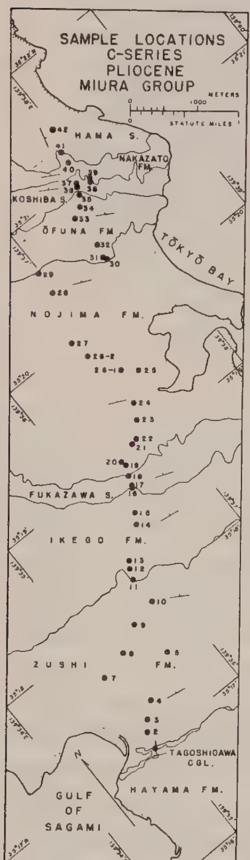

Fig. 1

Various classifications have been attempted in order to divide this group into smaller formational units (Geol. Soc. Japan, 1955, pp. 591–604). For convenience here, it is classified in the following way according to the lithologic changes observed along the surveyed course (Fig. 1). Namely, from the base to the top, the formations are: a) Tagoshigawa conglomerate, b) Zushi formation (sand and silt alternations), c) Ikego pyroclastic formation (involving tuffaceous sand in its middle and upper part), d) Fukazawa sandstone formation, e) Nozima tuffaceous sandstone formation, f) Ōfuna siltstone formation, g) Koshiba sandstone formation, h) Nakazato silstone formation, and i) Hama sandstone formation (NASU, 1950). The Hama sandstone mentioned last is different in its strike as well as dip from the others, and is of limited areal extent.

The samples were analyzed mechanically and the results are tabulated in Table I in the appendix. The thickness of the formations together with the size distribution measures for the samples are shown in Fig. 2.

The results of the investigations are as follows:

(1) Tagoshigawa conglomerate at the base of the Miura group (30 m±) consists of breccias including abundant fossils, and are rich

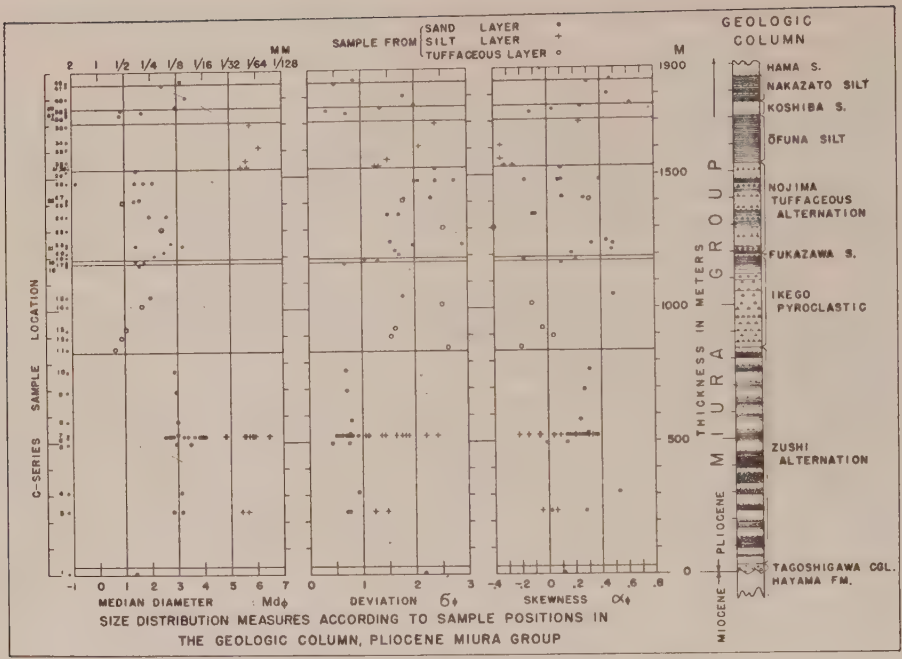

Fig. 2

in taffaceous materials. Sample C-1 was taken from the matrix consisting of coarse sand.

(2) The Zushi formation, consisting of sand and silt alternations, forms thick deposits (810 m ±). Each layer of sand or silt is several to several tens of centimeters thick. Occasionally white tuff layers are interbedded, and also, scattered volcanic lappillis are sometimes recognized in sand or silt layers.

(3) The outcrops of the Zushi alternations have generally a horizontal extent of several to several tens of meters. So far as the observed exposures are concerned, the thickness of each layer of sand and silt does not vary laterally. Occasionally there is a lateral change from sand to silt along the same horizon, and in all cases the change was in the form of sudden lensing out of a sand layer into a silt layer. A gradual change from a sand layer into a silt layer laterally has never been observed. This may be due to the limited length of the observed exposures, or it may be a truly characteristic feature of the alternations.

Fig. 3. Sand and Silt Alternation of the Zushi Formation, Pliocene Miura Group.
No. C–6 samples were collected here.
Dark bands are sand layers.
Light bands are silt layers.

(4) Vertical alternations in sediment type are shown in Fig. 3 and 4. Black bands are sand layers and white ones are silt layers. A sharp contact exists between each layer, as can be seen from the photographs. However, on closer observation, it is noticed that the boundary between a silt layer and the overlying sand layer is very distinct. However, the boundary between a sand layer and the overlying silt layer is not as sharp as in the other case and a rapid gradation is common. Generally speaking, inside a single layer of sand, the grain size is obviously coarsest at the base, but it is hard to judge by visual observations whether the grain size grades into finer toward the top of the layer. Size variation within a single layer of silt can not be recognized. These facts are commonly observed in a whole sequence of the Zushi formation.

(5) The microphotograph of several successive layers of sand and silt in the neighbourhood of C–9 is shown in Fig. 5. The position of each sample is indicated in the column drawn at left, and the corresponding microphotos are shown at the right. The things described in item (4) are also observed here. Nos. 1, 5, and 8 are silts,

Fig. 4. Sand and Silt Alternation in the Vicinity of Sample Location C-9 in the Zushi Formation, Pliocene Miura Group.
Dark bands are sand layers.
Light bands are silt layers.
The length of the scale is one meter.

and the rest are sands. The boundary between 1 and 2 is quite distinct, and sand grains decrease their sizes from the bottom to the top of a sand layer. This tendency can be seen from No. 2 through No. 4, as well as from No. 6 to No. 7. The boundary between Nos. 4 and 5, from a sand layer to an overlying silt layer, is also fairly distinct.

(6) The laminations in the sand layers are commonly parallel to the boundary described above, and cross-bedding is generally not recognized. Sometimes the laminations are characterized by chocolate brownish color which might be primarily organic matter, because the trace of plant fibers is recognized under a microscope.

(7) Generally speaking, it seems that the sand layers thicker than 40-50 centimeters show coarser grain sizes than those of thinner sand layers.

(8) From every single layer of sand and silt at location C-6, samples were collected successively and analyzed. Fig. 3 shows the alternation at this locality.

(9) Sometimes sand layers are thicker than silt layers, and sometimes the reverse is true. On the average, however, the silt layers are somewhat thicker, as shown in Figs. 3 and 4.

(10) As shown in Fig. 2, the median diameter is coarse and the sorting is poor at the base (Tagoshigawa cgl.) of sand and silt alternations of the Zushi formation, but the main part of the alternation shows median diameters in the fine to very fine sand range and also shows good sorting in each layer of sand. This might reflect stability of environment when they were deposited.

(11) This calm environment was finally broken by severe volcanic

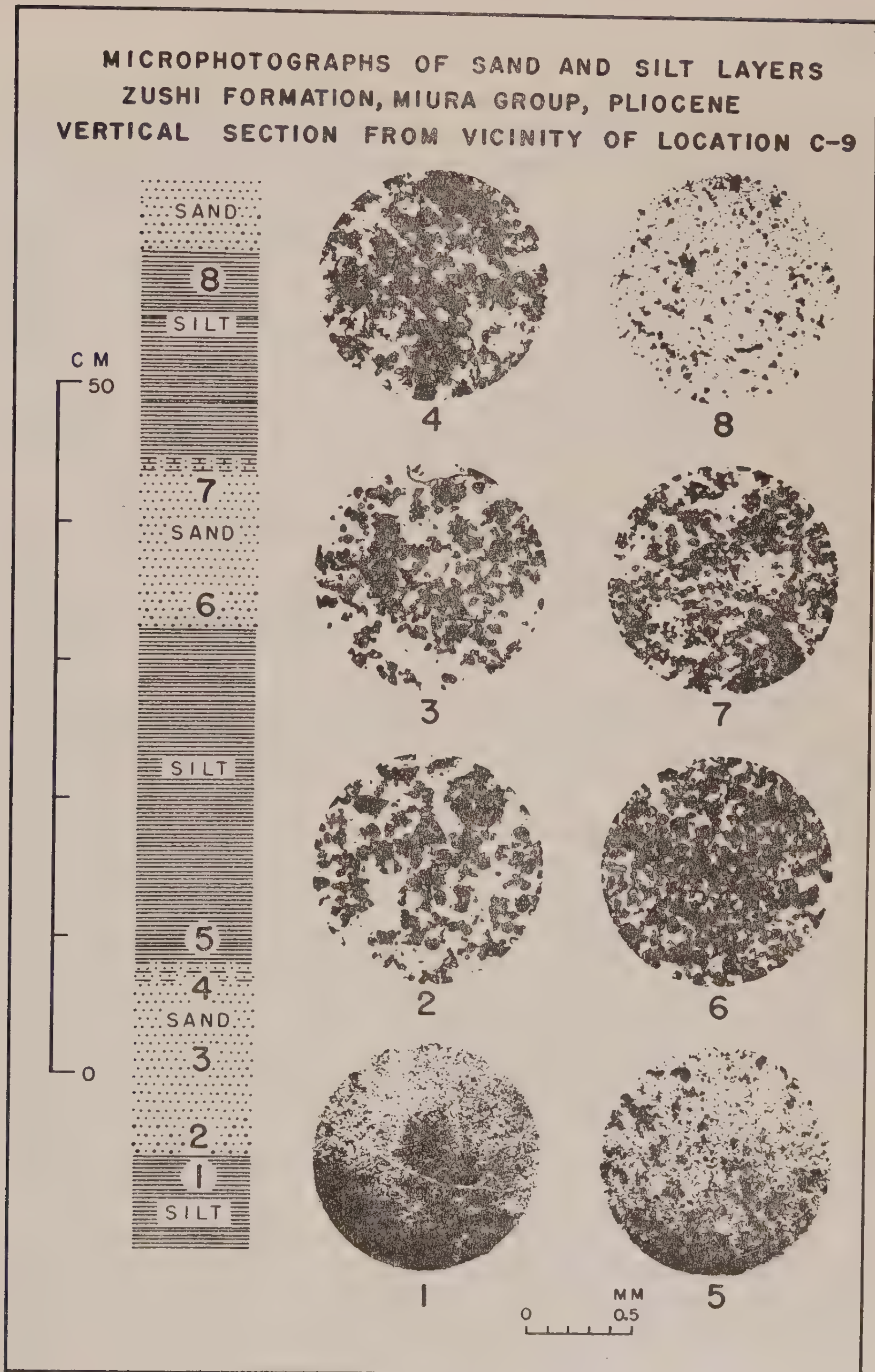
MICROPHOTOGRAPHS OF SAND AND SILT LAYERS
ZUSHI FORMATION, MIURA GROUP, PLIOCENE
VERTICAL SECTION FROM VICINITY OF LOCATION C-9
SAND
8
SILT
CM
50
7
SAND
6
SILT
5
4
SAND
3
0
2
1
SILT
4
8
3
7
2
6
1
5
MM
0
0.5

Fig. 5

activity. Namely, a few sheets of pyroclastic materials start to be involved at the uppermost part of the Zushi formation, succeeded by a thick pile of the main body of the Ikego pyroclastic rocks. The Ikego formation seems to be conformable to the Zushi formation.

(12) The Ikego formation (335 m ±) changes to the taffaceous sandstone in its central and upper portions, due to the decay of the volcanic activity. The stratification in sizes of several to several tens of centimeters thick is common at these parts of the formation, but there are no alternations like the Zushi formation which consists of heterogeneous successive layers.

(13) The Ikego formation is overlaid by the Fukuzawa sandstone (15 m ±). The latter is massive sand, and has been thought to be uncomformable to the Ikego formation.

(14) The roundness of sands in the Fukuzawa formation is much higher than that of the Zushi formation.

(15) Also, the median diameter of the Fukuzawa sands is generally coarser than that of sand layers of the Zushi alternations as shown in Fig. 2.

(16) The Nojima tuffaceous sandstone (340 m ±) overlies on the Fukazawa sands comformably. This formation should be accompanied by the extensive volcanism because it contains abundant fractions of scorias and lappillis. Occasionally, white tuff layers are inserted. The stratification indicated several to several tens of centimeters in its thickness for each single layer. The results of the particle size analyses of this formation indicate the bimodal distributions. It suggests the contamination of the local volcanic materials with sedimentary deposits of other origin. The sediments from the central and upper part of the Ikego formation also tend to be polymodal.

(17) The Ōfuna siltstone (175 m ±) covers the Nojima formation comformably. This formation consists dominantly of blue-greenish siltstone, and presents almost no stratification. A trace of volcanic activity is rarely seen, except a few layers of white tuff. The particle size distributions are somewhat similar to those from the silt layers of the Zushi formation.

(18) The Koshiba sandstone (55 m ±) overlies the Ōfuna formation. The shell fragments are abundant, and the false beds are well developed. The dip (15°) is steeper than those of the neighbourhood formations (9°). The median diameters of this formation are coarser

than those of sand layers in the Zushi alternations and approximate to those of the Fukazawa sands.

(19) The Nakazato siltstone (93 m ±) lies on the Koshiba sands conformably. This is brownish siltstone and is a little different from the Ōfuna siltstone in its characteristics. Sands are mixed, and occasionally sand layers are recognized. Stratification occurs only where the content of sands increases. The samples which were analyzed here were taken from sand layers.

(20) The Hama sands (50 m ±) cover the Nakazato siltstone. This formation is different in its dips and strikes from the others

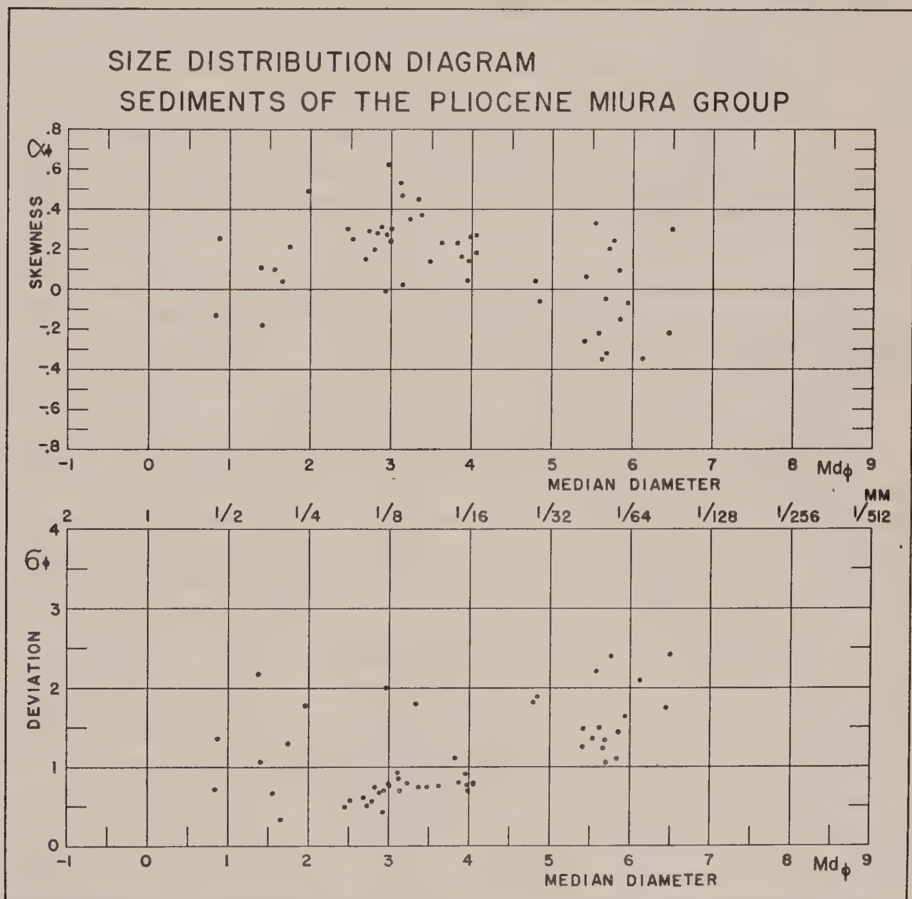

Fig. 6

previously mentioned. Only one sample is illustrated here, so it is hard to draw any kind of conclusion.

(21) In Fig. 6, σ_ϕ and α_ϕ values are plotted as ordinate and Md_ϕ values as abscissa. This diagram, however, is based upon the samples which do not involve the evident trace of the volcanic activity. The resulting points are fairly scattered, compared with those from modern sediments in the vicinity of the Sagami River mouth and the Obitsu Delta (NASU, 1956, Figs. 6 and 14). This is probably due to diagenesis, weathering effects and degradation effects during the process of the particle size analyses.

However, it is thought that the following statements will be correct insofar as tendencies are concerned. Phi deviation measures, σ_ϕ, are minimum and concentrated in a range of median diameter of 2ϕ to 4ϕ. The further the Md_ϕ values deviate from this range, the more the σ_ϕ values increase and scatter. The α_ϕ measures increase from zero or minus values to large positive values, then decrease gradually toward zero values according to the increase in value of Md_ϕ.

(22) The results of coarse fraction analyses of a few representative samples, i. e., of C-6-17, C-6-18, and C-37, together with the visual observation in the field, indicate that the terrigenous materials are definitely dominant in the Miura group, except the Koshiba formation which contains abundant shell fragments.

The results of mineral grain analyses of the same samples show that light minerals are dominant and the constituents of heavy minerals suggest the lack of metamorphic rocks in its source areas.

The composition of the sand size fraction of a typical sample would be about as follows:

% by weight	*Composition*
90	Feldspar and quartz
2	Rock fragments
8	Heavy minerals, predominantly augite, hornblende, hypersthene, and miscellaneous opaque minerals.

Hydrodynamics

It will be worthwhile to discuss briefly a few known principles

of hydrodynamics before entering into the interpretation of the origin of discontinuous graded beddings. However, this part of the problem has already been discussed by the author, so that readers are referred to NASU (1956, pp. 82–90).

The Origin of Sand and Silt Alternations (The Origin of Discontinuous Graded Beddings)

Detailed descriptions about the Zushi alternations among the Miura group have been made. It has been pointed out that there is a fairly sharp boundary between a sand layer and an overlying silt layer, which has somewhat been overlooked. Of course, the sharp boundary between a silt layer and an overlying sand layer has been explained adequately by various authors (for example, SHROCK, 1948, p. 78).

These sharp boundaries on both sides of each layer are not only observed in the Zushi formation, but also in the alternations in various areas such as the following: the middle to the upper part of the Miocene Shidara formations exposed in Aichi, Japan: parts of the Miocene Sagara group and the Pliocene Kakegawa group, Shizuoka, Japan. A part of the Pliocene formations in Ventura, California presents similar lithological characteristics (Fig. 7).

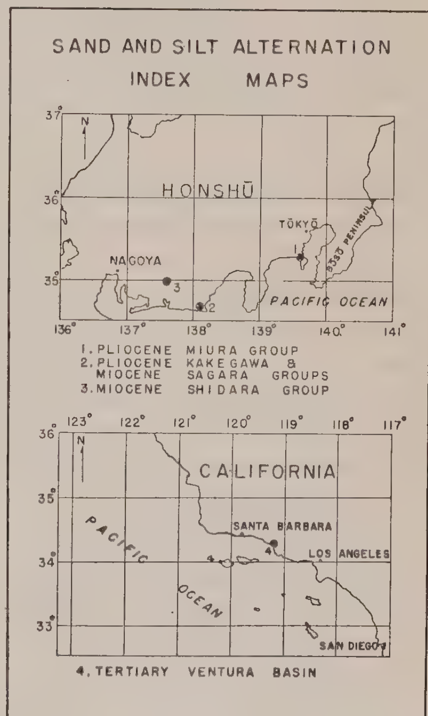

Fig. 7

Fig. 8 presents the picture of sand and silt alternations of the Pico formation along the Santa Paula creek, a branch of the Santa Clara River which extends NNW from the town of Santa Paula near Ventura, California (neighbourhood of the locality 5 by NATLAND and KUENEN, 1951). The

Fig. 8. Sand and Silt Alternation of the Pico Formation near Ventura, California.
The tip of hammer indicates the top of a sand layer at the right.

point of a hammer indicates the boundary between a sand layer on the right and a silt layer on the left.

The occurrence of this kind of alternation will be explained in the following manner. As mentioned previously, sands generally creep along the bottom during the processes of transportation until they reach the final place for deposition. On the other hand, muds are mostly in suspension when they are transported by horizontal advection or diffusion. Thus sands and silt-clays are separated during the common processes of transportation, which have already been explained hydrodynamically.

Sand and silt alternations can be considered as the vertical records of this separation preserved in the geologic column. Here, the attempt will be made to recreate the original process of deposition by speculating on the lithological conditions of the alternations.

Muds were being deposited, forming a widespread layer over the area. Suddenly sands invaded this area because of the sudden change of supply conditions of the sediments. But, the surface of a silt-clay sheet was not disturbed owing to the coagulation effect within it, and

to its higher critical tractive velocity. Thus, much vertical mixing between muds and newly invaded sands was avoided. Therefore, the sharp boundary was formed between a silt layer and an overlying sand layer.

After cessation of the sand invasion, which had taken an entirely different transporting form from that of mud which had been in suspension, the sand layer was gradually covered by the settling fractions of mud which continued to accumulate until the next invasion of sands occurred.

Here, the grading within a silt layer would not be so significant, because of the slow rate of deposition of muds which might result in a higher chance of mixing among a wide range of size fractions. Thus, the boundary between the sand layer and the overlying silt layer became fairly distinct because of the different type of transportation. This cycle process repeated many times, and, as a consequence, thick deposits of sand and silt alternations were formed.

Next, the horizontal distribution of sands and muds will be discussed (Fig. 9). It can be considered that the depositional areas of sands would be connected with those of muds by having narrow

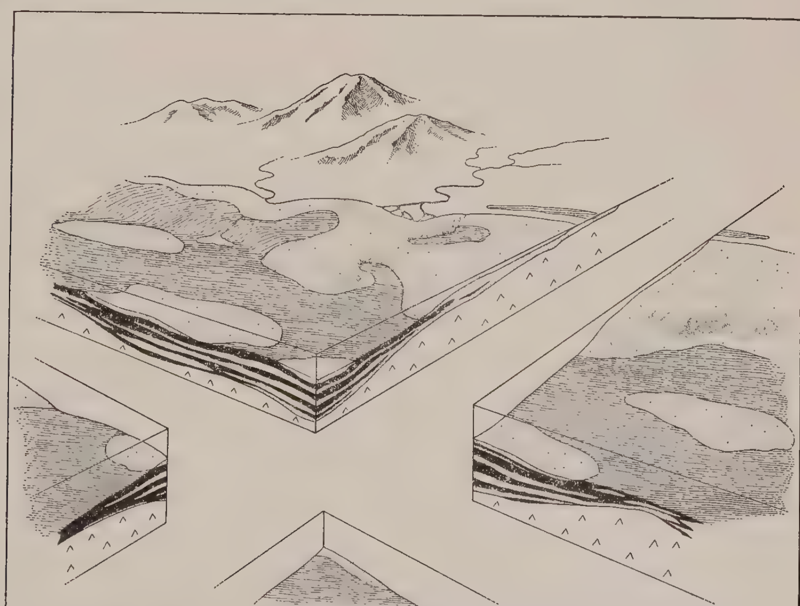

Fig. 9. Schematic Diagram of Sand and Silt Alternation.

transition zones as shown in the distributions of modern as well as older sediments (cf. p. 114; SHEPARD and COHEE, 1936; EMERY and BUTCHER et. al., 1952; NASU, 1955; RICH, 1948).

This zone would be shifted for a long distance during a short time owing to the sudden change of sediment supply conditions. Then, the heterogeneous sediments would start to settle in the area over which the transition zone migrated, and the homogeneous sediments would continue to settle elsewhere. Thus, the sand and silt alternations would be formed under the area where the sudden migration of the transition zone had been repeated. On the other hand, under the area where the migration did not reach, thick siltstone or sandstone would be formed without showing any kind of characteristic alternations, as shown in the Ōfuna siltstone, Fukazawa, Koshiba and Hama sandstones. In general, these sandstones present a little coarser median diameters than those of sand layers in the alternations, which may suggests the horizontal sorting of sand in a direction of the transportation of sediments.

Here, the question naturally arises as to the circumstances under which the sand and silt alternations were formed. Prior to the author's speculation concerning this point, several important works done previously will be introduced here.

The existence of deep sea sands has been pointed out by various authors during past several years, and the majority of them have suggested the possibility that the source of these sands might be of shallow water (for example, SHEPARD, 1951). PHLEGER (1951a, pp. 50–53; 1951b) gave a proof for it by pointing the contamination of shallow water Foraminifera into these deep sea sands. The turbidity currents have been suggested as the cause of this sand displacement (ERICSON, EWING and HEEZEN, 1952; KUENEN, 1953).

The term *turbidity currents* was proposed by KUENEN and MIGLIORINI (1950) by expanding the original concept of *density currents* by DALY (1936), and has been also applied as the major cause of graded beddings in the geologic formations, because of: (1) absence of insignificance of current bedding and ripple marking in graded deposits; (2) Deposition of coarse material on the unconsolidated fine-grained top of the preceding bed; (3) enormous extent of each individual member without apparent change in thickness or character.

They concluded that the graded beddings might be formed in the

deeps of geocynclines, and developed in the so-called greywackes. It might be associated with slump structures. DORREEN (1951) also observed the same sort of sedimentary sequence in the Tarala sandstones in Peru, as observed by KUENEN and MIGLIORINI in the Italian macigno type. The characteristics of alternations observed by the author coincide with those described by KUENEN, MIGLIORINI, and DORREEN except they did not point the fairly distinct boundary between a sand layer and the overlying silt layer.

So far as the Ventura group is concerned, NATLAND and KUENEN (1951) studied the lithological as well as paleontological features, and determined the content of shallow water Foraminifera with deep water faunas in a single layer of the graded beddings. They concluded that this is the result of the secondary displacement of the shallow water sediments by the action of turbidity currents into the deep water.

SUZUKI and KITAZAKI (1951) studied Foraminifera in the Miura group in detail, and described that the dominant Foraminifera groups in the Zushi alternations indicate the deep sea faunas. However, this study was not done from the same view point of PHLEGER, NATLAND and KUENEN, so that the fact of contamination is not clear. Since the sand layers in the alternaions might be carried from shallow water, it may be possible to prove the contamination in the Zushi formation if investigated from this viewpoint. The sporadic displacement of shallow water sediments into deep sea might very possibly occur.

The fact of contamination was already pointed in the alternations of the Seki formations, which are the easterly extension of the middle part of Miura group, and are exposed in the Bōsō Peninsula. (HIRAYAMA, 1954).

MAKIYAMA (1950) described that the sand and silt alternation of the Horinouchi formation of Kakegawa group is a typical Flysch type and contains the carbonized fragments of plants in sand layers. Thus, he speculated that the original sedimentation occured in the deep basin close to the mainland, and the density current would be counted as the transporting agency of sediments. The author tends to agree with MAKIYAMA's statements.

According to these statements, the sand and silt alternations might be formed in the deeps at the foot of the continental slopes or in the deeps quite close to the shore from where the plentiful supply of

sediments was expected; for example, as the Gulf of Sagami and the Gulf of Suruga at present, because the sand and silt alternations illustrated here for thick deposits of several hundreds to a few thousand meters in thickness. The original sedimentation basins of the alternations might not be the lagoons, estuaries or on the continental shelves.

The density currents, which consisted of sand and mud mixture, sometimes involving gravels (Ventura group), might slide down along the submarine slopes until it broke. Then, they might be separated into sand and mud, the latter in suspension, the former spreading over the bottom taking the creeping form. The final process before the deposition might be just a simple creeping form, or, as mentioned by STETSON and SMITH (1938); namely, the density currents would descend the continental slope until the point of similar density is reached, at which level the density currents would disperse and be suspended prior to deposition, controlling the distribution of sediments over the continental slopes as well as in the neighbourhood deeps. In Fig. 5, the particles are coarser at the bottom then decrease toward the top in a single layer of sand; therefore, STETSON's assumption is reasonable in this case.

When a part of the Pico formation near Ventura (in the vicinity of locality 2 by NATLAND and KUENEN (1951)) was investigated in 1954, the alternation of graded beddings consisting dominantly of conglomerate and sand was observed. NATLAND and KUENEN suggested that coarse sands had been deposited by turbidity currents, whereas the conglomerate appears to have resulted from submarine sliding or highly mobile flows, because the contamination of shallow and deep water faunas of Foraminifera was recognized in these beddings.

In this case, the graded beddings consist of much coarser sediments than those which have been discussed previously in this paper, and it is understandable from the viewpoint of hydrodynamics why these graded beddings indicated here do not show any characteristic abrupt grading within a single layer of bedding.

Furthermore, KUENEN and CAROZZI (1953) described their search results of the Flysch and Molasse of the Alps, and indicated that the Flysch shows remarkably clear stratification because of the regular alternations; on the other hand, the Molasse shows no distinct boundaries between each layer, and it is the post-orogenic deposits accom-

panied with the emergence of the Alps. This statement will give a certain suggestions.

Therefore, the following statement will be included here to make clear the distinction between discontinuous graded beddings consisting of sand and silt alternations and continuous graded beddings consisting only of sediments of sand and coarser sizes. If the source sediments consisted of a heterogeneous mixture of sand and mud, then they would tend to be sorted into sand and mud fractions prior to deposition if the course of transportation would be long enough, and would result upon deposition in sand and silt alternations showing discontinuous graded beddings within each single couplet. In the case where the source consists entirely of coarser sediments without mud, then upon deposition the resulting bed would tend to show continuous graded beddings.

Furthermore, the continuous graded bedding within a single couplet which may occur for the case of sand and mud mixture might be the result of poorer sorting during the process of transportation.

Summary and Conclusions

Sediments are commonly separated into sand and mud fractions during the common processes of transportation and deposition, reflected by the actual distribution of sediments in nature. The significance and geologic importance of this separation have been discussed in this paper as illustrated by Tertiary sediments, principally of the marine Pliocene Miura group exposed in the northern part of the Miura Peninsula in Japan (Fig. 1).

Phi median diameters, Md_{ϕ}, phi deviation measures (sorting factor), σ_{ϕ}, and phi skewness measures, α_{ϕ}, obtained from particle size distribution curves of the collected samples, were the principal measures for the interpretation.

Among the findings the following are important:

(1) The Zushi formation consisting of successive alternate layers of sand and silt occupies the lower half of the Pliocene marine Miura group, 1900 meters thick (Fig. 1).

(2) Characteristic features of these sand and silt alternations are: (a) the boundary between a silt layer and an overlying sand layer is always sharp, (b) the boundary between a sand layer and an overlying

silt layer is also sharp, but less distinct than the above, and sand grades into the overlying silt layer (Figs. 3, 4 and 5), (c) each layer of sand or silt has a thickness of several to several tens of centimeters.

(3) Sediments were collected from the representative layers in each formation among the Miura group and analyzed to obtain the particle size distribution curves. Some of these formations in the Miura group consisting of sandstone or siltstone do not show any characteristic stratification as seen in the Zushi formation.

(4) The median diameters of sand layers which alternate throughout the vertical section of the Zushi formation are close to 3ϕ. The phi deviation measures of the same samples are less than 1.0, and the phi skewness measures are positive. Therefore, sediments forming sand layers of the Zushi formation are well sorted sands having finer median diameters than, and containing more mud than the modern sands along the Gulf of Sagami and the Obitsu Delta (Fig. 6).

(5) The median diameters of sediments forming silt layers in the Zushi formation range from 5ϕ to 7ϕ, and the larger σ_ϕ values indicate poor sorting (Fig. 2).

(6) Md_ϕ, σ_ϕ, α_ϕ values of the Koshiba sandstone, which have well developed cross beddings, are similar to those from the Sagami and the Obitsu areas (Fig. 2).

(7) The above mentioned characteristic features are seen not only in the Zushi formation but elsewhere (Figs. 7 and 8).

These are the major results obtained from the investigations, and before entering into the interpretation of these facts, it will be desirable to mention a few known principles in hydrodynamics.

Muds of which settling velocities are quite slow and in accordance with STOKES' law are suspended in water for a long period and are transported for a long distance by the advection as well as the horizontal turbulence in water. The stronger the water turbulence, the longer will be the suspension. The settling velocities of sands are very fast and deviate from STOKES' law, because the resistance from water is not only caused by the viscosity but also by the form drag.

The turbulent boundary layer of fluids has a bottom laminar boundary layer which is very thin and has a very steep velocity gradient when the bottom is smooth. Muddy bottom will be considered smooth when silt-clays do not project above this thin layer and thus have rare chances to be plucked into water by the vertical component

of turbulence. In addition, the coagulation effect of muds will tend to make difficult the initiation of motion of muds by weak currents.

Medium to fine sands are most easily shifted by the weakest current, because at this stage of the bottom condition, the bottom laminar boundary layer may not exist any longer. Therefore, sediments will be plucked into water easily by the vertical component of turbulence and also will be moved by the horizontal force of the currents.

Gravels are not easily shifted simply due to their weight, and the only style of transportation will be rolling or sliding when their motion is initiated. Thus, the threshold mean flow velocity is minimal in medium to fine sands.

Therefore, gravels, sands and muds will be separated from each other during the process of transportation. The sedimentological significance of this separation can be possibly traced in the sequence of discontinuous graded beddings as follows.

Sand and silt alternations are generally formed in extroardinarily thick deposits, for example, as seen in the Zushi and the Pico formations. Each layer of sand or silt has sharp boundaries.

The mechanism forming these distinct boundaries between silt layers and an overlying sand layers has been throughly discussed in various papers. A combination of a sand layer and an overlying silt layer is commonly considered as a graded bed and the grain size has been assumed to change gradually from coarser at the bottom and finer at the top inside a single bed. However, in many cases there is a fairly distinct change in the grain size between the top of a sand layer and the base of an overlying silt layer, and this seems to have been overlooked.

The author assumes that these sharp boundaries between sand and overlying silt layers are the result of the sand and silt separation during the processes of transportation and deposition. Furthermore, the area covered by sands will be separated laterally from the area covered by muds. Transition zones between them may not be as wide and rapid changes of grain size and sorting value in this zones can be expected.

When plentiful sediments were supplied, for example, to the deeps close to the land, the density currents flowing down the slope sporadically would tend to separate the sediments into sands and muds, and

would cause sudden horizontal shifts of the transition zone due to sudden changes in sediment supply (Fig. 9).

Sand and silt alternations would be formed under the area on which the transition zones had shifted repeatedly. Sandstone would be the result of the accumulation under the area on which sands had been deposited continuously, and siltstone would result in the area of mud deposition.

Generally speaking, the median diameters of sands from beaches, dunes, sandstones, and top set beds of deltas are little coarser than those from sand layers of the alternations.

References cited

DALY, R. A., 1936, "Origin of submarine canyons," Amer. Jour. Sci., v. 31, pp. 401-420.

DORREEN, J. M., 1951, "Rubble bedding and graded bedding in Talara formation of northwestern Peru," Bull. Amer. Assoc. Pet. Geol., v. 35, n. 8, pp. 1829-1849.

EMERY, K. O., W. S. BUTCHER, H. R. GOULD, and F. P. SHEPARD, 1952, "Submarine geology off San Diego, California," Jour. Geol., v. 60, n. 6, pp. 511–548.

ERICSON, D. B., M. EWING, and B. C. HEEZEN, 1952, "Turbidity currents and sediments in north Atlantic," Bull. Amer. Assoc. Pet. Geol., v. 36, n. 3, pp. 489–511.

Geol. Soc. Japan, 1955, "Chisomei Jiten (Lexicon of stratigraphic names of Japan, Cenozoic Erathem)," Part II, pp. 295–789, (Japanese).

HIRAYAMA, J., 1954, "Gosō no mondai (Problems in sand and silt alternations among the Seki subgroup)," Taisekigaku Kenkyu, n. 7. pp. 2–5, (Japanese).

KRUMBEIN, W. C., and F. J. PETTIJOHN, 1938, "Manual of sedimentary petrography," Appleton-Century-Crofts, Inc., New York, 549 p.

KUENEN, Ph. H., 1953, "Significant features of graded bedding," Bull, Amer. Assoc. Pet. Geol., v. 37, n. 5, pp. 1044–1066.

——, and A, CAROZZI, 1953, "Turbidity corrents and sliding in geosynclinal basins of the Alps," Jour. Geol., v. 51, n. 4, pp. 363–373.

——, and C. I. MIGLIORINI, 1950, "Turbidity currents as cause of graded bedding," Jour. Geol., v. 58, n. 2, pp. 91–127.

MAKIYAMA, J., 1950, "Nippon chiho chishitsu shi, Chubu chiho." Asakura Book Co., Tokyo, 233 p., (Japanese).

NASU, N., 1950, "Taisekigan no ryudo hyoji, Miura Hanto hokubu (Particle size distribution of sediments of the Pliocene Miura group)," Jour. Geol. Soc. Japan, v. 56, n. 656, pp. 309–310, Abstract, (Japanese).

——, 1951, "Interpretation of sedimentation phenomena in terms of fluid dynamics," Jour. Geol. Soc. Japan, v. 57, n. 671, pp. 367–368, Short communication.

——, 1954, "Origin of sand and silt alternations (Discontinuous graded beddings)," Bull. Geol, Soc. Amer., v. 65, n. 12, p. 1290, Abstract.

——, 1955, "Significance of the separation of sediments into sand and mud fractions during common processes of transportation as illustrated by modern and Tertiary sediments," unpublished doctoral dissertation of the Scripps Institution of Oceanography,

University of California, 161 p.

——, 1956, "Particle size distribution in the vicinity off Sagami River mouth (The processes forming beach and dune sands)," Jour. Fac. Sci., Univ. Tokyo, Sec. II, v. 10, pp. 65–108.

——, and Y. SATO, (in preparation), "Particle size distribution of the Obitsu Delta (The occurrence of the steep marginal slope of a small scale delta)."

NATLAND, M. L., and Ph. H. KUENEN, 1951, "Sedimentary history of the Ventura Basin, California, and the action of turbidity currents," Soc, Econ. Paleo. & Mineral., Spec. Pub., n. 2, pp. 76–107.

OTUKA, Y., 1937, "Geologic structure of the south Kwanto region, Japan (Yokohama-Huzisawa district)," Bull. Earthquake Research Inst., Tokyo Imperial Univ., v. 15, Part 4, pp. 974–1040, (Japanese with English summary).

PHLEGER, F. B., 1951a. "Ecology of Foraminifera, northwest Gulf of Mexico," Part I, Geol, Soc. Amer. Memoir 46, 88 p.

——, 1951b, "Displaced Foraminifera faunas," Soc. Econ. Paleo. & Mineral., Spec. Pub., n. 2, pp. 66–75.

RICH, J. L., 1948, "Submarine sedimentary features on Bahama Bank and their bearing on distribution patterns of lenticular oil sand," Bull. Amer. Assoc. Pet. Geol., v. 32, n. 5, pp. 767–779.

SHEPARD, F. P., 1951, "Transportation of sand into deep water," Soc. Econ. Paleo. & Mineral., Spec. Pub., n. 2, pp. 53–65.

——, and G. V. COHEE, 1936, "Continental shelf sediments off the mid-Atlantic states," Bull. Geol. Soc. Amer., v. 47, n. 3, pp. 441–458.

SHROCK, R. R., 1948, "Sequence in layered rocks," McGraw-Hill Book Co., Inc., New York and London, 507 p.

STETSON, H. C., and J. F. SMITH, 1938, "Behaviour of suspension currents and mud slides on the continental slope," Amer. Jour. Sci., 5th Series, v. 35, n. 205, pp. 1–13.

SUZUKI, K., and U. KITAZAKI, 1951, "Applied micropaleontological studies of the Cenozoic formations on the northern part of Miura Peninsula," Jour. Geol. Soc. Japan, v. 57, n. 665, pp. 65–78, (Japanese with English summary).

Appendix

Table I. Data on Particle Size Distribution of Series C Samples Sediments of the Pliocene Miura Group

In this table, sand includes particles $-1<\phi<4$,
silt includes particles $4<\phi<8$,
clay includes particles $8<\phi$,
gravel includes particles $\phi<-1$

The percentage of gravel is not indicated here. because it is easy to calculate by subtracting from 100% the total percentage of the sediments tabulated.

Sample No.	M_ϕ	Md_ϕ	σ_ϕ	β_ϕ	α_ϕ	$\alpha_{2\phi}$	% Sand	% Silt	% Clay	Formation	Meters Above Base	Lithology of Sampled Layer
C-1	1.62	1.39	2.17	0.11	0.69	0.22	75	13	1	Tagoshigawa	0	cgl.
C-2	2.20	3.28	1.97	−0.55	0.81	−0.94	69	20	0	Zushi	196	sand
C-3-1	3.05	2.84	0.75	0.28	1.36	0.78	86	13	1	Zushi	238	sand
C-3-2	5.60	5.67	1.24	−0.05	0.92	0.05	11	83	6	Zushi	238+	silt
C-3-3	5.51	5.43	1.48	0.06	0.67	0.23	15	79	6	Zushi	238+	silt
C-3-4	3.16	3.15	0.71	0.02	1.25	0.38	86	13	1	Zushi	238+	sand
C-4	3.61	3.12	0.93	0.53	0.50	0.40	63	37	0	Zushi	309	sand
C-5-1	3.59	3.49	0.75	0.14	1.18	0.73	74	25	1	Zushi	494	sand
C-5-2	2.93	2.94	0.43	−0.01	1.49	−0.03	95	5	0	Zushi	494+	sand
C-6-1	4.00	3.96	0.92	0.04	0.71	0.22	52	47	1	Zushi	523	sand
C-6-2	5.10	5.59	2.20	−0.22			21	68	11	Zushi	523+	silt
C-6-3	4.08	3.97	0.77	0.14	1.13	0.68	52	44	4	Zushi	523+	sand
C-6-4	5.94	5.84	1.11	0.09	1.33	−0.08	9	84	7	Zushi	523+	silt
C-6-5	4.17	3.99	0.70	0.26	1.22	0.84	50	47	3	Zushi	523+	sand
C-6-6	4.73	4.85	1.88	−0.06	0.35	0.18	44	52	4	Zushi	523+	silt
C-6-7	4.20	4.06	0.78	0.18	0.69	0.48	47	51	2	Zushi	523+	sand
C-6-8	5.64	5.86	1.43	−0.15	0.56	−0.01	10	85	5	Zushi	523+	silt
C-6-9	4.01	3.88	0.81	0.16	0.89	0.38	57	41	2	Zushi	523+	sand
C-6-10	5.83	5.95	1.64	−0.07	0.75	−0.17	14	77	9	Zushi	523+	silt
C-6-11	3.66	3.38	0.75	0.37	1.06	1.03	76	22	2	Zushi	523+	sand
C-6-12	6.06	6.46	1.75	−0.22	0.64	−0.40	14	73	13	Zushi	523+	silt
C-6-13	4.27	4.06	0.80	0.27	1.58	0.94	46	50	4	Zushi	523+	sand
C-6-14	4.87	4.80	1.82	0.04	0.63	0.08	33	63	4	Zushi	523+	silt
C-6-15	3.80	3.63	0.77	0.23	0.84	0.57	68	30	2	Zushi	523+	sand
C-6-16	7.23	6.50	2.42	0.30			7	68	25	Zushi	523+	silt
C-6-17	2.89	2.74	0.52	0.29	1.16	0.93	93	7	0	Zushi	523+	sand
C-6-18	5.93	5.72	1.06	0.20	0.98	0.29	6	88	6	Zushi	523+	silt
C-6-19	2.91	2.80	0.57	0.20	1.25	0.82	92	7	1	Zushi	523+	sand
C-6-20	5.99	5.54	1.36	0.33	0.55	0.39	5	88	7	Zushi	523+	silt
C-6-21	2.67	2.53	0.58	0.25	1.43	1.03	92	7	1	Zushi	523+	sand
C-6-22	3.52	3.24	0.80	0.35	1.58	1.47	78	18	4	Zushi	523+	sand
C-6-23	4.08	3.83	1.11	0.23			59	31	10	Zushi	523+	sand
C-6-24	2.78	2.69	0.62	0.15	1.52	0.90	91	9	0	Zushi	523+	sand
C-7	3.24	3.01	0.76	0.30	1.23	1.06	84	15	1	Zushi	531	sand
C-8	3.19	3.00	0.79	0.24	1.33	0.84	84	14	2	Zushi	579	sand
C-9	3.14	2.95	0.71	0.27	1.56	0.47	86	13	1	Zushi	693	sand
C-10	3.10	2.89	0.68	0.31	1.31	1.13	87	12	1	Zushi	767	sand
C-11	0.10	0.63	2.63	−0.20			62	5	3	Ikego	853	pyroclastic
C-12	0.94	0.88	1.55	0.04	0.65	0.11	87	3	0	Ikego	895	pyroclastic
C-13	0.99	1.05	1.63	−0.04	1.15	0.37	82	6	1	Ikego	924	pyroclastic
C-14	1.34	1.65	2.52	−0.12	0.36	−0.08	67	14	0	Ikego	1016	pyroclastic
C-15	2.84	1.97	1.78	0.49	0.92	0.92	80	17	2	Ikego	1048	sand
C-16	1.62	1.56	0.67	0.10	0.85	0.16	99	1	0	Ikego	1174	sand
C-17	2.02	1.75	1.30	0.21	1.61	1.41	88	11	1	Fukazawa	1176	sand
C-18	1.22	1.42	1.07	−0.18	1.01	0.20	94	3	1	Fukazawa	1185	sand
C-19	2.44	2.14	1.70	0.18	0.81	0.82	83	15	2	Nozima	1203	sand
C-20	3.29	2.50	1.63	0.48	1.25	0.71	78	18	4	Nozima	1215	sand
C-21-1	3.86	3.21	1.98	0.33	0.55	0.43	62	36	2	Nozima	1244	sand
C-21-2	2.86	1.43	2.90	0.49	0.41	0.76	77	19	4	Nozima	1244+	sand
C-22	3.45	2.77	1.54	0.44	0.75	0.73	74	24	2	Nozima	1249	sand
C-23	1.38	2.41	2.54	−0.40	0.81	−0.17	68	13	2	Nozima	1303	sand
C-24-1	1.80	1.93	1.50	−0.09	0.99	0.34	89	8	1	Nozima	1354	sand
C-24-2	2.39	2.59	1.70	−0.11	0.93	0.35	82	15	2	Nozima	1354+	sand
C-25	1.47	0.92	1.78	0.31	0.95	1.06	90	9	1	Nozima	1407	pyroclastic
C-26-1	1.83	1.34	1.80	0.27	0.75	0.55	83	12	1	Nozima	1411	sand
C-26-2	2.28	1.93	2.36	0.15	0.41	0.19	72	23	0	Nozima	1411+	tuff
C-27	1.82	1.58	2.32	0.11	0.58	0.38	75	16	1	Nozima	1415	sand
C-28-1	0.95	1.40	2.75	−0.17	0.36	−0.18	63	9	1	Nozima	1481+	sand
C-28-2	0.10	−0.84	2.40	0.39	0.93	0.97	44	8	2	Nozima	1481+	cgl.
C-28-3	1.94	1.73	2.06	0.10	0.90	0.42	77	14	2	Nozima	1481+	sand
C-28-4	2.24	2.07	2.01	0.08	0.48	0.35	81	17	1	Nozima	1481+	sand
C-29	1.67	1.43	2.40	0.10	0.52	0.19	70	17	0	Nozima	1530	sand
C-30	5.08	5.42	1.26	−0.26	1.09	0.34	20	75	5	Ōfuna	1530+	silt
C-31	5.26	5.69	1.34	−0.32	0.46	−0.30	18	79	3	Ōfuna	1532	silt
C-32	5.10	5.63	1.50	−0.35	0.39	−0.39	23	75	2	Ōfuna	1557	silt
C-33	5.39	6.13	2.09	−0.35	0.44	−0.50	25	69	6	Ōfuna	1610	silt
C-34	4.27	3.51	3.17	0.24			56	31	13	Ōfuna	1637	tuff. silt
C-35	6.34	5.77	2.39	0.24			17	62	21	Ōfuna	1694	silt
C-36	0.74	0.84	0.72	−0.13	0.84	−0.06	98	0	0	Koshiba	1737	sand
C-37	1.67	1.66	0.34	0.04	0.70	0.16	100	0	0	Koshiba	1745	sand
C-38	1.22	0.88	1.36	0.25	1.74	1.38	87	6	2	Koshiba	1757	sand
C-39	4.21	2.97	2.00	0.62	0.54	0.91	72	23	5	Nakazato	1760	sand
C-40	4.14	3.34	1.80	0.45	0.89	1.00	64	30	6	Nakazato	1798	sandy silt
C-41	2.62	2.47	0.50	0.30	1.76	1.50	93	6	1	Nakazato	1853	sand
C-42	3.54	3.14	0.86	0.47	1.49	1.49	78	20	2	Hama	1859	sand

JOURNAL OF THE FACULTY OF SCIENCE
UNIVERSITY OF TOKYO

The JOURNAL is on sale at

MARUZEN CO., LTD.

6, Nihonbashi Tōri-Nichōme, Chūō-Ku, Tokyo

Price in Tokyo: Yen 220 for this Part.

CONTENTS

昭和三十一年九月二十五日印刷
昭和三十一年九月三十日発行

編纂兼発行者 東京大学

東京都港区芝浦一丁目一番地
印刷者 富田元

東京都港区芝浦一丁目一番地
印刷所 ヘラルド社

東京都中央区日本橋通二丁目六番地
売捌所 丸善株式会社